PHYSICAL REVIEW
LETTERS

VOLUME 6 FEBRUARY 1, 1961 NUMBER 3

VELOCITY-SPACE PLASMA INSTABILITIES OBSERVED IN A MIRROR MACHINE*

Richard F. Post and Walton A. Perkins
Lawrence Radiation Laboratory, University of California, Livermore, California
(Received January 9, 1961)

We have previously reported[1,2] our first observations of a deliberately induced velocity-space instability of magnetically compressed plasma, adiabatically confined in a mirror machine. Search for this instability was prompted by theoretical calculations, to our knowledge first performed by Rosenbluth,[3] predicting that hydromagnetic instabilities could arise in magnetically confined plasmas, the particle distributions of which are anisotropic in velocity space. The observations reported in this Letter show that plasma instability can be induced in an otherwise stable plasma, under the conditions predicted by theory. The instability is detected by observing the greatly enhanced rate of transport of particles (across the flux lines of the confining magnetic field) which it causes, as compared to a stable case.

Aside from its relevance to plasma research, the instability we have observed may be of more general interest because it can be made to appear at very low plasma densities. Thus it might arise in situations (such as in some high-current accelerators) where cooperative effects are normally considered unimportant.

The instability in question is the so-called "mirror instability," predicted to occur in plasmas where $p_\perp > p_\parallel$ (the pressure tensor component perpendicular to the lines is greater than that parallel to the lines), whenever the local value of $\beta = (p_\perp)/[(B^2/8\pi) + p_\perp]$ exceeds a local critical value β_c. In these regions where $\beta > \beta_c$, theory predicts that random perturbations in the magnetic field should rapidly develop exponentially (until some nonlinear limit is reached). As suggested by its name, one can understand this instability by noting that within the plasma any local perturbation, depending on whether it increases or decreases the field, must create either a local "magnetic mirror," or else a trapping region between two mirrors. If the plasma velocity distribution is anisotropic, this in turn must lead either to the turning back or to the trapping of some particles by the perturbation. The diamagnetic effects associated with these excluded or trapped particles will in either case then act to amplify the initial perturbation, the effects becoming regenerative if $\beta > \beta_c$. One therefore expects that in unstable regions turbulent "rippling" of the magnetic field would develop, destroying the adiabaticity of the particle motions, and thus leading to enhanced transport effects.

Clearly, the more anisotropic the distribution, the smaller will be the value of β_c. Conversely, in the mirror machine, confined plasmas which have reached diffusion equilibrium with the end losses are normally only slightly anisotropic and will therefore be characterized by large β_c values, typically 0.5 or greater.[4] To observe the mirror instability at smaller values of β, the anisotropy must therefore be made anomalously large.

Theoretical expressions from which β_c can be calculated for an "infinite" plasma in a uniform magnetic field have been reported.[3,5-7] To calculate β_c for a finite plasma in pressure equilibrium in a nonuniform magnetic field (as in the mirror machine), a condition derivable from the work of Newcomb[8] will be used. The condition is

$$\beta < \beta_c = [\tfrac{1}{2}|(\nabla p_\perp/p_\perp)/(\nabla B/B)| + 1]^{-1} \text{ stable}, \quad (1)$$

the gradients being taken in the direction of the

magnetic field. This condition is to be applied at any point in the plasma. In deriving this expression, individual particle motions have been assumed to be governed by the usual adiabatic invariants, i.e., the magnetic field varies slowly in time, and particle orbit diameters are small.[9]

In these experiments the confined anisotropic plasma is produced by the adiabatic magnetic compression of an injected "blob" of low-energy plasma. As previously discussed[10,11] this process can be used in a mirror machine to generate a stably confined plasma of very high electron temperature (~25 kev); we induce the instability in these experiments by manipulation of the electron component of the plasma, the ions playing an unimportant role. Because magnetic compression acts primarily to increase the "temperature" of only one component of particle motion, that perpendicular to the lines of force, anisotropy results. It is appropriate therefore to describe the final particle distribution by two "temperature" parameters, $T_\perp$ and $T_\parallel$, and to take the midplane distribution function to be a "two-temperature Maxwellian,"

$$f = \exp\{-\tfrac{1}{2}m[(v_\perp^2/T_\perp)+(v_\parallel^2/T_\parallel)]\}, \qquad (2)$$

within the allowed values of $v_\perp/v_\parallel$. Calculating $p_\perp$ from (2), (1) can be evaluated for various values of the mirror ratio, $R = B_{max}/B_0$, as a function of position between the midplane (B_0) and the mirrors (B_{max}). For values of $t = T_\parallel/T_\perp \ll 1$, it is found that the minimum β_c occurs at the midplane. Figure 1 shows β_c(min) as a function of t, for various values of R. Since in our experiment $R \approx 2$, Fig. 1 shows β_c(min) $= t$, to close approximation. Parenthetically, it can be shown that the curves of Fig. 1 also represent β_c(min) for a midplane distribution function which is any differentiable function of the variable $(v_\perp^2/T_\perp + v_\parallel^2/T_\parallel)$, not merely the special exponential form assumed above.

To observe the instability at small values of β, the anisotropy must be large; this requires a large magnetic compression ratio. But since collisions tend to destroy anisotropy, it is also necessary that the initial plasma density be low enough that collision effects are unimportant during the compression, but not so low that β lies below its critical value. Therefore, in order to produce the instability, it was necessary to reduce the initial density about a factor 10 below that normally used.[11] Magnetic compression ratios $B_f/B_i = 10^3$ or more were used, so that $t = \beta_c \approx 10^{-3}$. The peak magnetic field, B_f, was 10 kilogauss.

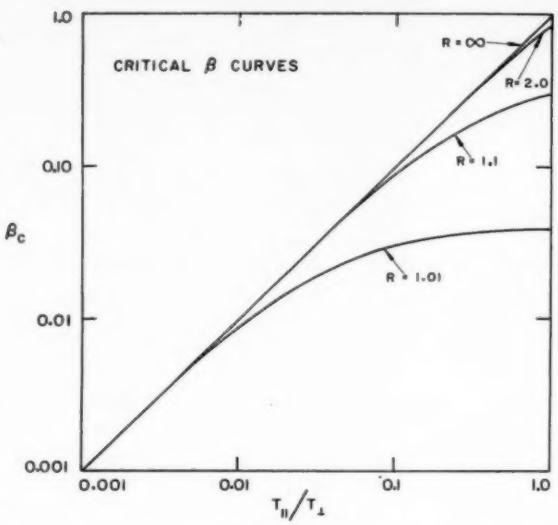

FIG. 1. Critical β curves for the midplane for several values of the mirror ratio R.

Figure 2 shows the experimental arrangement used. Scintillation probes were used to detect the fluxes of radially and axially escaping electrons. The plasma conditions, which determined whether or not instability occurred, were varied by changing (a) the initial magnetic field, (b) the intensity and the timing (relative to the pulsed magnetic field) of the injected plasma burst, and (c) the residual gas pressure.

Most of the observations consisted of correlating the intensity of signals received at the radial scintillation probe (see Fig. 2), with changes in the plasma or compression parameters. The most striking feature of the signals received by this probe was the extreme variation in intensity between stable and unstable cases. Whereas strong signals, several orders of magnitude above multiplier noise, were detectable in the unstable cases, signal levels dropped below detectability when the plasma was rendered stable. Figure 3 illustrates the effect of changing plasma density (by varying the plasma-source-pulse-capacitor charging voltage). Although the signal received by the end scintillation probe increases monotonically until detector saturation occurs, the time-integrated radial probe signal increases only up to a critical density and then falls rapidly to zero with further increase in density. At this density we believe that collisional randomization becomes important and suppresses the instability. This interpretation is apparently borne out by

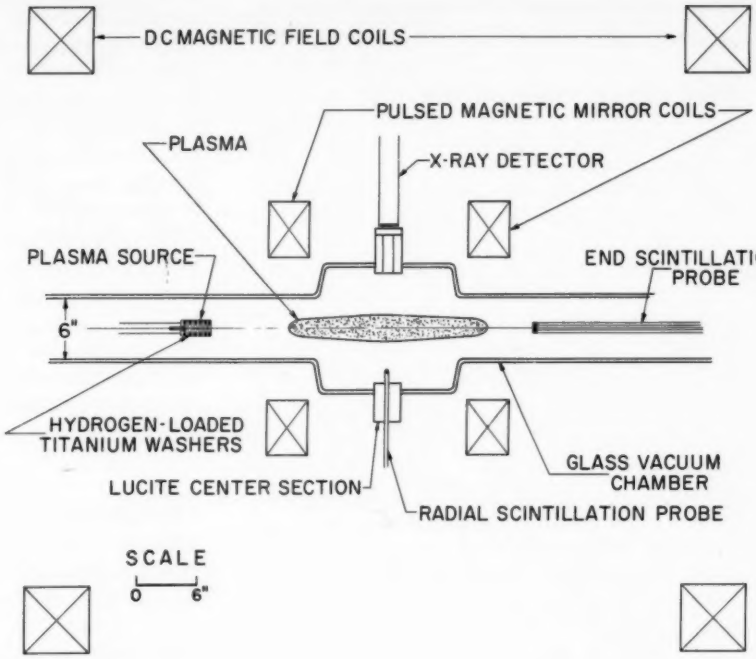

FIG. 2. Experimental arrangement.

experiments in which a neutral "scattering gas" (helium) was admitted to the chamber. As the helium density was raised above about 3×10^{12} cm^{-3}, the ratio of radial-to-axial signal dropped rapidly to zero. From scattering theory one can calculate that, for electrons of mean energy of 20 kev, this density of helium scattering centers would smooth out all anisotropies in about 300 microseconds, i.e., in a time comparable to the compression time of 500 microseconds.

The velocity of plasma transport (across the magnetic field lines) caused by the instability was estimated by three methods: (1) Calculation from the rate of collapse of flux tubes during compression; the plasma collected during compression must possess at least enough velocity to "paddle upstream" to the detectors. (2) Time correlation between signals received by scintillation probes at two different radial positions. (3) Observation of the effect of a movable obstacle which projects into the chamber at a point diametrically opposite the radial probe. By inserting this probe into the chamber to a radius less than that of the radial scintillator probe we decreased its signals; from these data and from the known mean precession time of electrons around the chamber (about 8 microseconds), the radial transport velocity can be calculated. The mean velocities deduced by the above three methods ranged between 2×10^4 and 2×10^5 cm/sec. These velocities are more than 10^7 times the "classical" diffusion velocities appropriate to the plasma density and temperature, and are at least 10^4 times the upper limits experimentally deduced[11,12] for the stable, higher density, plasmas studied earlier in the same apparatus.

Associated with the presence or absence of the instability one expects substantial changes in the radial density distribution of the compressed plasma. By using a movable scintillator probe located just outside one of the mirrors, the radial distribution of the escaping electrons was measured; from such measurements radial density distributions can be inferred. Figure 4 shows these data for two cases: (1) plasma density in the range where instabilities are observed; (2) "low" plasma density, i.e., $\beta<\beta_c$. The differences are striking. Similar constricting effects were found upon increasing the initial field (lowering B_f/B_i, therefore reducing anisotropy), even though the theoretical radial compression itself was thereby reduced.

Approximate quantitative agreement between the theoretical β_c and experimental β values was obtained from the following considerations: The theoretically predicted axial variation of plasma density [calculated by using Eq. (2)] was compared with the experimental data (obtained by axial move-

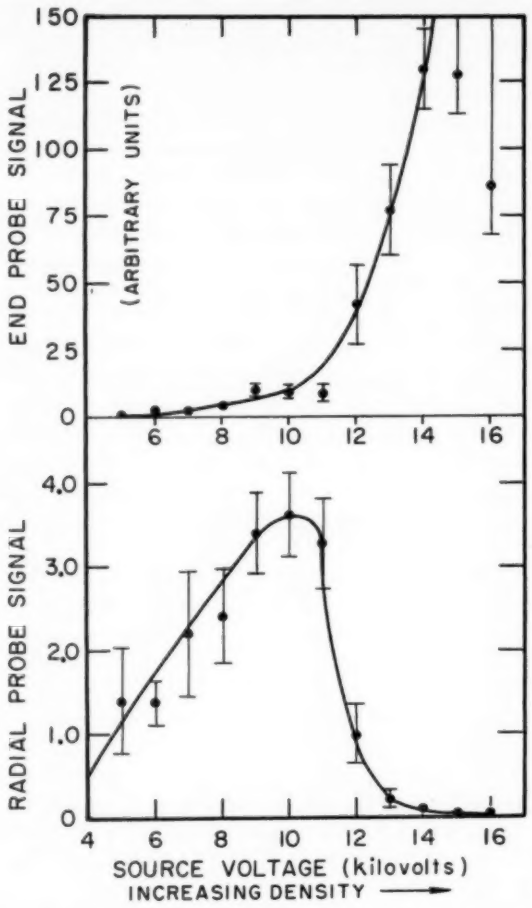

FIG. 3. Probe signals as a function of plasma-source pulse-capacitor charging voltage.

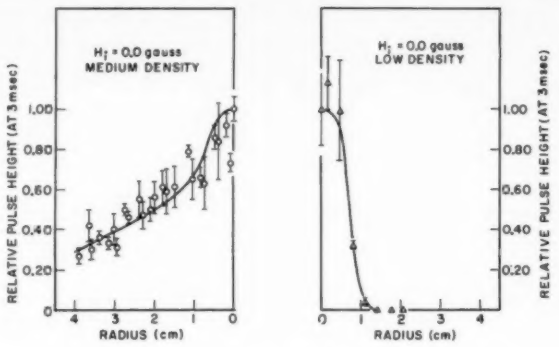

FIG. 4. End escaping flux as a function of radius for an initial magnetic field of 0.0 gauss for medium and low densities.

ment of a scintillator probe about the midplane) to determine the anisotropy. In the cases analyzed $t \approx 10^{-3}$, so that, from Fig. 1, $\beta_C \approx 10^{-3}$. From calorimetric measurements[13] of the energy flux carried radially by the escaping plasma, and from the measured plasma volume, experimental values of β could be deduced. For a plasma that had diffused out to the scintillator, these ranged between 1×10^{-3} and 4×10^{-3}, i.e., between about 1 and 4 times the "theoretical" value of β_C. (The corresponding plasma density was therefore of order 10^{11} cm^{-3}.) However, the value of β prior to expansion of the plasma out to the detector should be larger than its value after expansion. This means that we believe that whenever the pressure of the compressed plasma was initially only slightly above the critical value, only the most anisotropic components were able to diffuse out to the radial probe, the pressure of the rest of the plasma dropping below β_C (so that the plasma became "frozen" to the field lines) before it could reach the detector. We have obtained experimental evidence for this interesting selective transport effect by method (3), above, used to measure radial transport velocity. These measurements showed a clear separation of the radial probe signals into two groups: (1) a "fast" group, appearing within about 500 μsec of the initiation of compression; (2) a "slow" group, appearing several milliseconds after peak field, i.e., not until inner field lines of the collapsing field had expanded out to the detector. For the "slow" group a relative motion of the obstacle and detector of only 0.005 inch was sufficient to extinguish most of the detected signal. The "late" plasma particles appeared therefore to be frozen to the expanding field lines. In support of this interpretation, it was found from the axial variation of the radial flux about the midplane that only the "fast" group was characterized by a very large ratio of $p_\perp/p_\parallel$. These measurements also apparently resolve an old mystery; we had earlier discovered[10] that under certain conditions the outermost energetic electrons of an otherwise stable compressed plasma core could apparently diffuse rapidly to the chamber walls, producing x rays. Their rate of radial transport was much greater than that predicted by classical theory. We now believe that this effect was early evidence of the "mirror" instability here discussed, but occurring only in the outer, low-density, portion of the plasma core.

In summary, we believe that we have established the existence and some of the manifestations of a

hydromagnetic velocity-space instability of the "mirror" type. In our experiments, using high-energy electrons, it has been observed to cause an enhanced rate of transport of particles across field lines. It may also cause other effects, such as more rapid thermalization of the plasma, or the emission of plasma radiation. These effects, or those which might arise when the instability is associated with anisotropies in the ionic component of the plasma rather than the electronic component, we have not investigated. Although it is possible to avoid the instability by controlling the plasma parameters, we have shown that it may occur in plasma compression experiments. It also seems likely that any method of creating a hot plasma which results in anomalously large anisotropies (such as the method of injecting highly directed high-energy particles), may stimulate this instability during buildup, even if the final plasma state aimed for is stable. Finally, since this instability feeds on perturbation in energy density, and is not of electrostatic origin, it should persist in the limit of very low particle densities, provided the anisotropy becomes correspondingly large. For this reason, it (or related instabilities) might occur in some astrophysical situations or in particle accelerators, even though the conditions are such that cooperative effects would normally be considered unimportant.

*Work performed under the auspices of the U. S. Atomic Energy Commission.

[1]W. A. Perkins and R. F. Post, Bull. Am. Phys. Soc. 5, 353 (1960).

[2]R. F. Post and W. A. Perkins, Bull. Am. Phys. Soc. 5, 353 (1960).

[3]M. N. Rosenbluth, Los Alamos Report LA-2030, 1956 (unpublished).

[4]R. F. Post, Proceedings of the Conference on the Theoretical Aspects of Controlled Fusion Research, Gatlinburg, Tennessee, April 28-29, 1959 [Atomic Energy Commission Report TID-7582 (unpublished), p. 158].

[5]S. Chandrasekhar, A. Kaufman, and K. Watson, Proc. Roy. Soc. (London) A245, 435 (1958).

[6]L. I. Rudakov and R. Z. Sagdeev, Plasma Physics and the Problem of Controlled Thermonuclear Reactions (Pergamon Press, New York, 1959), Vol. III, p. 321.

[7]A. A. Vedenov and R. Z. Sagdeev, reference 6, p. 332.

[8]W. Newcomb, Ann. Phys. (to be published).

[9]These conditions (of adiabaticity) are undoubtedly not essential to the growth of instabilities of this type. H. Furth and K. Neil (private communication), when investigating the instabilities of relativistic electron streams, have also been able to show that the "mirror" instability should persist even in the limit of large orbit sizes.

[10]F. H. Coensgen, F. C. Ford, and R. E. Ellis, Proceedings of the Second United Nations International Conference on the Peaceful Uses of Atomic Energy, Geneva, 1958 (United Nations, Geneva, 1958), Vol. 32, p. 266; also R. F. Post, ibid, p. 245.

[11]R. F. Post, R. E. Ellis, F. C. Ford, and M. N. Rosenbluth, Phys. Rev. Letters 4, 166 (1960).

[12]W. A. Perkins, R. E. Ellis, and R. F. Post, Bull. Am. Phys. Soc. 5, 309 (1960).

[13]T. Passell (private communication), also reported at American Physical Society Plasma Physics Division Meeting, Gatlinburg, Tennessee, November 2-5, 1960.

SUPERCONDUCTIVITY IN Nb_3Sn AT HIGH CURRENT DENSITY IN A MAGNETIC FIELD OF 88 kgauss

J. E. Kunzler, E. Buehler, F. S. L. Hsu, and J. H. Wernick
Bell Telephone Laboratories, Murray Hill, New Jersey
(Received January 9, 1961)

We have observed superconductivity in Nb_3Sn at average current densities exceeding 100 000 amperes/cm^2 in magnetic fields as large as 88 kgauss. The nature of the variation of the critical current (the maximum current at a given field for which there is no energy dissipation) with magnetic field shows that superconductivity extends to still higher fields. Existing theory does not account for these observations. In addition to some remarkable implications concerning superconductivity, these observations suggest the feasibility of constructing superconducting solenoid magnets capable of fields approaching 100 kgauss, such as are desired as laboratory facilities and for containing plasmas for nuclear fusion reactions.[1,2]

The highest values of critical magnetic fields previously reported for high current densities

have been less than 18 kgauss.[3,4] However, values as large as 30 kgauss have been reported[5] for low current densities.

The discovery of the existence of Nb_3Sn with its high critical temperature of 18.0°K by Matthias, Geballe, Geller, and Corenzwit[6] immediately suggested that the critical field might be high. The existence of superconductivity in Nb_3Sn at high fields is also indicated by the recent susceptibility observations of Bozorth, Williams, and Davis.[7]

Nb_3Sn is very brittle and is thus not readily fabricated into specified configurations. However, a method of minimizing this difficulty was developed during the current investigation. Two distinctly different types of samples were studied. The first type consisted of rectangular rods cut from an ingot which was prepared by first sintering a stoichiometric mixture of Sn and Nb powders at 1800°C and then melting the compact in a zirconia crucible in an argon atmosphere at about 2400°C. X-ray diffraction data confirmed the existence of essentially a single homogeneous phase of the β-wolfram structure. The rods were about 2 cm long and had thicknesses varying from 0.025 cm to 0.063 cm. The second type consisted of small niobium tubes which contained thin cores of Nb_3Sn. These were prepared by packing 0.6 cm o.d.−0.3 cm i.d. niobium tubes with either a mechanical mixture of powdered Nb_3Sn + a 10 weight percent excess of powdered Sn or similar mixtures of unreacted Sn and Nb powders. The ends of the tubes were closed with Nb plugs and the sealed tubes were mechanically reduced in size to 0.038 cm o.d. Each tubular sample was heated to a prescribed temperature between 970°C and 1400°C for a predetermined period of time, as long as 24 hours.

Current and potential leads were attached to each of the samples using an ultrasonic soldering iron and indium solder. The potential leads were about 1 cm apart. The samples were mounted transverse to the axis of a solenoid magnet capable of a maximum steady-state field of 88 kgauss. Observations were made by selecting a fixed value for the magnetic field and slowly increasing the current through the sample until a potential drop across the sample of a few hundredths of one microvolt was observed. The results for three sizes of parallelepiped samples cut from the Nb_3Sn ingot are shown in Fig. 1.

In addition to the high magnetic fields and current densities for which superconductivity exists in Nb_3Sn, there are two other interesting features of the data of Fig. 1. First, the average current density does not scale as the perimeter of the cross-sectional area as is expected for a "soft" superconductor, nor as the cross-sectional area as is observed for "hard" superconductors, such as mechanically deformed Mo_3Re,[4] but is about midway between the two types of behavior. This variation with sample size suggests that appreciable current is being carried both by the surface and by "filaments." Secondly, the variation of the maximum permissible applied magnetic field with temperature, at constant current, is far from parabolic. Although T_c is about 18°K for Nb_3Sn,[6] the magnetic field increases more than 50% between 4.2°K and 1.5°K. We have not been able to account for these observations in terms of existing theory.

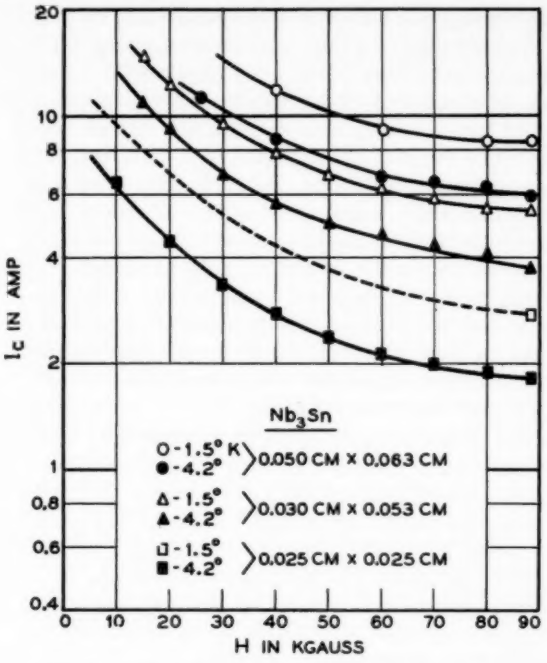

FIG. 1. Critical current vs applied magnetic field for three sample sizes at 1.5°K and 4.2°K. The magnetic field was perpendicular to the current direction. Each experimental point represents the maximum current, at the value of magnetic field indicated, for which no voltage drop along the sample was observed, the smallest detectable voltage being a few hundreths of one microvolt.

Critical current vs applied magnetic field curves for several characteristic samples of "Nb_3Sn" cores clad with Nb are shown in Fig. 2. It is of considerable interest that all of the curves

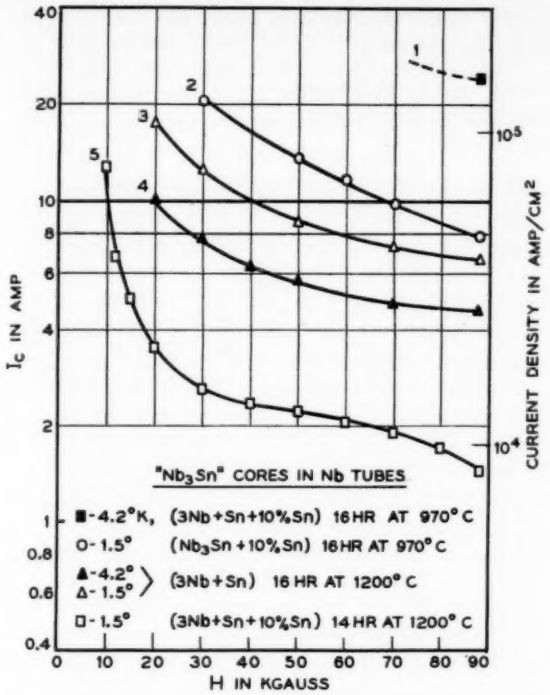

FIG. 2. Critical current vs applied magnetic field for Nb-clad cores of "Nb_3Sn." The o.d. of the cores was about 0.015 cm and the o.d. of the Nb jackets was about 0.038 cm. "+ 10% Sn" in the table legend means 10 wt. % more Sn than is required to form Nb_3Sn assuming no reaction with the Nb tube. The magnetic field was perpendicular to the current direction. Each experimental point represents the maximum current, at the value of magnetic field indicated, for which no voltage drop along the sample was observed, the smallest detectable voltage being a few hundreths of one microvolt.

represent significantly higher average current densities at the highest fields than the samples cut from the Nb_3Sn ingot. The single point shown on Curve 1 in Fig. 2 represents an average current density nearly 50 times higher than the data of Fig. 1. The average current density of this "Nb_3Sn" core exceeds 100 000 amperes/cm². The Nb tubes do not contribute since it is found that annealed niobium becomes normal in fields well below 20 kgauss. A comparison of Curve 3 of Fig. 2 with Curve 5 suggests that a stoichiometric mixture of Nb and Sn powders is preferable to an excess of Sn. A comparison of these curves with Curves 1 and 2 indicates that it is preferable to start with the elemental powders, with or without an excess of Sn, rather than with powdered Nb_3Sn + excess Sn powder. Also, the curves of Fig. 2 and similar data for heat treatment at temperatures as high as 1400°C show that a lower temperature of heat treatment consistently yields material capable of higher critical current density. This rapid trend with temperature suggests that still higher current densities might be obtained at still lower reaction temperatures.

The data of Fig 2 and data from related samples suggest that the difference in properties between pure dense Nb_3Sn and the Nb-clad samples is not principally one of chemistry but rather is in some manner associated with the physical state of the "Nb_3Sn" in the core. However, the critical temperature of the fused dense Nb_3Sn was found to be 17.8°K (when extrapolated to the limit of zero current through the sample) while that of the clad sample having the highest critical current density (Curve 1 of Fig. 2) was found to be 17.9°K. Although the pertinent physics of the situation is not yet clear, it is tentatively concluded that the conditions of preparation of the clad samples are such as to lead to a structure containing large numbers of "filaments." It is fortunate that these conditions are compatible with those which are expected to permit fabrication of the material into high-field superconducting electromagnets.

We are indebted to B. T. Matthias for encouraging the investigation of Nb_3Sn for high-field studies. Encouragement and stimulation from R. Kompfner and M. Tanenbaum contributed significantly to this work as did assistance from H. Dail and C. V. Wahl.

[1]S. H. Autler, Bull. Am. Phys. Soc. 5, 367 (1960).
[2]D. J. Rose, Bull. Am. Phys. Soc. 5, 367 (1960).
[3]S. H. Autler, Rev. Sci. Instr. 31, 369 (1960).
[4]J. E. Kunzler, E. Buehler, F. S. L. Hsu, B. T. Matthias, and C. V. Wahl, J. Appl. Phys. (to be published).
[5]J. C. McLennan, J. F. Allen, and J. O. Wilhelm, Trans. Roy. Soc. Can. 24, 25 (1930); 24, 53 (1930).
[6]B. T. Matthias, T. H. Geballe, S. Geller, and E. Corenzwit, Phys. Rev. 95, 1435 (1954).
[7]R. M. Bozorth, A. J. Williams, and D. D. Davis, Phys. Rev. Letters 5, 148 (1960).

SUPERCONDUCTORS AS QUANTUM DETECTORS FOR MICROWAVE AND SUB-MILLIMETER-WAVE RADIATION*

E. Burstein, D. N. Langenberg, and B. N. Taylor
University of Pennsylvania, Philadelphia, Pennsylvania
(Received January 6, 1961)

Giaever[1] and Nicol, Shapiro, and Smith[2] have reported experiments on electron tunneling through metal oxide barriers between a metal and a superconductor, $M|B|S$, and between two superconductors, $S_1|B|S_2$. The tunneling process which involves "unpaired" charge carriers can be simply described in terms of a quasi-particle energy band picture in which the superconductor is represented, at temperatures below its transition temperature, as an intrinsic semiconductor with a temperature-dependent energy gap, $E_G = 2\epsilon_0$, and equal effective masses for electrons and holes [Fig. 1(a)].

For small bias voltages, V_b, such that $|eV_b|$ is less than $E_G/2$ in the case of $M|B|S$ and less than $(E_{G_1} + E_{G_2})/2$ in the case of $S_1|B|S_2$, the tunneling current depends on the density of thermally excited carriers. For larger bias voltages, the tunneling current is essentially independent of the density of thermally excited carriers and results in the "injection" of electrons and holes into the conduction and filled bands of the superconductor. The concept of "photo-injection" of carriers by optical excitation across the energy gap of the superconductor follows quite naturally. These considerations suggest the use of "low-voltage" tunneling in $M|B|S$ and $S|B|S$ structures for the quantum detection of microwave and sub-millimeter-wave radiation in a manner which is analogous to the detection of visible and near infrared radiation by p-n junctions in semiconductors [Fig. 1(b)]. Such superconductor photodetectors would have long-wavelength limits, λ_{max}, determined by the energy gap of the superconductor used. Thus, for aluminum $\lambda_{max} = 3.9$ mm corresponding to $E_G = 3.2\times10^{-4}$ ev, and for lead $\lambda_{max} = 0.46$ mm corresponding to $E_G = 2.7\times10^{-3}$ ev.[1,2]

The magnitude of the tunneling current due to optically excited carriers will depend, among other things, on the lifetime of the carriers. The processes which limit the lifetime include (a) the recombination of electrons and holes across the gap, (b) the pairing of electrons in the conduc-

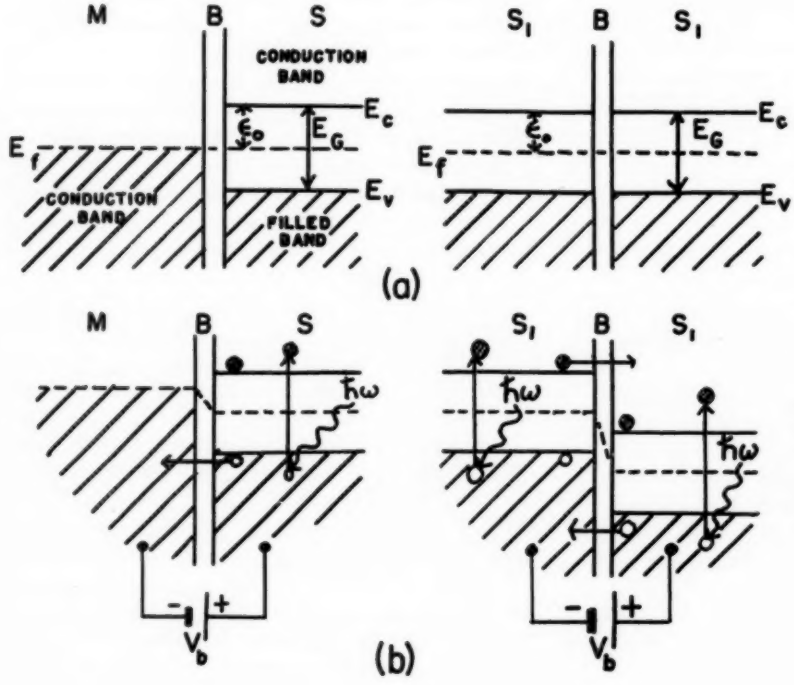

FIG. 1. (a) Quasi-particle energy band diagrams for an $M|B|S$ structure and an $S_1|B|S_2$ structure in which the two superconductors are the same. (b) Tunnelling of optically excited carriers in $M|B|S$ and $S_1|B|S_1$ structures under "low bias voltage" conditions.

tion band and the corresponding pairing of holes in the filled band, and (c) in the case of $M|B|S$ structures, the simultaneous tunneling of electrons and holes into the metal from the superconductor and their subsequent transition to the Fermi surface of the metal. At the present time, estimates for the lifetimes for these processes which may be radiative or nonradiative are not available. We have carried out an estimate of the electron-hole radiative recombination lifetime, τ_{opt}, for lead at 2°K using the theory of van Roosbroeck and Shockley[3] (Fig. 2). The dependence on frequency of $\eta^2\kappa$, where $\eta+i\kappa$ is the complex refractive index, was derived from theoretical expressions for $\sigma_1+i\sigma_2$, the complex conductivity, obtained by Mattis and Bardeen,[4] while the density of thermally generated carriers, n_i, was calculated from the quasi-particle density of states of superconductors given by the Bardeen, Cooper, and Schrieffer theory[5] and a value of $N(0)=2.2\times10^{22}/\text{cm}^3$ which Gold[6] proposed for the density of states at the Fermi surface of lead in the normal state. The theoretical values of σ_1 and σ_2 are in reasonable agreement with the experimentally determined values obtained by Glover and Tinkham[7] and Ginsberg and Tinkham[8] but do not show any of the structure near the

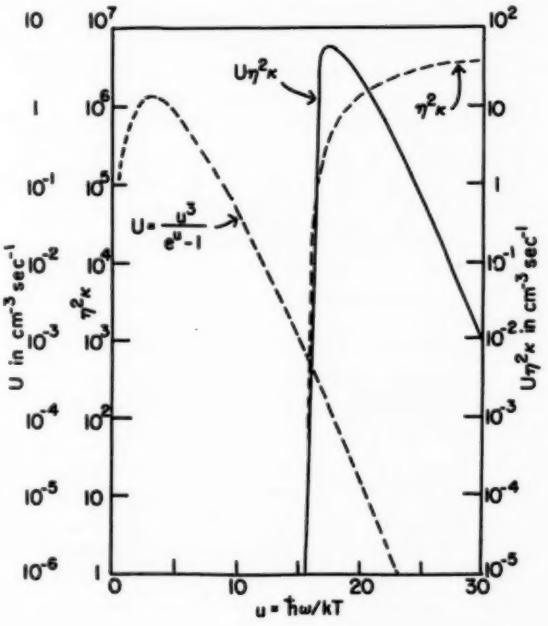

FIG. 2. The dependence of $\eta^2\kappa$ and of $U\eta^2\kappa$, which is proportional to the radiative recombination rate per unit frequency interval, on $u=\hbar\omega/kT$ for lead at 2°K.

band gap which is present in the experimental spectrum. We obtain $n_i=5.5\times10^{15}/\text{cm}^3$ and $\tau_{opt}=0.4$ sec. It is, therefore, very unlikely that the radiative recombination of electrons and holes is the dominant process which determines the lifetime. Measurements of the tunneling current due to optically and electrically injected carriers should provide an effective means for obtaining information about the lifetime, and, in appropriate configurations, about the diffusion length of the unpaired carriers in superconductors.

B. Rosenblum of RCA Laboratories has pointed out that photoexcited carriers in the metal of the $M|B|S$ structure may also contribute to the tunneling current. This would extend the photoresponse to longer wavelengths with λ_{max} controlled by the bias voltage. The magnitude of the photoresponse of the metal would be expected to be much smaller than that of the superconductor since the lifetime of the excited carriers in the metal is very much shorter than the corresponding lifetime in the superconductor.

The metal and superconductor films used in the superconductor photodetectors must be much smaller than the wavelength of the radiation in the films in order to decrease the reflection and, thereby, to increase the absorption of the incident radiation by the superconductor. An $S_1|B|S_2$ structure is an ideal configuration for such detectors. On the one hand, it avoids the annihilation of electrons and holes by simultaneous tunneling of electrons and holes from the superconductor into the metal which can occur in $M|B|S$ structures, and on the other hand it allows an optimum absorption of the incident radiation by the superconductor layers. The absorption of radiation by an $S_1|B|S_1$ structure can be calculated by considering the composite structure as a single superconductor film. Curves of the absorptivity, A, and of $A/(\hbar\omega/E_G)$ which is proportional to the number of photons absorbed per unit intensity of incident radiation, are plotted as a function of $\hbar\omega/E_G$ in Fig. 3 for lead films having thicknesses of 5, 15, and 150 angstroms. We see that the absorptivity of the 15-angstrom film approaches the maximum value of 0.5 at $\hbar\omega/E_G\approx2.5$. However, the 150-angstrom film still exhibits an appreciable absorptivity, having a value of 0.15 at $\hbar\omega/E_G\approx3$. The photoresponse of the $S_1|B|S_1$ structure may be expected to differ somewhat from the photon absorption spectrum as a result of two effects: (a) a dependence of the lifetime of the excited carriers on energy,

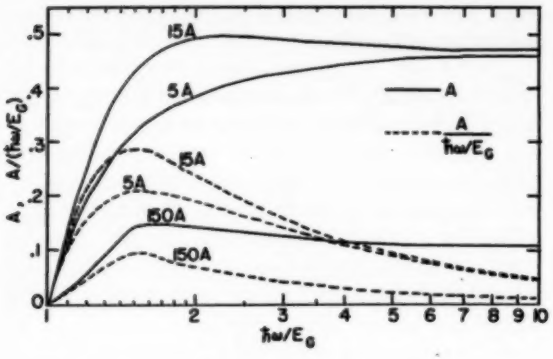

FIG. 3. Absorptivity and photon absorption spectra for superconducting lead films of 5, 15, and 150-angstrom thicknesses.

and (b) an increase in quantum efficiency for high-energy photons due to secondary impact ionization processes, as has been observed in the case of photoconductors.[9] The latter effect would increase the photoresponse at the higher frequencies and, thereby, would compensate for the decrease in photoresponse resulting from the decrease in the number of photons absorbed per unit intensity of radiation with increase in frequency. However, the photoresponse may also be expected to exhibit a sharp drop-off at frequencies greater than the "collision" frequency of the carriers (not shown in Fig. 3) where σ_1 exhibits a $1/\omega^2$ dependence.

Operating conditions for the superconductor photodetector are straightforward. The superconductor should be maintained at a temperature well below its transition temperature in order to diminish the thermal generation of carriers. Under these conditions ($kT \ll E_G$) the thermally excited carriers obey Maxwell-Boltzmann statistics and the equilibrium density of excited carriers is, to a good approximation, given by $n_i = N(0)(\pi E_G kT)^{1/2} \exp(-E_G/2kT)/2$ which has the same temperature dependence as a one-dimensional intrinsic semiconductor. For optimum response the temperature is lowered to a point where the rate of optical generation of carriers by background radiation is greater than the rate of thermal generation.[10] Under these conditions the fractional change in carrier density produced by a small radiation signal is given by $\Delta n/n_i = G_S/G_b$, where G_S is the rate of generation by the radiation signal and G_b is the rate of generation by the background radiation accompanying the radiation signal. The frequency response of the photodetector should be limited only by the lifetime of the excited carriers. It should also be noted that the photodetector can be operated with bias voltages of either polarity, as contrasted to the semiconductor photodiode.

It is a pleasure to acknowledge the valuable discussions we have had with R. Amado, M. Cohen, R. Parmenter, A. Rose, B. Rosenblum, A. Rothwarf, P. Stiles, and R. deZafra. This research was supported in part by the U. S. Atomic Energy Commission.

---

*Contribution from the Laboratory for Research on the Structure of Matter.

[1]I. Giaever, Phys. Rev. Letters 5, 147 (1960); 5, 464 (1960).

[2]J. Nicol, S. Shapiro, and P. H. Smith, Phys. Rev. Letters 5, 461 (1960).

[3]W. van Roosbroeck and W. Shockley, Phys. Rev. 94, 1558 (1954).

[4]D. C. Mattis and J. Bardeen, Phys. Rev. 111, 412 (1958).

[5]J. Bardeen, L. N. Cooper, and J. R. Schrieffer, Phys. Rev. 108, 1175 (1957).

[6]A. V. Gold, Phil. Mag. 5, 70 (1960).

[7]R. E. Glover and M. Tinkham, Phys. Rev. 108, 243 (1957).

[8]D. M. Ginsberg and M. Tinkham, Phys. Rev. 118, 990 (1960).

[9]V. S. Vavilov, J. Phys. Chem. Solids 8, 223 (1959).

[10]E. Burstein, G. Picus, and N. Sclar, Photoconductivity Conference (John Wiley & Sons, Inc., New York, 1956), p. 353.

STIMULATED OPTICAL EMISSION FROM EXCHANGE-COUPLED IONS OF Cr^{+++} IN Al_2O_3

Irwin Wieder and Lynn R. Sarles
Varian Associates, Palo Alto, California
(Received December 19, 1960)

The advantages of chromium ions in aluminum oxide crystals (ruby) for double resonance experiments have been pointed out[1,2] and utilized in several microwave-optical experiments.[3-5] Recently, stimulated emission[6] and coherence[7] of the characteristic "R_1" fluorescence at 6943 A has been observed in pink ruby (~0.07% Cr^{+++} by weight). We wish to report the observation of stimulated emission at wavelengths 7010 A and 7040 A from transitions in red ruby (~0.7% Cr^{+++} by weight) which arise[8] from exchange coupling between neighboring chromium ions.

The observations were made by monitoring the fluorescence of a $\frac{1}{6}$-in.$\times 1\frac{1}{2}$-in. red crystal rod following an intense excitation flash. By virtue of the broad optical absorption bands and the efficient radiationless transfer to sharp excited states, these levels accumulate an excess population which may satisfy the requirements[9] for stimulated optical emission. At high excitation energy the fluorescence at 7010 A and 7040 A exhibits the initial decrease from the natural radiative lifetime which is characteristic of stimulated emission. However, the decay curves show significant differences from the previous results with the R_1 line. Figure 1 is a comparison of the R_1 line in pink ruby, the 7010A line in red ruby, and the R_1 line in red ruby, all under similar conditions of excitation at 77°K. The decay curves at low excitation are all similar in appearance to Fig. 1(c), and in two cases the shapes change progressively with increasing excitation until they reach the curves shown in Fig. 1(a) and Fig. 1(b). A plot of the areas under the fluorescence curves of R_1 and 7010 A as a function of flash energy is shown in Fig. 2.

Our interpretation of the data is as follows: It is apparent that the R_1 line in red ruby does not exhibit stimulated emission. This follows from the fact that the absorbed flash energy is not sufficient to overcome the ground-state population, and is corroborated by the approximately linear relationship between R_1 and flash energy in Fig. 2. (The increased linewidth in red ruby would not change conditions enough to prevent stimulated emission from occurring.) The behavior of the 7010A line (and 7040A line) is a little more complicated. The fact that it exhibits enhanced emission while the R_1 line in this sample does not is a result of the relatively unpopulated terminal state for the 7010A transition (negligible optical absorption for this wavelength at 77°K). Since the number of atoms radiating 7010A light saturates at intermediate energy (Fig. 2), it appears that the total number of equivalent ion pairs which have this line in their spectrum is excited at this energy. This number

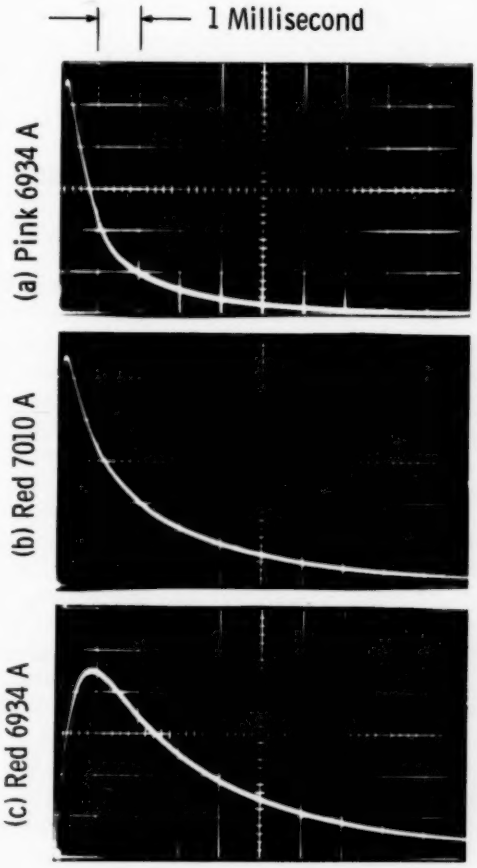

FIG. 1. Fluorescence decay curves of pink and red ruby taken at 77°K under approximately the same high excitation conditions.

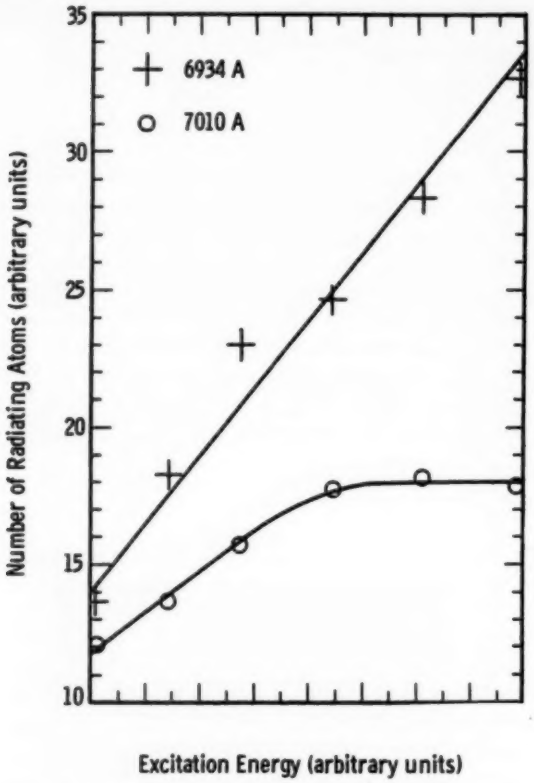

FIG. 2. A plot of area under fluorescence decay curves for R_1 and 7010 A in the same red ruby at 77°K as a function of excitation flash energy.

is not sufficiently greater than the threshold number needed for stimulated emission to exhibit the degree of lifetime shortening observed in pink ruby [compare Fig. 1(a) and Fig. 1(b)].

These experimental results also yield information on the excitation processes of the coupled ions. Since more than half of the single ions are in the ground state even at high excitation, direct excitation via the broad absorption bands is not likely for those ion pairs near the center of the rod. On the other hand, thermal transfer of excitation between single ions and paired ions is ruled out by the saturation behavior of the 7010A line. One possibility which seems promising is radiative excitation by trapped 6934A light. As a preliminary check we have observed absorption lines in the red sample which overlap the 6934A line and have also observed the 7010A fluorescence when the red rod is excited by a pulse of 6934A light from a pink sample. Further experiments to clarify the nature of the excitation processes of exchange-coupled ions are in progress.

[1]I. Wieder, Proceedings Ann Arbor Conference on Optical Pumping, June, 1959 (unpublished).
[2]A. L. Schawlow, Proceedings of the Quantum Electronics Conference, Shawanga, New York, September, 1959 [Quantum Electronics, edited by C. H. Townes (Columbia University Press, New York, 1960)].
[3]I. Wieder, Phys. Rev. Letters 3, 468 (1959).
[4]S. Geschwind, R. J. Collins, and A. L. Schawlow, Phys. Rev. Letters 3, 545 (1959).
[5]T. H. Maiman, Phys. Rev. Letters 4, 564 (1960).
[6]T. H. Maiman, Nature 187, 493 (1960); British Communications and Electronics 7, 674 (1960).
[7]R. J. Collins et al., Phys. Rev. Letters 5, 303 (1960).
[8]A. L. Schawlow, D. L. Wood, and A. M. Clogston, Phys. Rev. Letters 3, 271 (1959).
[9]A. L. Schawlow and C. H. Townes, Phys. Rev. 112, 1940 (1958).

SIMULTANEOUS OPTICAL MASER ACTION IN TWO RUBY SATELLITE LINES

A. L. Schawlow and G. E. Devlin
Bell Telephone Laboratories, Murray Hill, New Jersey
(Received December 19, 1960)

We have obtained pulsed maser oscillations simultaneously at wavelengths of 7009 A and 7041 A in concentrated ruby. The lines involved are two of the strongest of the satellite or neighbor lines,[1] which have been known and studied for many years but are not yet fully analyzed.[2-5] It is known[5] that these lines disappear at low concentrations, but appear strongly in emission at chromium concentrations of the order of 0.5%. In absorption, they are weak and disappear entirely at low temperatures.

Since these lines terminate on states which are far enough above the ground states to be empty at low temperatures and since their upper states can be populated easily by white light illumination, it was proposed that the strongest of them be used for an optical maser.[6] A very low estimate of the fluorescence efficiency (0.1%) was used, but with the advantage of an empty lower state, pulsed operation seemed possible at low

temperatures. Now that the fluorescence efficiency for the main R lines is known to be nearly unity,[7] it is apparent that much less pumping light is needed. Moreover, recent investigations of the 7009A line in absorption have shown that its lower state is about 100 cm^{-1} above the ground state. Thus liquid hydrogen or neon temperatures would be sufficiently low to depopulate this lower state.

However, operation should also be possible at higher temperatures. This is expected because even at 77°K the line is so strong in emission, but so weak in absorption. It seems possible that the very numerous individual chromium ions absorb the pumping radiation and transmit it to the much rarer paired ions which emit the N lines.[6] Thus even if we have to invert the population of the N-line levels by pumping to empty the lower level, this can be accomplished with only enough pumping light to excite a small fraction of the isolated ions.

Maser operation was sought first in a ruby rod containing about 0.5% Cr_2O_3, having a diameter of 2 mm and a length of 4 cm. The ends of the rod were silvered, one of them completely, and the other to a transmission of about 1%. The rod was immersed in liquid nitrogen in a small clear Dewar flask, with its upper end supported in a cone which allowed emergence only of light coming through the silver film. Pumping radiation was supplied by a General Electric $FT524$ xenon flash tube. When a 400-microfarad capacitor bank was charged to 3500 volts and discharged through the flash tube, the relative intensity of the 7041A line was greatly enhanced over the other lines in the spectrum. At about 3700 volts it was joined by the 7009A line. Figure 1 shows these two lines photographed in a single flash at about 3900 volts. For comparison, part of the spectrograph slit was covered by a concentrated ruby at room temperature. When the latter was illuminated by a microscope lamp, it gave a comparison spectrum similar to that of the ruby below the maser threshold except for a small wavelength shift of all lines.

The observation of enhancement thresholds is a strong indication of maser action.[8] Further confirmation was obtained by observation of parallelism in the output radiation, as shown by a sharply defined spot on a distant surface. The beam width, well above the pumping threshold energy, was about 1 degree. This approximate parallelism implies considerable spatial coherence in the output.[9]

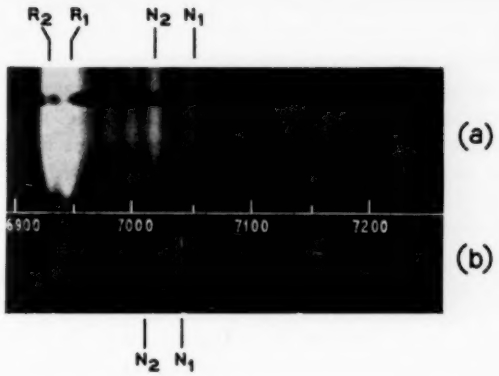

FIG. 1. (a) Spectrum of a concentrated ruby at room temperature with a 10-second exposure. (b) Spectrum of a ruby rod at 77°K showing N-line maser oscillations as described in the text, with a single flash lasting about 1/2000 second. All lines are shifted slightly because of the temperature difference between (a) and (b). The wavelength scale is in angstroms.

It may seem surprising that optical maser action occurs at two frequencies simultaneously. If the upper levels of the two lines are identical, or relax rapidly to each other, as with the $\bar{E}$ and $2\bar{A}$ levels of the isolated Cr^{3+} ions, this will not happen. In such a case, when maser action starts to empty one of the levels rapidly, it prevents the additional buildup of population needed for maser action from the other level. However, it had already been suspected that the 7041A line has an origin not closely connected with the 7009A and other neighbor lines. The evidence for this different origin is that the relative intensity of the two lines varies erratically from sample to sample. The intensity of the 7009A line varies with concentration in much the same way as most of its neighbors, whereas the 7041A line is usually weaker, but occasionally brighter than the 7009A line.[10] Occurrence of simultaneous maser action is confirmation of their separate origin.

The pumping power needed for this sample is no less than that required for R_1-line maser action in dilute ruby.[8,9] There are many ways in which the power required can be reduced. Of these, the simplest is to cool it further, and this is being studied. Preliminary attempts produced too much heat in the sample, so that its temperature rose far above that of the bath. Indeed, heating may have increased the threshold

power even when the sample was in liquid nitrogen. It is believed that more careful filtering of the light source to remove all but the useful pumping radiation will permit low-temperature operation at greatly reduced pump power.

It has thus been shown that optical maser operation at the wavelength of the 7009A line (N_2) does occur in concentrated ruby as predicted.[6] Moreover, simultaneous maser oscillations at 7041 A (N_1) show that these two lines are not closely related, and probably come from different kinds of chromium ion pairs.

We wish to thank W. L. Bond for polishing the ruby rod, D. F. Nelson for lending us the flash tube mount and power supply, and E. M. Kelly for silvering the ends of the rod. We are also indebted to W. S. Boyle for pointing out the importance of sample heating by the flash, and to A. M. Clogston and D. L. Wood for helpful discussions on the origin and properties of the satellite lines.

[1]Deutschbein labelled these lines N_1 and N_2, where N stands for Nebenlinien. This usage has advantages now that the word "satellite" is used so often in its astronomical sense – even in connection with masers.

[2]C. E. Mendenhall and R. W. Wood, Phil. Mag. 30, 316 (1915).

[3]O. Deutschbein, Ann. Physik 14, 712 (1932); 14, 729 (1932); 20, 828 (1932).

[4]S. F. Jacobs, thesis, John Hopkins University, Baltimore, 1956 (unpublished).

[5]A. L. Schawlow, D. L. Wood, and A. M. Clogston, Phys. Rev. Letters 3, 271 (1959).

[6]A. L. Schawlow, talk at Quantum Electronics Conference, Shawanga, New York, September 16, 1959 [Quantum Electronics, edited by C. H. Townes (Columbia University Press, New York, 1960)].

[7]T. H. Maiman, Phys. Rev. Letters 4, 564 (1960).

[8]T. H. Maiman, Nature 187, 493 (1960); British Communications and Electronics, 7, 674 (1960).

[9]R. J. Collins, D. F. Nelson, A. L. Schawlow, W. Bond, C. G. B. Garrett, and W. Kaiser, Phys. Rev. Letters 5, 303 (1960).

[10]D. L. Wood and R. A. Ford (private communications).

INTERPRETATION OF THE Fe^{57} ISOMER SHIFT

L. R. Walker, G. K. Wertheim, and V. Jaccarino
Bell Telephone Laboratories, Murray Hill, New Jersey
(Received January 3, 1961)

We have made a systematic study of the Mössbauer effect[1] of Fe^{57} in di- and tri-valent iron compounds and in d-group metals. The observed "isomer shift"[2] measures the total s-electron density at the nucleus. The shift in compounds is shown to depend mainly upon the $3d$ configuration of iron involved and to a lesser extent upon the "chemical" bond. The Hartree-Fock calculations of Watson[3] on the various $3d$ configurations of iron are combined with the data on the shifts in the most ionic compounds to obtain a calibration of the shift in terms of s-electron density. This enables us to estimate the difference in charge radius of the ground state and isomeric state of Fe^{57}. We associate the shift of an Fe solute ion in a d-group metal with the addition of some fraction of a $4s$ electron to an Fe $3d^7$ configuration; an estimate of the $4s$-electron wave function density at the nucleus from the Fermi-Segrè-Goudsmit (FSG) formula[4] enables this fraction to be determined.

Kistner and Sunyar[5] first observed in the recoil-free emission and resonant absorption of the 14.4-kev nuclear gamma ray of Fe^{57}, that the energies of the emitted and absorbed gamma rays were noticeably different if the emitter and absorber were two dissimilar lattices containing iron. The origin of this effect is as follows.

The ground and isomeric levels of the nucleus have different effective charge radii; the electrostatic interaction with the electronic charge is then different in the two states and the gamma-ray energy is consequently changed (relative to its value for a point nucleus) by an amount proportional to the s-electron density at the nucleus. If the s-electron density is different for the absorber and emitter, the difference in gamma-ray energies, $E_a - E_e$, is defined as the isomer shift.

$$E_a - E_e = \tfrac{2}{3}\pi Ze^2[R_{is}^2 - R_{gr}^2][|\psi(0)_a|^2 - |\psi(0)_e|^2], \quad (1)$$

where R_{is} and R_{gr} are the radii of the isomeric and ground states and $|\psi(0)_a|^2$ and $|\psi(0)_e|^2$ are the total s-electron densities at the nucleus for absorber and emitter, respectively.[6] It is to be noted that the sign of the shift has its origin in the fact that the level energy is lower the more

compact the charge distribution.

An examination of the restricted Hartree-Fock calculations of Watson[3] shows that there are significant differences in the value of $|\psi_{3S}(0)|^2$ for different $3d$ configurations of iron; the change in $|\psi_{1S}(0)|^2$ and $|\psi_{2S}(0)|^2$ is substantially smaller.

It is perhaps worthwhile to point out that unrestricted Hartree-Fock calculations, which exhibit the imbalance of up and down spin density (exchange polarization effect), appear to give the same total density at the nucleus as the restricted procedure.[7] The variation of $|\psi_{3S}(0)|^2$ is such as to correspond to different degrees of shielding of $3s$ by $3d$ electrons. To calibrate the observed shifts in terms of total s-electron density, we associate the difference in the shifts for the most ionic Fe^{2+} and Fe^{3+} compounds with the difference in Watson's values of $\sum_{n=1}^{3}|\psi_{nS}(0)|^2$ for $3d^6$ and $3d^5$ configurations. When an Fe atom is introduced into a d-group host metal, $\sum_n|\psi_{nS}(0)|^2$ will also contain a contribution from $4s$ conduction electrons. Hartree-Fock calculations do not exist for single $4s$ electrons outside $3d^n$ configurations, but the FSG[4] formula, combined with the known term value of $3d^n4s$ configurations,[8] provides an entirely adequate estimate of $|\psi_{4S}(0)|^2$.

In Fig. 1 is shown a possible interpretation of the observed shifts making use of the above ideas. The total s-electron density in atomic units is plotted as ordinate. Watson's values for $2\sum_{n=1}^{3}|\psi_{nS}(0)|^2$ for the Fe $3d^n$ configurations from $n=4$ to $n=8$ are indicated on the left. The scale on the right for Mössbauer center-of-gravity shifts relative to stainless steel is established by identifying the shifts in the most ionic Fe^{2+} and Fe^{3+} with Watson's densities for $3d^6$ and $3d^5$, respectively. The solid straight lines represent s-electron densities for hypothetical $3d^n4s^x$ configurations. They are drawn on the assumption that the density for such a configuration is of the form $|\psi(3d^n)|^2+x|\psi_{4S}(0)|^2$, where $|\psi_{4S}(0)|^2$ is calculated from the FSG formula for a single $4s$ electron outside the $3d^n$ configuration. This assumes no screening of inner s electrons by the single $4s$ electron.[9] Curves for the configurations $3d^{8-x}4s^x$ and $3d^{7-x}4s^x$ are indicated by dashed lines and were obtained by extrapolation and interpolation of the FSG formula. The experimental data are given in Table I.

The shifts for Fe in various metals have been represented as horizontal lines of a length sufficient to cover what appear to be the most plausible configurations. Since for Fe in Fe metal there are certainly 8 electrons to be accounted

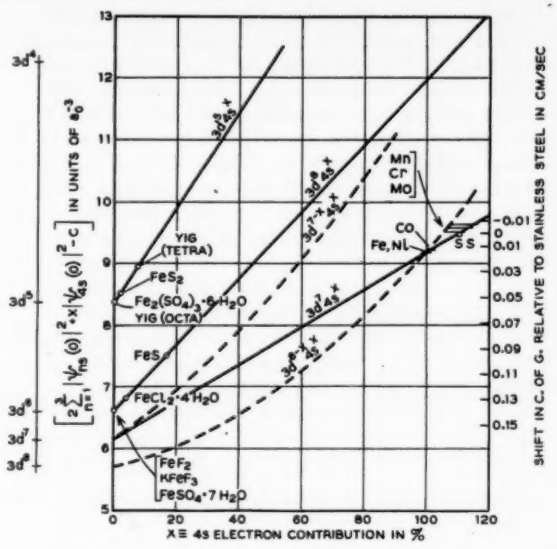

FIG. 1. A possible interpretation of the Fe^{57} Mössbauer isomer shifts in various solids. The total s-electron density is plotted as a function of the percentage of $4s$ character for various d-electron configurations. The reasons for placing the experimental data on given theoretical curves are discussed in the text. The constant $C=11\,873\ a_0^{-3}$.

for, the evidence seems to point clearly to the configuration $3d^74s$ for this case. The smallness of the spread in shifts between the different metals indicates strongly that the configuration of the solute Fe is substantially the same in the metals investigated. For the Fe^{2+} and Fe^{3+} compounds, the experimental data are entered upon the $3d^64s^x$ and $3d^54s^x$ curves, respectively. This is consistent with the idea that in these covalent compounds the $4s$ atomic orbitals are partially occupied by electrons from the ligand ions (bonding orbitals).[10,11] The data for the "ferro" and "ferri" cyanides of potassium have not been plotted since it is not clear how to fit them into the above scheme. Indeed, since they have ground states which do not follow Hund's rule, it is unlikely that Watson's calculations are applicable to them. The fact that the isomer shifts in both cyanides are very small relative to each other and to stainless steel appears to be fortuitous.

From the observed isomer shift and the calculated difference in $|\psi(0)|^2$ for the d^5 and d^6 free-ion configurations we may compute the difference of the excited and ground-state charge

Table I. Observed shifts in gamma-ray energy in various iron compounds and d-group metals measured relative to type 310 stainless steel. (Source and absorber at room temperature.) The measured shifts contain contributions from the second-order Doppler shift and the zero-point energy shift in addition to the isomer shift discussed here. Measurements at 77°K[a] indicate that the second-order Doppler shift contributions are small compared to the total shift. Moreover, since the Doppler shifts are likely to be of similar magnitudes in the compounds considered, they will cancel, since we are ultimately concerned only with differences in the shifts between similar materials. The same is true of the zero-point energy shift. The uncertainty in comparing metals with salts is considerably greater. To convert the shifts from cm/sec to Mc/sec, one should multiply the values by 116. The errors indicated reflect the uncertainty in the last significant figure.

		Shift (cm/sec)
$3d^6$	FeF_2 (single crystal)	0.140 ±5
$3d^6$	$KFeF_3$	0.139 ±5
$3d^6$	$FeSO_4 \cdot 7H_2O$	0.140 ±5
$3d^6$	$FeCl_2 \cdot 4H_2O$	0.130 ±5
$3d^6$	FeS	~0.11 ±1
$3d^5$	$Fe_2(SO_4)_3 \cdot 6H_2O$	0.052 ±5
$3d^5$	Fe_2O_3[b]	0.047 ±5
$3d^5$	Yttrium-iron garnet, octahedral	0.057 ±5
$3d^5$	Yttrium-iron garnet, tetrahedral	0.026 ±5
	FeS_2 (pyrites)[c]	0.048 ±5
	FeS_2 (marcasite)	0.048 ±5
Metals	Fe[b]	0.015 ±5
	Co	0.012 ±5
	Ni	0.015 ±5
	Mn	-0.008 ±2
	Cr	-0.005 ±2
	Mo	-0.001 ±2
Cyanides	$K_4Fe(CN)_6 \cdot 3H_2O$	0.0083 ±10
	$K_3Fe(CN)_6$	0.0000 ±10

[a]R. L. Ingalls, G. Lang, and S. DeBenedetti, Bull. Am. Phys. Soc. 5, 429 (1960).
[b]See reference 5.
[c]See reference 6.

radii using Eq. (1), assuming the usual charge radius dependence on mass number, i.e., $R = 1.20A^{1/3} \times 10^{-13}$ cm. We obtain $\delta R/R = 1.8 \times 10^{-3}$ as the fractional change in the charge radius, with the effective radius of the ground state larger than that of the excited state. This result is not unexpected[12] in sign and magnitude. The shell model predicts that the ground state for 3 odd neutrons outside a closed shell (28 neutrons), corresponding to a hole in the $2p_{3/2}$ shell, is one for which $I = 3/2$, as is the case for the 14-kev excited state. The large spin-orbit coupling precludes the possibility of a $2p_{1/2}$ configuration being the ground state.

Using the radial moments for an isotropic square well[13] and even assuming a proton excitation corresponding to $\Delta l = 3$ or 4, one still obtains a value of only 2×10^{-3} for $\delta R/R$. (The more likely case of a neutron excitation would leave the charge radius unchanged in a first approximation.) It is most unlikely therefore that the ground state is a simple shell state. It is interesting to note that the charge radius change expected for the addition of one particle (isotope shift at $A = 57$) is $\delta R/R \equiv \frac{1}{3}(\delta A/A) = 5.9 \times 10^{-3}$.

In the isomeric transition of Hg^{197} ($I_{gr} = 1/2 \rightarrow I_{ex} = 13/2$), it was estimated[2] that the charge redistribution corresponded to an increase of one-fourth to one-fifth of that observed experimentally for the addition of one neutron at $A = 157$. (The excited state has the larger charge distribution in this case.) Since both states are identifiable as single-particle neutron states, it is clear that a general charge redistribution accompanies the isomeric transition.

We would like to thank W. E. Blumberg, A. M. Clogston, and M. Goldhaber for several critical discussions.

[1]R. L. Mössbauer, Z. Physik 151, 124 (1958).
[2]Isomer shift was first observed in the optical spectra of Hg^{197} (ground state $I = 1/2$, excited state $I = 13/2$); A. C. Melissinos and S. P. Davis, Phys. Rev. 115, 130 (1959). If one accepts "isotope shift" to be the proper name for charge redistribution effects resulting from addition of particles, the name "isomer shift" is the logical choice for the effect discussed herein. Unfortunately, the phrase "chemical shift" has been used to describe Mössbauer isomer shifts in the past.
[3]R. E. Watson, Solid State and Molecular Theory Group, Technical Report No. 12, Massachusetts Institute of Technology, June 15, 1959 (unpublished).
[4]E. Fermi and E. Segrè, Z. Physik 82, 729 (1933); S. A. Goudsmit, Phys. Rev. 43, 636 (1933).
[5]O. C. Kistner and A. W. Sunyar, Phys. Rev. Letters 4, 412 (1960). A temperature-dependent shift had been

previously observed and identified as a second-order Doppler shift resulting from the thermal motion of the atoms. See R. V. Pound and G. A. Rebka, Jr., Phys. Rev. Letters 4, 274 (1960).

[6]I. Solomon, Compt. rend. 250, 3828 (1960). Apart from the numerical constant which was not given in this reference, our Eq. (1) is the same as the result given there.

[7]R. E. Watson and A. J. Freeman, Phys. Rev. 120, 1125 (1960).

[8]C. E. Moore, Atomic Energy Levels, National Bureau of Standards Circular No. 467 (U. S. Government Printing Office, Washington, D. C. 1952), Vol. 2.

[9]R. E. Watson, Phys. Rev. 119, 1934 (1960). An estimate of the charge $|\psi_0(0)|^2$ for the inner s electron was made from this reference in which the configurations $3d^{n-2}4s^2$ are considered.

[10]J. S. Van Wieringen, Discussions Faraday Soc. No. 19, 118 (1955).

[11]The effect of covalency on the occupation of d orbitals is neglected.

[12]M. Goldhaber (private communication).

[13]J. Eisinger and V. Jaccarino, Revs. Modern Phys. 30, 528 (1958).

EVIDENCE FOR THE EXISTENCE OF SURFACE EXCITONS IN TETRACENE MICROCRYSTALS*

J. Katul and A. B. Zahlan
Physics Department, American University of Beirut, Beirut, Lebanon
(Received January 9, 1961)

During the past few years there have been a number of predictions of new types of excitons in molecular crystals.[1]

Selivanenko[2] predicted the existence of surface excitons in molecular crystals with a high heat of fusion. Ferguson and Schneider[3] observed a b-polarized shoulder in a 0.2μ anthracene film which was not observed in thicker films. These authors believed that it was unlikely that this band be due to a surface exciton. However, McClure[1] interpreted this 25100-cm^{-1} band as the b-polarized factor group component of the pure electronic transition occurring in these surface molecules.

We have observed two absorption bands in thin tetracene (microcrystalline) films prepared by rapid sublimation under conditions which produce a high surface-to-volume ratio. Rapid sublimation is essential[2] to increase the density of surface states.

No absorption above 5200 A was observed in thick crystals grown from the vapor under vacuum. However, when these same crystals were sublimed rapidly, under vacuum, onto a quartz disk forming a highly imperfect surface, a band at about 5400 A was observed. The two bands in the range 530-600 mμ could not be observed in the solutions made by dissolving the films in suitable solvents. This proves that these bands were not due to an impurity produced during the preparation.

Films were prepared under a pressure of 30 μ, but with different rates of sublimation. No absorption in the range 520-600 mμ occurred in slowly sublimed films. However, films prepared by rapid sublimation (at 130°C) exhibited one strong band when the film was about 0.5 μ and two strong bands at a thickness of 1 - 1.5 μ. The 1 μ need not be the thickness of the microcrystals involved. This observation of a critical thickness is an indication that the 5330A band (I) involves either a minimum crystalline length or a crystalline structure that can exist in stable form only above a certain thickness. Below such a thickness either the strains or the large number of imperfections, due to the high (surface/volume) ratio, make such a crystalline structure unstable. Table I summarizes sample data on the positions and extinction coefficients. Band II at 5350 A shifts continuously to about 6000 A with increasing thickness. Band I is very sharp

Table I. Dependence of the position and intensity of the surface excitons on thickness.

Wavelength (A)	Thickness (μ)	$\epsilon \times 10^{-3}$ (cm^{-1})	Bandwidth (cm^{-1})
5344 (I)	1 - 2	...	25 - 75 (80°K)
5650 (II)	0.4 - 2	...	100 - 300 (300°K)
5340 (II)	0.4	4.2	...
5410 (II)	1	4.4	...
5540 (II)	1.3	4.9	...
5680 (II)	1.5	4.4	...

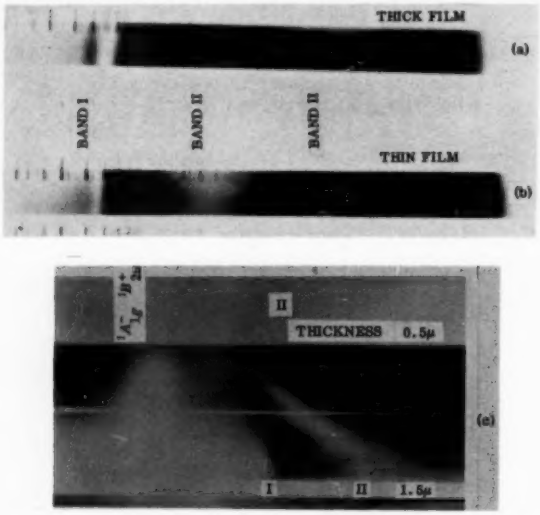

FIG. 1. In (a) and (b), bands I and II are clearly seen at 80°K. The thickness of the film in (a) is about 1.5 μ and in (b) it is about 0.5 μ. Note the shifts of I and II with thickness. In (c) the continuous shift of II with thickness is seen clearly at 300°K. Note that I appears suddenly at a critical thickness (see text). The 0-0′ of the molecular $^1A_{1g}^- \rightarrow {}^1B_{2u}^+$ transition is shown for comparison. A large Hilger spectrograph with glass optics was used throughout.

and shifts with thickness (see Fig. 1) about 100 A over the range 1 - 2 μ. The critical thickness depends on temperature. At 80°K, I is observed in a thinner film that at 300°K.

Besides the shift in the position of band II with thickness, its intensity may increase or decrease as it shifts to longer wavelength. We do not report oscillator strength, and due to variations in bandwidth with thickness, the intensity of the band is not linearly proportional to the extinction coefficient.

Heating in air up to 130°C for 3 hours did not induce any absorption in films where the bands are absent. Furthermore, a similar heat treatment did not change the bands when these were present. Tetracene is extremely sensitive to oxidation in solution but stable in the solid state. The lack of sensitivity of these bands to oxidation means that these states involve several "crystalline" layers of tetracene, and due to the packing in a crystal, the oxygen molecules cannot penetrate deep enough to produce observable damage.

Using a 10^3 magnification and polarized light, a difference between films that do not display "surface states" and those that do was observed: The nonabsorbing films consisted of microcrystals whose linear dimensions were of the order of 5 microns, about 1 micron thick, and appeared to be of the flaky type. As for the "absorbing" films, their dimensions were just at the limit of visibility and must be less than a micron. It was not possible to determine the shape, or dimensions, of these microcrystals. Furthermore, a large number of needle-like crystals were observed along with these microcrystals. Thus two different crystalline forms exist in these films. I and II might then arise in the same crystal or in two different types of crystalline structure.

Two arguments in favor of surface states rather than surface imperfections are the shift of the energy with thickness and the sharpness of the bands. The shift in the energy is of the order of 10%, i.e., 0.2 ev, from the thin to the thick edge of a film. It has been pointed out[3] that surface imperfections could lead to new states but theoretical and experimental proofs do not exist to support this hypothesis. Surface imperfections are, however, important perturbations of surface states. Since such imperfections act to decrease the degree of surface order they also act to raise the energy levels. This might account for the observed shift with thickness—it being assumed that film thickness determines approximately the size of the microcrystals.

Since there should be a large variety of surface imperfections, there should be an equally broad distribution in the energy levels. This would lead to broad absorption bands, whereas we observe a very sharp band I and band II is still sharper than the molecular $^1A_{1g}^- \rightarrow {}^1B_{2u}^+$ bands (these bands have half-widths of 480, 340, 480, 780 cm^{-1}) in the solid state at 90°K.

---

*This work was supported by the Research Corporation, American Chemical Society Petroleum Research Fund, and the American University Arts and Sciences Rockefeller Research Grant.

[1]D. S. McClure, Solid State Physics, edited by F. Seitz and D. Turnbull (Academic Press, Inc., New York, 1959), Vol. 8, p. 1.

[2]A. S. Selivanenko, J. Exptl. Theoret. Phys. (U.S.S.R.) 32, 75 (1957) [translation: Soviet Phys.-JETP 5, 79 (1957)].

[3]J. Ferguson and W. A. Schneider, J. Chem. Phys. 28, 761 (1958).

CYCLOTRON AND PARAMAGNETIC RESONANCE IN STRAINED CRYSTALS

G. E. Pikus and G. L. Bir
Semiconductor Institute, Academy of Sciences, Leningrad, U.S.S.R.
(Received January 11, 1961)

Recent studies on cyclotron and paramagnetic resonance in strained p-Si[1,2] have confirmed the earlier developed theory,[3,4] and have shown that investigations of this kind give important information concerning band structures and the nature of impurity centers. In connection with this, some new possibilities offered by measurements of the resonance effect in strained crystals are pointed out.

I. Measurements of the cyclotron resonance in strained Ge and Si make it possible to find not only the values of the constants A, B, and D determining the spectrum $E(\vec{k})$ in these crystals[5] but also the ratio of the deformation potential constants, b/d, which is very important for the theory of scattering.[6] Thus, according to reference 3, when the crystal is strained along [110], the inverse effective masses on the main axes, [110], [1$\bar{1}$0], and [001], are equal to

$$A \pm \frac{D}{2}\frac{1+\gamma B/D}{(1+\gamma^2)^{1/2}}, \quad A \mp \frac{D}{2}\frac{1-\gamma B/D}{(1+\gamma^2)^{1/2}}, \quad A \mp \frac{B\gamma}{(1+\gamma^2)^{1/2}}, \tag{1}$$

where

$$\gamma = \frac{2(b/d)c_{44}}{c_{11}-c_{12}}.$$

Here we assume that the upper choice of signs corresponds to $d\epsilon < 0$ while the lower one corresponds to $d\epsilon > 0$. The signs of the constants B and D cannot be determined by cyclotron resonance. Such experiments as well as measurements of the piezoresistance at high temperatures[7] allow us to determine only the signs of the products Bb and Dd. From the data[1] as well as from Smith's experiments[8] it is evident that for Si, $Bb > 0$ and $Dd > 0$.

II. The use of strained crystals with an InSb-type lattice makes it possible to obtain semiconductors with some special kind of spectrum when the surfaces of constant energy have toroidal shape and the extremum is in the ring. Taking into consideration terms linear[9] in $\vec{k}$ at low $\vec{k}$ for the lower band corresponding to the minimal energy of the holes, we obtain from the calculations

$$E(\vec{k}) = E^0(\vec{k}) \pm \frac{K}{(\mathcal{E}_\epsilon)^{1/2}}\left(\sum_{i,j}\alpha_{ij}k_ik_j\right)^{1/2}. \tag{2}$$

Here $E^0(\vec{k})$ has significance for the strained p-Ge corresponding to that determined by Eq. (18) of reference 3, K is Kane's constant,[9] $\mathcal{E}_\epsilon$ is determined by Eq. (16) of reference 3, and

$$\alpha_{xx} = 3b^2(\epsilon_{yy}-\epsilon_{zz})^2 + 4d^2(\epsilon_{xy}^2+\epsilon_{xz}^2),$$

$$\alpha_{xy} = -2\sqrt{3}(\mathcal{E}_\epsilon)^{1/2}d\epsilon_{xy} + 2d^2\epsilon_{xz}\epsilon_{yz}, \text{ etc.}$$

This formula is just for the strains when the band splitting, which is equal to $2(\mathcal{E}_\epsilon)^{1/2}$, exceeds kT and the difference $E(0)-E(k)_{\min}$, i.e., under conditions similar to those attained during the above-mentioned experiments.[1]

Toroidal surfaces occur, in particular, in the strains on the axes [001] and [111]: When $b\epsilon > 0$,

$$E(\vec{k}) = (A+\tfrac{1}{2}B)(k_\perp \pm k_{\perp 0})^2 + (A-B)k_z^2; \tag{3}$$

when $b\epsilon < 0$,

$$E(\vec{k}) = (A-\tfrac{1}{2}B)(k_\perp \pm k_{\perp 0})^2 + (A+B)k_z^2; \tag{4}$$

where

$$k_\perp^2 = k_x^2 + k_y^2, \quad k_{\perp 0} = \frac{\sqrt{3}}{2}\frac{|K|}{A \pm \frac{1}{2}B}.$$

Correspondingly, when $d\epsilon > 0$,

$$E(\vec{k}) = \left(A + \frac{D}{2\sqrt{3}}\right)(k_\perp \pm k_{\perp 0})^2 + \left(A - \frac{D}{\sqrt{3}}\right)k_z^2, \tag{5}$$

where

$$k_{\perp 0} = \frac{|K|}{A + D/2\sqrt{3}}.$$

On the contrary, when $d\epsilon < 0$,

$$E(\vec{k}) = \left(A - \frac{D}{2\sqrt{3}}\right)k_\perp^2 + \left(A + \frac{D}{\sqrt{3}}\right)(k_z \pm k_{z0})^2,$$

where

$$k_{z0} = \frac{\sqrt{2}\,|K|}{A + D/\sqrt{3}}.$$

The properties of semiconductors with toroidal energy surfaces have been studied in detail by Rashba et al.[10] Of great interest is the investigation of the cyclotron resonance and the combined resonance predicted by Rashba in these semiconductors.

III. In strained crystals p-Ge and p-Si it seems possible to observe a spin resonance of free carriers. In these nonstrained crystals such a resonance cannot be seen, because as a result of the large spin-orbit interaction an effective magnetic moment of the hole depends on its impulse direction. Therefore, instead of a resonance line, a broad resonance spectrum would result.

In strained crystals all the holes with low $\vec{k}$ possess the same effective magnetic moment depending on the strain direction, and their resonance frequency is determined by

$$(\hbar\omega_p)^2=(\mu_0{}^2\mathfrak{K}^2/\mathcal{E}_\epsilon)\langle\vec{H},\vec{H}\rangle, \tag{6}$$

where

$$\langle\vec{A},\vec{B}\rangle=\sum\beta_{ij}A_iB_j, \tag{7}$$

$$\beta_{xx}=[(\mathcal{E}_\epsilon)^{1/2}+b(\Delta-3\epsilon_{xx})]^2+3d^2(\epsilon_{xy}{}^2+\epsilon_{xz}{}^2),$$

$$\beta_{xy}=\sqrt{3}\,d\{\sqrt{3}\,d\epsilon_{xz}\epsilon_{yz}-\epsilon_{xy}[2(\mathcal{E}_\epsilon)^{1/2}-b(\Delta-3\epsilon_{zz})]\},\ \text{etc.},$$

where $\Delta=\epsilon_{xx}+\epsilon_{yy}+\epsilon_{zz}$ and $\mathfrak{K}$ is Luttinger's constant.[11] In the case of strain along [001] and [111],

$$(\hbar\omega_p)^2=\mu_0{}^2\mathfrak{K}^2(g_\parallel{}^2H_z{}^2+g_\perp{}^2H_\perp{}^2), \tag{8}$$

where $g_\parallel{}^2=(1\mp2)^2$, $g_\perp{}^2=(1\pm1)^2$, $H_\perp{}^2=H_x{}^2+H_y{}^2$, and μ_0 is the Bohr magneton. Here the upper sign corresponds to $b\epsilon>0$ and $d\epsilon>0$ while the lower one corresponds to $b\epsilon<0$ and $d\epsilon<0$.

The matrix element determining the probability of the transition under the influence of an alternating magnetic field h is equal to

$$|W_{12}|^2=\frac{\mathfrak{K}^2\mu_0{}^2}{\mathcal{E}_\epsilon}\,\frac{\langle\vec{H},\vec{H}\rangle\langle\vec{h},\vec{h}\rangle-\langle\vec{H},\vec{h}\rangle^2}{\langle\vec{H},\vec{H}\rangle}, \tag{9}$$

where $\langle\vec{A},\vec{B}\rangle$ may be determined according to (7). For the indicated directions [001] and [111], when $b\epsilon>0$ or $d\epsilon>0$,

$$|W_{12}|^2=\mathfrak{K}^2\mu_0{}^2\,\frac{[\vec{h}\vec{H}]^2+3[\vec{h}\vec{H}]_z{}^2}{H^2+3H_\perp{}^2}; \tag{10}$$

when $b\epsilon<0$ or $d\epsilon<0$, $W_{12}=0$.

Significant changes in the resonance frequency of the hole of the acceptor center occur when the splitting of the ground fourfold-degenerate state[12] due to the strain exceeds the term splitting in the magnetic field. However, in the case of strains obtained in practice,[2] a main contribution to the ψ function of the impurity center comes from states with large k for which Eq. (6) does not apply. That is why the resonance frequency of the bound hole depends not only on the constants b and d but also on the ψ function.[2] Therefore it is not to be believed, as is accepted in Kleiner and Roth,[13] that the term splitting is equal to the splitting of the valence bands at $k=0$, for the term splitting also depends on the change of the corresponding effective masses.

Only in cases when the strain is so large that the main contribution to the ψ function comes from states of low k, i.e., when the band splitting $2(\mathcal{E}_\epsilon)^{1/2}$ exceeds the activation energy of the impurity center E_i, will the resonance frequency be the same as for free holes. Therefore, in the case of lower strains this frequency must depend notably on the strain value according to

$$\Delta_p/\omega_p\simeq 2(\mathcal{E}_\epsilon)^{1/2}/E_i. \tag{11}$$

In the above-mentioned experiments[2] $\Delta g_\perp/\epsilon g_\perp=30$ which, according to (11), gives for the constant b a value about 0.5 ev.

We have no grounds to believe that in this instance the ratio $g_\parallel/g_\perp$ undergoes considerable changes for the bound states when compared with the free ones. Therefore, comparing the results of the experiments[2] with Eq. (8), the conclusion may probably be drawn that in Si both constants b and d are negative; hence B and D are also negative, which corresponds to the theoretical estimate.[5]

---

[1]J. C. Hensel and G. Feher, Phys. Rev. Letters 5, 307 (1960).

[2]G. Feher, J. C. Hensel, and E. A. Gere, Phys. Rev. Letters 5, 309 (1960).

[3]G. E. Pikus and G. L. Bir, Fiz. Tverd. Tela 1, 139, 1642 (1959)[translations: Soviet Phys.–Solid State 1, 136, 1502 (1959)].

[4]G. E. Pikus and G. L. Bir, report at the International Semiconductor Conference, Prague, August, 1960 (unpublished).

[5]G. Dresselhaus, A. F. Kip, and C. Kittel, Phys. Rev. 981, 368 (1955).

[6]G. L. Bir and G. E. Pikus, Fiz. Tverd. Tela 2, 2287 (1960).

[7]G. E. Pikus and G. L. Bir, Fiz. Tverd. Tela 1, 1828 (1959)[translation: Soviet Phys.–Solid State 1, 1675 (1960)].

[8]C. Smith, Phys. Rev. 94, 42 (1954).

[9]G. Dresselhaus, Phys. Rev. 100, 580 (1955); E. Kane, J. Phys. Chem. Solids 1, 249 (1957).

[10]E. I. Rashba and B. I. Sheka, Fiz. Tverd. Tela, Collected Articles 2, 162 (1959); E. I. Rashba, Fiz.

Tverd. Tela 2, 1224 (1960); I. I. Boiko and E. I. Rashba, Fiz. Tverd. Tela 2, 1874 (1960).
[11]J. M. Luttinger, Phys. Rev. 102, 1030 (1955).
[12]W. Kohn, in Solid-State Physics, edited by F. Seitz and D. Turnbull (Academic Press, New York, 1957), Vol. 5, p. 257.
[13]W. H. Kleiner and L. M. Roth, Phys. Rev. Letters 2, 334 (1959).

SELECTION RULE FOR THE INTERACTION OF MICROWAVE ULTRASONICS WITH SPINS

N. S. Shiren and E. B. Tucker
General Electric Research Laboratory, Schenectady, New York
(Received December 27, 1960)

Theory and results for iron-group paramagnetism in crystals[1] show that the dominant contribution, of noncubic crystalline fields, to the ground-state spin Hamiltonian is quadratic in the spin. This indicates a quadrupolar form for the relevant spin operator in spin resonance transitions induced by lattice vibrations. Quadrupole selection rules for spin-phonon transitions have been explicitly derived by Mattuck and Strandberg[2] for non S-state ions of the iron group. However, their low-frequency acoustic experiments[3] were unable to verify the selection rule. Using microwave ultrasonics in conjunction with standard spin resonance techniques,[4] we have experimentally confirmed the quadrupole selection rule for a non S-state ion, Cr^{3+} in Al_2O_3, and also for two S-state ions, Mn^{2+} and Fe^{3+} in MgO.

9-kMc/sec longitudinal phonons were generated in quartz rods bonded to the paramagnetic host crystals.[5,6] The wave propagation direction was parallel to the c axis in the Al_2O_3, and parallel to a cubic axis in the MgO. CW resonance saturation techniques were used to observe the interaction of the ultrasonics with the spin resonances, and relative spin-phonon matrix elements were extracted by comparison of the saturation by ultrasonics with saturation by a microwave source, at the resonance frequency, which was not coherent with the electron spin resonance spectrometer power.[6] Measurements of the matrix elements were made as a function of the angle θ between the dc magnetic field direction and the wave axis.

The dominant quadrupole nature of the relevant spin operator is shown by comparison of the observed angular variations with those computed, using the quadrupole spin operator. Good agreement was obtained for all three ions. As an example, Fig. 1 shows the experimental and theoretical angular variations of the square of the matrix element for the (-3/2, -1/2) transition of Fe^{3+} in MgO. In the absence of crystal field terms in the spin Hamiltonian, m_S is a good quantum number along H_{dc}, independent of the angle θ, and the probability for $\Delta m_S = \pm 1$ transitions, caused by a longitudinal wave, varies as

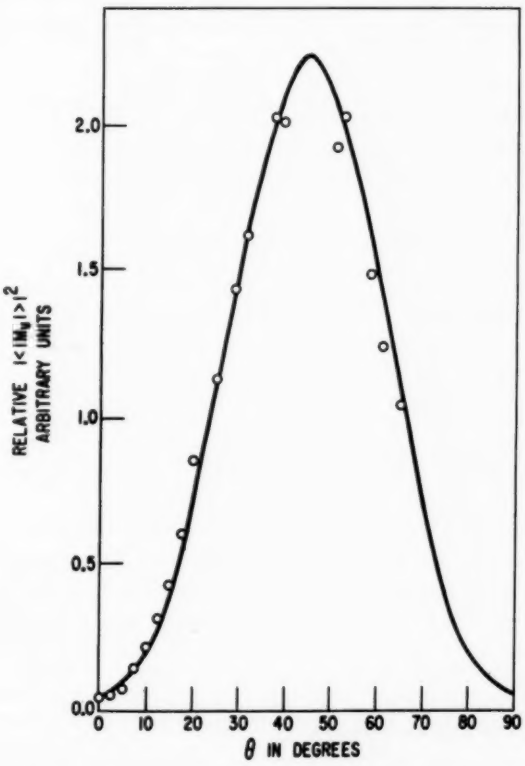

FIG. 1. Angular variation of the spin-phonon matrix element for the (-3/2, -1/2) transition of Fe^{3+} in MgO. The theoretical expression is normalized to the average of the experimental values. The small background level is believed due to generation of other acoustic modes, either in the quartz-MgO bond, or in the MgO crystal.

$\cos^2\theta \sin^2\theta$. However, for Fe^{3+} ions in MgO the cubic field causes a small admixing of states[1] and consequently, a slight deviation of the transition probability from a simple $\cos^2\theta \sin^2\theta$ dependence. Therefore, exact wave functions have been used in computing the theoretical angular variation.

A quadrupole spin operator cannot induce transitions between pure -1/2 and +1/2 states, and the near-zero ultrasonic effect observed on this transition for all three ions is further evidence for the quadrupole interaction.

The authors would like to thank Dr. G. D. Watkins for helpful discussions, and Mr. T. G. Kazyaka for his aid in taking the data.

[1]W. Low, Paramagnetic Resonance in Solids (Academic Press, New York, 1960).
[2]R. D. Mattuck and M. W. P. Strandberg, Phys. Rev. Letters 3, 369 (1959).
[3]R. D. Mattuck and M. W. P. Strandberg, Phys. Rev. 119, 1204 (1960).
[4]E. H. Jacobsen, N. S. Shiren, and E. B. Tucker, Phys. Rev. Letters 3, 81 (1959).
[5]E. B. Tucker, Bull. Am. Phys. Soc. 5, 157 (1960).
[6]N. S. Shiren, Bull. Am. Phys. Soc. 5, 343 (1960).

POPULATION INVERSION AND CONTINUOUS OPTICAL MASER OSCILLATION IN A GAS DISCHARGE CONTAINING A He-Ne MIXTURE

A. Javan, W. R. Bennett, Jr., and D. R. Herriott
Bell Telephone Laboratories, Murray Hill, New Jersey
(Received December 30, 1960)

This Letter is intended to give a summary of the results of experimental determinations of several physical properties of a gaseous discharge consisting of a He-Ne mixture which have led to the successful operation of a continuous-wave maser at five different wavelengths in the near-infrared. Population inversions are achieved between several Ne levels by means of excitation transfer from the metastable He($2\,^3S$) to the $2s$ levels of Ne.[1,2] The maser oscillation takes place in a narrow beam with a diameter of 0.45 inch. The power in our strongest beam at the wavelength 11 530 A is 15 milliwatts. The measured linewidth is in the range of 10 to 80 kc/sec. The angular spread of the beam is less than one minute of arc.

In the present system, the He($2\,^3S$) metastables are used as carriers of energy to excite the levels of Ne. Due to the resonant nature of this process, the excitation cross section is large only to those levels of Ne which fall in energy within a few kT of that of the He($2\,^3S$). Figure 1 gives the pertinent energy levels of He and Ne. As may be seen from Fig. 1,[3] the energy separations between the He($2\,^3S$) and Ne($2s$) states are small enough to insure an appreciable degree of transfer to the $2s$ states; however, the energy gap between the $2\,^3S$ and $2p$ levels is much too large to permit direct population of the $2p$ states in the collision process. Although the $2s_2$ and $2s_4$ levels

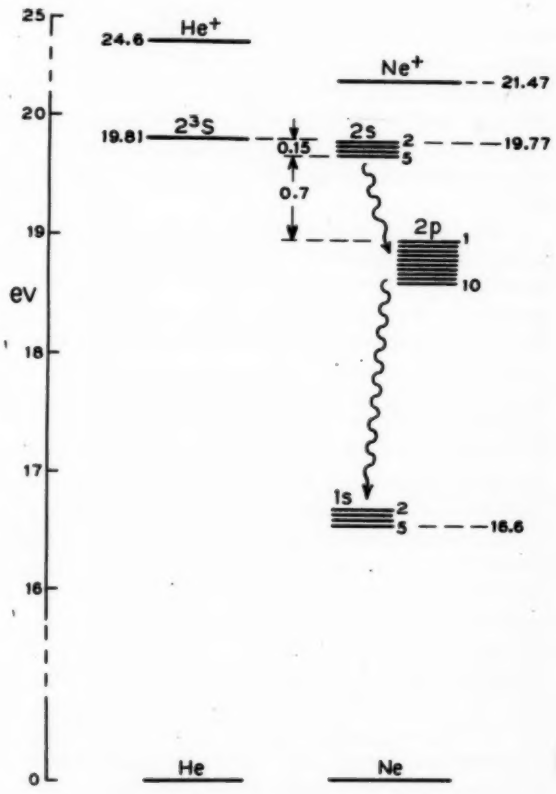

FIG. 1. Energy level diagram of He and Ne atoms.

of Ne may radiate to the Ne ground state, in the limit of complete resonance trapping their lifetimes are determined primarily by radiative decay to the $2p$ levels. Under this condition, the lifetimes of all of the $2s$ levels are about one order of magnitude longer than those of the corresponding $2p$ states. (The decay of the $2p$ levels is due to their radiative decay to the $1s$ levels.) Thus population inversions may be obtained on each of the thirty allowed $2s \rightarrow 2p$ transitions (see below).

In order to determine the transfer cross section and spurious sources of excitation of Ne levels, the afterglow of a pulsed rf discharge containing varying amounts of He and Ne was studied in detail. The time variation of the densities of the $2s$ and $2p$ levels was observed by the fluorescent decay of these levels using appropriate isolated transitions. The time variation of the $2\ ^3S$ density was determined through the absorption of the $2\ ^3P \rightarrow 2\ ^3S$ He transition.

The conditions were found under which the dominant mode of excitation of Ne levels arose from the He($2\ ^3S$) transfer. Among other sources of excitation of the Ne levels it was found that inelastic collisions of energetic electrons with Ne metastables[2] (i.e., the $1s$ levels[4]) were by far the most important. It should be noted that certain amounts of $2p$ excitation, arising from sources other than $2s$ - $2p$ cascade, can be tolerated without upsetting the presence of a population inversion. For instance, let us consider the population inversion between the $2s_5$ and $2p_9$ levels. The $2p_9$ is optically connected to only one of the $2s$ levels, namely the $2s_5$. The Einstein A coefficient for the $2s_5 - 2p_9$ transition was measured and found to be at least 25 times smaller than the rate of decay of the $2p_9$ level to within an accuracy of 20%. (This measurement was done by means of two independent techniques. The first was a spectroscopic technique to be described in a later publication. The second is discussed below.) This means that even an order of magnitude added excitation of $2p_9$ over that due to the cascade from the $2s_5$ still yields a population of the $2s_5$ levels larger than twice the population of the $2p_9$. In view of this effect, the adjustment of the electron density was found to be most critical.

In the afterglow, the energetic electrons thermalize within 10 to 20 μsec. The excitation transfer from He($2\ ^3S$), however, continues until the time when all of the $2\ ^3S$ states are quenched. This effect gives rise to a decay of the $2s$ levels identical to the time variation of the He($2\ ^3S$). The afterglow of the $2p$ levels also shows an identical decay due to the cascade transition from the $2s$ levels. Our observations indicate that the time variations of the $2\ ^3S$, $2s$, $2p$ levels in the afterglow are indeed identical to a high degree of accuracy. The possibility of the direct transfer from the $2\ ^3S$ to the $2p$ levels was ruled out by a process of relative intensity measurement at a fixed time in the afterglow to be described elsewhere.

Study of the fluorescent decay rate of the $2s$ and $2p$ levels as a function of several Ne pressures gave a total velocity-averaged inelastic cross section of $\langle\sigma\rangle = (3.7 \pm 0.5) \times 10^{-17}$ cm^2 for destroying He($2\ ^3S$) metastables in two-body collisions with Ne ground-state atoms at 300°K. This cross section can safely be assigned to the excitation transfer to the $2s$ levels of Ne since we have been able to show that other sources of destruction of the He($2\ ^3S$) by Ne ground-state atoms such as the one leading[5] to a formation of $HeNe^+$ are negligible. Our cross-section measurement at the same time furnishes the value of the diffusion coefficient of $2\ ^3S$ He metastables. Our result is in excellent agreement with the value of (470 ± 25 cm^2/sec) determined by Phelps.[6]

The radiative lifetimes of the $2s$ and $2p$ levels were determined using techniques described previously.[7] Our tentative values of the lifetimes of the $2s_2$, $2s_3$, $2s_4$, and $2s_5$ fall in the range from about 100 to 200 mμsec. Our results for the $2p$ levels are in general agreement with Ladenberg's[8] results. These measurements are still in progress and will be reported more fully at a later date. Each of the $2s$ levels decays into several of the ten $2p$ levels. The measured and estimated branching ratios for the transitions originating from each of the $2s$ levels, together with their total rate of radiative decay obtained from the above lifetimes, give the values of the individual Einstein A coefficients connecting the various $2s$ and $2p$ levels.

From the early stages of this experiment we were able to observe single-pass amplification of a transmitted signal at an infrared frequency where the inverted population was expected. Several electronic detection schemes were devised for this purpose. One of these schemes responded only during a small portion of the time and was in synchronism with the rf pulsed discharge. This technique enabled us to observe a larger value of amplification in the afterglow than during the glow; the latter is to be expected

since the added excitation of the $2p$ levels by electron impact is absent in the afterglow. However, in addition to extreme difficulties encountered in the interpretation of the results, the gain measurement alone was not sufficient to shed insight into the nature of the physical processes involved in the discharge.

In view of the above considerations, we were able to determine an optimum condition for the maser action prior to the observation of oscillation as described below.

The continuous-wave maser oscillation is observed in a discharge containing 0.1 mm Hg of Ne and 1 mm Hg of He. The optical feedback[9] is obtained through high-reflectance Fabry-Perot plates placed within the gas chamber. This chamber consists of a long quartz tube with an inside diameter of 1.5 cm and length of 80 cm. The quartz tube is terminated at each end with a larger metal chamber containing the high-reflectance plates. Flexible bellows are used in the end chambers to allow external mechanical tuning of the Fabry-Perot plates. Two optically flat windows at the extremes of this system are provided to allow the maser beam to leave the instrument undistorted. The separation of the plates is one meter. The discharge is excited by means of external electrodes using a 28-Mc/sec generator. The estimated power dissipation is around 50 watts.

The high reflectance is achieved by means of 13-layer evaporated dielectric films on the hundredth wavelength flat surface of the fused silica plates. The reflectance is 98.9% with 0.3% transmission in the wavelength range 11 000 A to 12 000 A. Outside of this range of wavelength the reflectance decreases rapidly.

The initial adjustment of the plates prior to starting of the discharge is done using an autocollimator. We have observed oscillations at the following wavelengths: 11 180, 11 530, 11 600, 11 990, and 12 070 A. The strongest oscillation occurs at 11 530 A with an output power of 15 mw.

An image converter tube is used visually and with a camera to observe and record structure of the beam. Two types of beam patterns have been studied.

A cross section of the emergent beam can be intercepted by the photocathode of the image converter and the intensity distribution recorded. This near-field pattern is shown in the two upper photographs of Fig. 2 for two Fabry-Perot plate angles.

The intensity pattern that the beam would form

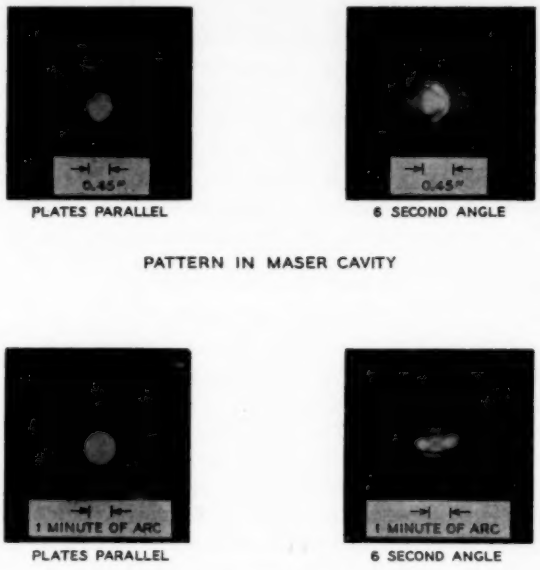

FIG. 2. Far-field and near-field patterns from maser beam at two plate angles.

at an infinite distance can be observed by imaging the maser beam to a point and observing the distribution of light in this image with an image converter microscope. The intensity distribution in this image represents the angular distribution in the maser beam. The two lower pictures in Fig. 2 show this far-field pattern at the indicated plate positions. The structures seen in the near- and far-field patterns would indicate the existence of several modes at a finite plate angle. The patterns shown in Fig. 2 were made at constant exposure and are therefore greatly overexposed by the increased intensity with parallel plates. The half-intensity width of the parallel plate output is less than one minute of arc.

The phase variation over the area of the beam was studied by placing a double or multiple slit in the beam and recording the diffraction pattern. A nine-slit mask of 0.050-in. spacing and 0.002-in. slit width covering the full 0.45-in. aperture of the beam results in a diffraction pattern shown in Fig. 3. The minima are very low, indicating small phase variation over the aperture. A double-slit pattern at 0.0175-in. is also shown.

Since the linewidth of the maser oscillation is many orders of magnitude narrower than the resolution of the best available spectrometers or

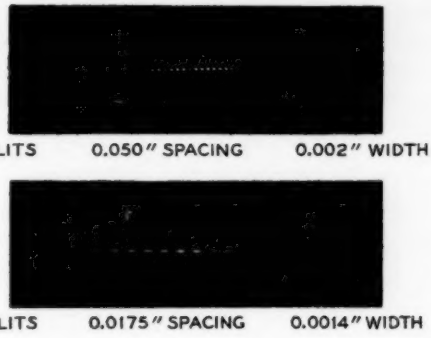

FIG. 3. Far-field diffraction patterns obtained by inserting multiple slits in the maser beam.

interferometers, standard optical techniques could not be used to measure the linewidth. Of the several possible methods examined, the most practical was found to be one based on analysis of the Fourier spectrum observed through a photomultiplier tube of the maser output. The photomultiplier is essentially a perfect square-law detector and should respond to beat frequencies. Hence, one can observe the spectral distribution obtained by beating all of the components of the line. The exact width of the original line determined from this distribution is independent of detailed assumptions on the line shape to within a factor of about two, providing the original line is not multiply peaked. In practice, this spectral distribution will be superimposed on top of the flat spectrum obtained from shot noise in the photomultiplier tube, and the latter may be used to check the bandwidth of the system.

The system was first checked by observing the spectrum from an intense line emitted in an ordinary discharge tube using a spectrum analyzer. The latter was flat within the frequency range of our analyzer, covering from 100 cps to 13 Mc/sec. Using a grating spectrometer to isolate the strong line at 11 530 A, the maser output was next examined. Our initial observations indicated a strong signal starting at zero frequency and extending to a half-width of about 100 kc/sec. Further examination showed the presence of an additional series of anharmonically related beats centered about frequencies other than zero. The location of these beats depended critically on the Fabry-Perot plate alignment. As the angular alignment of the plates was changed from 0 to 3 seconds, the beats became more widely spaced and weaker in intensity. Several possible spurious sources of beats were carefully examined and found not to be responsible for the observed signal. The possibility of "blocking oscillation" of the maser giving rise to an amplitude modulation of the output signal can be ruled out by the following observation: The peak frequency of a beat note is only a function of the plate adjustment and is independent of the factor by which the maser gain exceeds the oscillation threshold. The most plausible explanation found was that the beats arose from simultaneous oscillation in several different modes separated by frequencies in the Mc/sec range. Such a conclusion is not in disagreement with detailed calculations of the oscillatory modes by Fox and Li.[10] A distinct

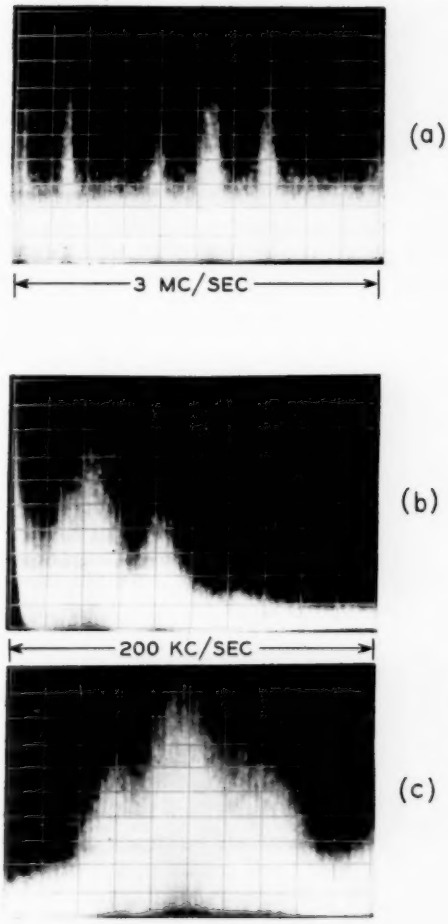

FIG. 4. Frequency spectra of the beat notes between various maser beam components.

correlation was found between the visual structure of the beam observed through the infrared image converter, and the presence of the beats as the angular alignment of the plates was varied. Figure 4(a) shows several beat notes ranging from 50 kc/sec to 2 Mc/sec. Figures 4(b) and 4(c) show the structure of these beats on an expanded scale. It should be noted that in our present system the angular adjustment of the plates is also accompanied by a slight change in plate separation. The important conclusion to be drawn here regards the linewidth of the maser oscillation. As is evident from Figs. 4(b) and 4(c), the beat notes imply linewidths in the range from 10 to 80 kc/sec.

The use of excitation transfer for production of inverted population was suggested[1,2] by one of the authors. The He-Ne mixture described above is the first gaseous system which has led to maser oscillations at optical frequencies. Recently some evidence for the presence of inverted populations in a Hg-Zn mixture has been reported[11] which supports the wide applicability of this principle.[1,2]

In the course of this research, a number of co-workers have contributed in the design, construction, and measurement. We are indebted to F. Muller, P. S. Kubik, A. R. Strnad, D. MacNair, E. Koch, G. J. Wolff, and G. E. Reitter. Dr. A. F. Turner of Bausch & Lomb has been very helpful in supplying the special evaporated reflectance films. In particular we would like to acknowledge the expert and patient assistance given by Mr. E. A. Ballik in the later stages of this experiment.

[1]A. Javan, Phys. Rev. Letters 3, 518 (1959).
[2]A. Javan, in Quantum Electronics, edited by C. H. Townes (Columbia University Press, New York, 1960).
[3]For simplicity, Paschen notation is used to describe the Ne energy levels.
[4]Not all of the 1s levels are truly metastables: the $1s_2$ and $1s_4$ undergo transitions to the ground state; however, due to the trapping of the resonant ultraviolet photons these levels are effectively long-lived and quasi-metastable.
[5]M. Pahl and U. Weimer, Z. Naturforsch. 12a, 926 (1957).
[6]A. V. Phelps, Phys. Rev. 99, 4, 1307 (1955).
[7]W. R. Bennett, Jr., A. Javan, and E. A. Ballik, Bull. Am. Phys. Soc. 5, 496 (1960).
[8]R. Ladenberg, Revs. Modern Phys. 5, 243 (1933).
[9]A. L. Schawlow and C. H. Townes, Phys. Rev. 112, 1940 (1958).
[10]A. G. Fox and P. Li, Proc. Inst. Radio Engrs. 48, 1904 (1960).
[11]V. K. Ablekov, M. S. Pesiu, and I. L. Fabelinski, Zhur. Eksp. i Teoret. Fiz. 39, 892 (1960).

MASS SPECTROGRAPHIC IDENTIFICATION OF THE ION OBSERVED IN HYDROGEN MOBILITY EXPERIMENTS*

W. S. Barnes, D. W. Martin, and E. W. McDaniel
Engineering Experiment Station and School of Physics,
Georgia Institute of Technology, Atlanta, Georgia
(Received January 9, 1961)

In a Letter appearing in a recent issue of this journal, Varney[1] pointed out that previous studies of the mobility of ions in pure hydrogen have probably been misinterpreted. In the majority of experiments performed to date, only one ion has been observed, and it has commonly been thought to be H_2^+. Indications of a second ion, generally assumed to be H^+, have been seen in a few experiments but the actual existence of this ion remains in doubt. Upon consideration of a study by Stevenson and Schissler[2] of the cross section for formation of H_3^+ by the reaction $H_2^+ + H_2 \rightarrow H_3^+ + H$, Varney has made the following assertions: (1) The H_2^+ ion is never observed in hydrogen mobility experiments; (2) the ion which invariably appears in these experiments is H_3^+; (3) it is reasonable to assume that the second ion, if actually present, is H^+. The purpose of this Letter is to report evidence which tends to corroborate Varney in each of these assertions.

We have recently constructed and put into operation apparatus designed to permit identification of the ions appearing in mobility experiments and to yield information concerning the various types of reactions which can occur at low energy between ions and molecules.[3] Ions are produced by electron bombardment inside a long drift tube containing gas at a pressure up to about 700 microns. The ions diffuse down the drift tube under the influence of a weak electric

field. A sample of the ion population at the end of the drift tube is extracted through a two-stage differential pumping chamber and passed into a 60° magnetic deflection mass spectrometer. The number of ion-molecule collisions in the drift tube may be varied over a wide range by changing the source position and/or the gas pressure. Information concerning the nature and probability of the reactions occurring is revealed by the resulting changes in the ionic mass spectrum.

In studies of hydrogen, the three known species (H^+, H_2^+, and H_3^+) are all observed at very low drift-tube pressures, p, and for short drift distances, d. The H_3^+ ion is by far the most abundant throughout the range covered. As pd is increased, the abundances of H^+ and H_2^+ relative to that of H_3^+ diminish, the H_2^+ abundance falling off more rapidly than that of H^+. Taking into account the increasing ion losses due to diffusion, recombination, etc., it appears that the H_3^+ population increases mainly at the expense of H_2^+. This is consistent with Stevenson and Schissler's finding that the reaction $H_2^+ + H_2 \rightarrow H_3^+ + H$ has a large cross section. The persistence of H^+ ions in our spectrum to higher pd values than that at which H_2^+ disappears indicates that the cross section for the reaction $H^+ + H_2 \rightarrow H_3^+$ is much smaller, consistent with the conclusions of other investigators.

In mobility experiments, pd is always made rather large in order that a steady state, constant drift velocity be achieved. Values of pd of 10 cm-mm Hg, and higher, are commonly used. At $pd \gtrsim 1.5$, only the H_3^+ ion is seen in our spectrometer. This fact appears to corroborate Varney's first and second assertions. Furthermore, since the H^+ ion persists to much higher pd than does the H_2^+ ion, it seems reasonable to assume that if a second ion is observed, it is H^+. Of course, the possibility exists that the second ion sometimes reported is an impurity.

A more complete discussion of the work reported here will be presented in another paper which will also contain a detailed description of the apparatus.

---

*This research was supported by the U. S. Air Force through the Air Force Office of Scientific Research of the Air Research and Development Command.

[1]R. N. Varney, Phys. Rev. Letters 5, 559 (1960).

[2]D. P. Stevenson and D. O. Schissler, J. Chem. Phys. 29, 282 (1958).

[3]E. W. McDaniel and D. W. Martin, Bull. Am. Phys. Soc. 5, 380 (1960); also see Air Force Office of Scientific Research Document No.. TN-60-661, June 20, 1960 (unpublished).

COLLISIONAL DETACHMENT IN MOLECULAR OXYGEN*

A. V. Phelps and J. L. Pack
Westinghouse Research Laboratories, Pittsburgh, Pennsylvania
(Received December 30, 1960)

The measurements reported in this Letter show that the electron affinity of the negative ion of molecular oxygen formed in low-energy swarm experiments is 0.46 ± 0.02 ev. This value is three times that used in the analyses of recent photodetachment experiments.[1] In addition, we show that the frequency of electron detachment collisions between oxygen negative ions and a thermal distribution of oxygen or nitrogen molecules in the lower ionosphere is at least two orders of magnitude smaller than the accepted value.[2] Therefore, a new mechanism for electron detachment must be found in order to explain the appreciable electron densities found in the lower ionosphere at night.

The experimental apparatus used in these measurements is the same as that used by Chanin, Phelps, and Biondi[3] to measure electron attachment coefficients. In the present experiments, either (a) a pulse of voltage is applied to the grid to collect negative ions and electrons in the vicinity of the grid and thus reduce the current reaching the collector in proportion to the sum of electron and negative-ion currents reaching the grid, or (b) a pulse of high-frequency voltage (~1 Mc/sec) is used to collect only electrons[4] and reduce the collector current in proportion to the electron current reaching the grid. The waveforms obtained are shown in Fig. 1. The upper waveform for $T = 423°K$ shows an initial peak due to electrons which have crossed the tube without attachment. This peak is followed by an exponen-

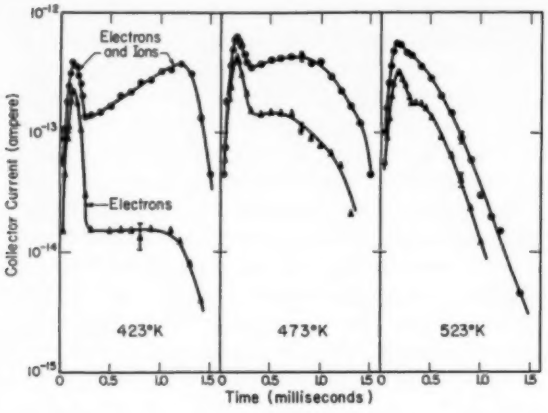

FIG. 1. Change in collector current as a function of time of application of voltage pulse to control grid at various temperatures for $N = 10^{18}$ molecules/cc, $E/N = 3.1 \times 10^{-17}$ volt cm^2, and a drift distance of 2.5 cm. The durations of the light pulse and the grid voltage pulses were 120 μsec.

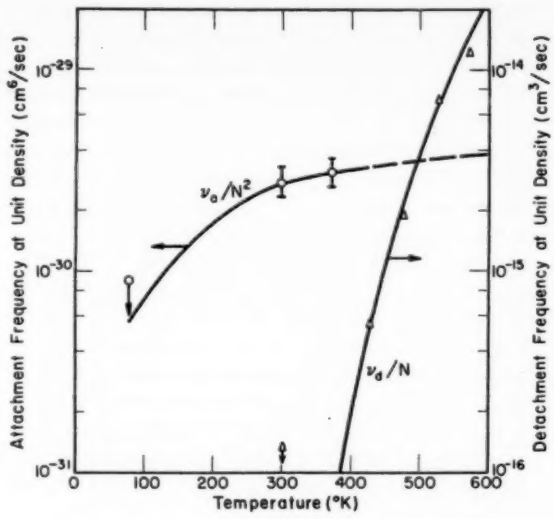

FIG. 2. Thermal attachment and detachment coefficients in molecular oxygen as a function of gas temperature.

tially increasing current due to negative ions. The lower waveform shows the initial electron peak and a delayed component due to electrons which are detached from the ions as they drift across the tube. At higher temperatures the ion-current waveform is distorted and the relative magnitude of the delayed electron current is increased. These waveforms agree well with theoretical predictions. For a sufficiently narrow pulse width (Δt), the ratio of the electron current immediately after the initial pulse (I_d) to the peak value of the initial electron-current pulse (I_e) is given by $I_d/I_e = \nu_a t_e \nu_d \Delta t$, where ν_a and ν_d are the frequencies of electron attachment and detachment collisions and t_e is the electron transit time. Under the conditions of these experiments, $\nu_a t_e$ is obtained from the ratio of the total current (I_t) to the current of electrons reaching the grid without attaching to the oxygen (I_{es}). Thus, $\nu_a t_e = \ln(I_t/I_{es})$. I_{es} is obtained by applying a large enough grid voltage pulse at the time of the initial peak to collect all of the electrons. The resultant values of ν_d are directly proportional to the oxygen density, N. At the value of E/p used, the negative ions are in thermal equilibrium with the gas.

Figure 2 shows the measured values of ν_d/N as a function of the oxygen temperature. Also shown are the results of measurements of the three-body attachment coefficient, ν_a/N^2, for thermal electrons in oxygen.[3] Similar values have been obtained by van Lint, Wikner, and Trueblood.[5] The results presented are consistent with the assumption that we are studying the reaction $e + 2O_2 \rightleftarrows O_2^- + O_2$. By equating rates of attachment and detachment and using the law of mass action, one finds that

$$\frac{\nu_a}{\nu_d N(O_2)} = \frac{N(O_2^-)}{N_e N(O_2)} = \frac{g(O_2^-)}{g_e g(O_2)} \left(\frac{h^2}{2\pi m k T}\right)^{3/2} \exp\left(\frac{e\Delta E}{kT}\right),$$

where the N's and g's are, respectively, the densities and statistical weights of the negative ions, the electrons, and the oxygen molecules and ΔE is the electron affinity. Meyerott, Landshoff, and Magee[6] state that $g(O_2^-)/g_e g(O_2) = 2/3$. The data of Fig. 2 show that $\Delta E = 0.46 \pm 0.02$ ev. This value is within the limits set by Loeb[4] and intermediate between the previously proposed values.[7] Further experiments will be necessary to determine whether the O_2^- ions are formed in the ground vibrational state or in a vibrationally excited state. There is no evidence of vibrational relaxation due to the approximately 5×10^5 ion-molecule collisions occurring during the experiment.

If our electron affinity is combined with the thermal attachment coefficients in Fig. 2, the

calculated collisional detachment coefficient at 230°K is 4×10^{-20} cm^3/sec compared to values of 10^{-17} cm^3/sec or greater used in the analysis of ionospheric data.[2] Preliminary measurements in dry air show that, as expected, nitrogen has very little effect on the collisional detachment rate. Therefore, if the negative ions formed in the ionosphere are O_2^-, then the detachment observed at night must be due to an excited species, such as vibrationally excited O_2 resulting from the recombination of oxygen molecules, electronic excitation, etc. In addition, if the O_2^- ions in the photodetachment experiments of Burch, Smith, and Branscomb[1] are assumed to be in the same vibrational state as those described above, then the radiative attachment coefficient for 230°K electrons in molecular oxygen will be increased from about 3×10^{-21} cm^3/sec to as much as 2×10^{-18} cm^3/sec.

*This work was supported in part by the Air Research and Development Command.

[1]D. S. Burch, S. J. Smith, and L. M. Branscomb, Phys. Rev. 112, 171 (1958).

[2]See for example S. K. Mitra, The Upper Atmosphere (The Asiatic Society, Calcutta, 1952), 2nd ed. pp. 306 and 309; and D. K. Bailey and L. M. Branscomb, Bull. Am. Phys. Soc. 5, 123 (1960).

[3]L. M. Chanin, A. V. Phelps, and M. A. Biondi, Phys. Rev. Letters 2, 344 (1959).

[4]L. B. Loeb, Basic Processes in Gaseous Electronics (University of California Press, Berkeley, California, 1955), Chap. V.

[5]V. A. J. van Lint, E. G. Wikner, and D. L. Trueblood, Bull. Am. Phys. Soc. 5, 122 (1960).

[6]R. E. Meyerott, R. K. M. Landshoff, and J. Magee, Lockheed Aircraft Corporation Report LMSD-48361, December, 1959 (unpublished).

[7]L. M. Branscomb, Advances in Electronics and Electron Physics, edited by L. Marton (Academic Press, Inc., New York, 1957), Vol. 9, p. 43; and R. S. Mulliken, Phys. Rev. 115, 1225 (1960).

NEW ISOTOPE OF CARBON: C^{16}

S. Hinds and R. Middleton
Atomic Weapons Research Establishment, Aldermaston, Berkshire, England

and

A. E. Litherland* and D. J. Pullen
Clarendon Laboratory, Oxford, England

(Received December 30, 1960)

Estimates of the neutron binding energies of a number of neutron-rich light nuclei have been made recently by Zel'dovich.[1] In particular, from these estimates the $C^{14}(t,p)C^{16}$ reaction was expected to have a Q value lying between -3 and -4 Mev. This reaction has now been observed and the measured Q value is -3.014 ± 0.016 Mev. In addition, the decay of C^{16} has been studied and the measured half-life is 0.74 ± 0.03 second.

A 6-Mev triton beam from the Aldermaston electrostatic generator was used to bombard a thin C^{14} target and the emitted protons were analyzed with a broad-range magnetic spectrograph.[2] The targets were prepared by polymerizing acetylene gas containing 33% C^{14} directly onto nickel backing foils. Several exposures were made with the spectrograph using different magnetic field strengths and at angles ranging from 15° to 65°. On five of these an intense proton group was observed which could not be accounted for by the known target impurities. Further analysis established that this group varied in energy characteristically of a mass-14 target nucleus and probably corresponded to the formation of C^{16} in its ground state. The kinematics of the reaction, however, do not allow the $C^{14}(t,p)C^{16}$ reaction to be distinguished from either the $C^{14}(He^3,p)N^{16}$ or the $N^{14}(t,p)N^{16}$ reactions. The He^3 contamination of the ion beam was measured to be less than 0.1% by observing the elastically scattered particles and was therefore unlikely to give rise to significant reaction groups. It was also noted that, although several intense groups were observed arising from the $C^{12}(t,p)C^{14}$ reaction, none could be attributed to the $C^{12}(He^3,p)N^{14}$ reaction. To eliminate the possibility of the $N^{14}(t,p)N^{16}$ reaction, two exposures were made with a target containing nitrogen. No group was observed with the same energy as the group ascribed to C^{16}. Also no proton groups were observed corresponding to the known lower excited states of N^{16} in the spectra obtained with the C^{14} target, and only a weak continuum of protons was observed from a typical nickel target backing.

The energy of the incident triton beam was determined in terms of the Q value of the $C^{12}(t,p)C^{14}$ reaction[3] and from this the Q value of the $C^{14}(t,p)C^{16}$ reaction was calculated to be -3.014 ± 0.016 Mev. This is consistent with a C^{16} mass excess of 13.694 ± 0.017 Mev and a mass of 16.014702 ± 0.000017 mass units, both referred to the scale on which the mass excess of C^{12} is zero.

An energy level diagram showing the possible modes of decay of C^{16} is shown in Fig. 1.[4-6] As a change of parity is required for the high-energy beta transitions, the beta decay of C^{16} was expected to leave N^{16} in neutron-unstable 1+ states. This expected delayed-neutron emission has been observed experimentally and used to determine the half-life of C^{16}.

A one-microampere triton beam from the electrostatic generator was interrupted by a mechanical shutter some 20 feet away from the neutron detector which was a block of polystyrene, 45 cm long by 45 cm in diameter, containing five BF_3 counters. A hole of 10-cm diameter through the polystyrene block allowed the C^{16} nuclei to be formed at the center of the assembly. The efficiency of the detector was between 1 and 2%. The pulses from the neutron detector and associated electronic equipment were fed into a circuit which converted their time of arrival into a pulse height. The time distribution of the pulses could then be displayed on a 100-channel pulse-amplitude analyzer immediately after the interruption of the beam. The time scale of the analyzer was calibrated using the 50-cps mains frequency.

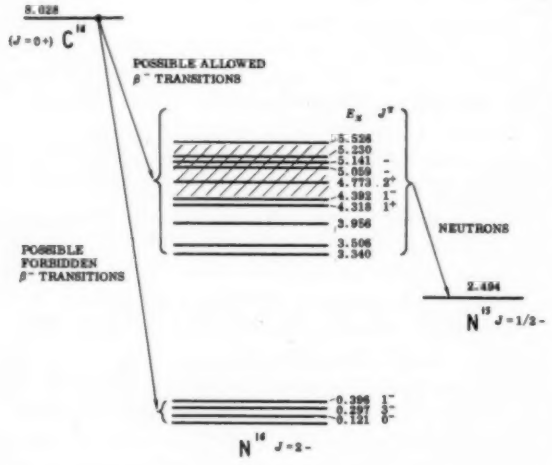

FIG. 1. An energy level diagram showing the possible modes of decay of C^{16}.

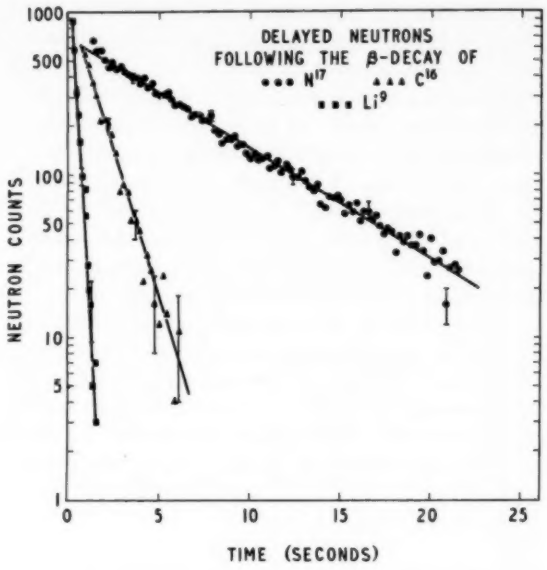

FIG. 2. A logarithmic plot of the decay of the delayed-neutron intensity from C^{16}. Also shown are the decay curves for the other two delayed-neutron emitters Li^9 and N^{17}.

Targets containing Li^7, C^{14}, and O^{18} were bombarded by the 6-Mev triton beam for periods between 2 and 10 seconds. The delayed neutrons from, respectively, Li^9, O^{16}, and N^{17} were displayed in the time-analyzer for periods ranging from 2 to 25 seconds. A fraction of a second delay between the end of each beam pulse and the start of the counting period was provided manually. No delayed neutrons were observed from the target backings though there was a very small background which was thought to arise from the triton beam striking the mechanical shutter. Figure 2 shows the decay of the delayed neutrons following the $Li^7(t,p)Li^9$, the $C^{14}(t,p)C^{16}$, and the $O^{18}(t,\alpha)N^{17}$ reactions. The half-lives of Li^9 and N^{17} were found to be 0.17 ± 0.01 and 4.20 ± 0.08 seconds, respectively, and these are in good agreement with the published values.[4] The half-life of C^{16} was found to be 0.74 ± 0.03 second.

The measured mass of C^{16} implies that the first $T=2$ state in O^{16} is at approximately 23.0 Mev. In the future it would be interesting to determine the neutron-unstable states of N^{16} to which C^{16} decays and to determine the beta-ray branching ratio to the low-lying negative-parity states of N^{16}.

We wish to thank Dr. K. W. Allen and Professor

D. H. Wilkinson for their interest in this work and several helpful discussions.

*Seconded from Atomic Energy of Canada, Chalk River, Ontario, Canada.

[1]Ya. B. Zel'dovich, J. Exptl. Theoret. Phys. U.S.S.R. 38, 1123 (1960)[translation: Soviet Phys. - JETP 11, 812 (1960)].

[2]S. Hinds and R. Middleton, Proc. Phys. Soc. (London) 74, 196 (1959).

[3]F. Everling, L. A. Konig, J. H. E. Mattauch, and A. H. Wapstra, Nuclear Phys. 18, 529 (1960).

[4]F. Ajzenberg-Selove and T. Lauritsen, Nuclear Phys. 11, 1 (1959).

[5]C. P. Sikkema and R. Van Wageningen, in Proceedings of the International Conference on Nuclear Structure, Kingston, edited by D. A. Bromley and E. W. Vogt (University of Toronto Press, Toronto, Canada, 1960), p. 513.

[6]N. Jarmie, M. G. Silbert, and D. B. Smith (private communication).

MATRIX ELEMENTS IN THE FORBIDDEN BETA DECAY OF Ce^{141}

D. D. Hoppes
National Bureau of Standards, Washington, D. C. and Catholic University of America, Washington, D. C.

and

E. Ambler, R. W. Hayward, and R. S. Kaeser
National Bureau of Standards, Washington, D. C.

(Received January 6, 1961)

We have performed measurements on oriented Ce^{141} in which the energy and angular distribution of the beta particles are determined with respect to the nuclear spin orientation. These measurements give information on the relative contribution of the various nuclear matrix elements contributing to the beta transitions.

The 33-day Ce^{141} undergoes beta decay to Pr^{141} via two beta groups according to the schemes

$$\tfrac{7}{2}- \xrightarrow{\beta_1} \tfrac{7}{2}+ \xrightarrow{\gamma} \tfrac{5}{2}+$$

and

$$\tfrac{7}{2}- \xrightarrow{\beta_2} \tfrac{5}{2}+.$$

The 70% abundant β_1 transition with a maximum energy of 435 kev and a $\Delta J=0$ will depend on all six first forbidden (real) matrix elements: $\mathfrak{M}(i\vec{\sigma}\cdot\vec{r})$, $\mathfrak{M}(\gamma_5)$, $\mathfrak{M}(i\vec{r})$, $\mathfrak{M}(\vec{\sigma}\times\vec{r})$, $\mathfrak{M}(\vec{\alpha})$, and $\mathfrak{M}(iB_{ij})$. The 30% abundant ground-state β_2 transition with a maximum energy of 580 kev and a $\Delta J=1$ will depend on only the last four matrix elements, i.e., those of tensor rank one and two.

The energy and angular distribution function, which has been calculated by Morita and Morita[1] and by Bincer,[2] has the form

$$W(\hat{p}\cdot\hat{J})=N_0(E)+N_1(E)\frac{p}{E}f_1P_1(\hat{p}\cdot\hat{J})+N_2(E)\frac{p^2}{E}f_2P_2(\hat{p}\cdot\hat{J})$$

$$+N_3(E)\frac{p^3}{E}f_3P_3(\hat{p}\cdot\hat{J}),$$

where $N_k(E)$ gives the energy dependence of the term of order k and contains products of the reduced matrix elements. The orientation parameter f_k describes the nuclear orientation, given in terms of an average over the population of the magnetic sublevels. The electron momentum and energy are p and E, respectively, and $P_k(\hat{p}\cdot\hat{J})$ is a Legendre polynomial. $N_0(E)$ gives the usual energy distribution for an unoriented beta emitter apart from the statistical factors.

The experimental apparatus and the procedure for the reduction of the data are similar to those used in earlier studies on the angular distribution of beta particles from oriented nuclei.[3] A single crystal of neodymium ethyl sulfate used for both cooling and orienting purposes is mounted with the c axis vertical in the demagnetization apparatus. On the uppermost surface of this crystal is grown a thin surface layer containing the Ce^{141} activity. Located about one centimeter above this is a thin anthracene scintillator which provides the input to a 100-channel pulse-height analyzer for the analysis of the beta spectra. Three 2-in. by 2-in. NaI gamma counters are located equatorially about 15 cm from the axis of the apparatus. These counters monitor the gamma-ray anisotropy which, combined with nuclear hyperfine splitting data for Ce^{141} neodymium ethyl sulfate, allows one to determine the nuclear orientation parameters f_k. The outputs of the gamma-ray counters are also compared for time coincidence with the output of the beta channel by

means of a fast-slow coincidence circuit in order to separate the distribution of the 435-kev inner beta group from the 580-kev ground-state transition.

The quantities $N_1(E)/N_0(E)$ and $N_2(E)/N_0(E)$ can be measured independently. The measurements of the ratio $N_2(E)/N_0(E)$ were made by determining the beta distribution when the sample has been aligned by the Bleaney method after cooling the sample by adiabatic demagnetization from a horizontal magnetic field of 23 kilogauss at 1.0°K. After a counting period of about thirty minutes the temperature of the sample was raised to 1°K again, destroying the nuclear alignment. The normalization for the gamma-ray anisotropy depended on a reliable measurement of a uniform gamma-ray distribution. In the case of nuclear alignment f_1 and f_3 are always zero.

The ratio $N_1(E)/N_0(E)$ was determined under similar conditions except that here a magnetic polarizing field of 200 gauss was applied along the c axis of the source-crystal so that the Ce^{141} nuclei were polarized by the Rose-Gorter method. Since this polarizing field was applied adiabatically, the sample temperature was not as low as in the case when no field was applied. By taking different combinations of the ratio of beta counts before and after orientation for two opposite field directions one can obtain values for both N_1/N_0 and N_2/N_0. The accuracy of the latter is poorer than in the alignment experiments where a larger f_2 is achieved. Counting was continued for alternating polarizing field directions for periods up to one hour. At the end of this period the sample was warmed and the orientation destroyed. The contribution of the f_3 term is calculated to be negligible at the temperatures achieved.

The observed distributions were corrected for backscattering effects in the source and for the finite energy and angular resolution of the apparatus; the limits on our experimental values include estimates of errors in these corrections as well as those due to counting statistics.

The experimentally determined distribution function for the ground-state 580-kev transition is

$$W(\hat{p}\cdot\hat{J})/N_0 = 1 - (1.11 \pm 0.10)\frac{p}{E} f_1 P_1(\hat{p}\cdot\hat{J}) + (0.36 \pm 0.10)\frac{p^2}{E} f_2 P_2(\hat{p}\cdot\hat{J}),$$

where we have evaluated the coefficients for an average $E = 1.85$ in relativistic units. A rough measurement of the energy distribution $N_1(E)/N_0(E)$ is also obtained.

The interpretation of these results requires that accurate radial Coulomb wave functions for the electron be employed. We have used exact radial wave functions taking into account nuclear finite-size effects. These functions have been calculated in a similar manner to those calculated by Bhalla and Rose.[4]

Each $N_k(E)$ contains products and squares of the matrix elements, each multiplied with energy-dependent factors. In principle one can get three independent nonlinear simultaneous equations for any individual $N_k(E)$ at three energies or for all three $N_k(E)$ at one energy. However, in the first case the energy dependence of $N_k(E)$ on the matrix elements is so insensitive that in practice only a rough limitation on the matrix elements can be determined. There is no evidence for a deviation from a statistical shape of $N_0(E)$ as measured by Freedman and Engelkemier[5] and Jones and Jensen,[6] and of $N_1(E)$ within the accuracy of our experiments.

For the purposes of illustration only, we employ an approximation where the radial functions are expanded in powers of $\xi = \alpha Z/2R$ and retain only those terms involving the highest power of ξ multiplying each matrix element product in each particle parameter (see reference 2). This approximation is useful only when the matrix element ratios are such that energy-independent factors dominate, giving the statistical shapes to the spectra. When we do this we obtain rather simple expressions for the $N_k(E)$, which are evaluated at the average energy $E = 1.85$ and compared with experiment in Figs. 1 and 2. We find that the allowable values of certain matrix element combinations are greatly restricted by experiment. In order to fix the relative values of the individual matrix elements, we must resort to a model to fix at least one ratio theoretically.

Fortunately the ground states of both $_{58}Ce_{83}^{141}$ and $_{59}Pr_{82}^{141}$ have configurations that should be adequately described by shell-model wave functions. For Ce^{141} the measured spin and magnetic moment establish the ground state of the eighty-third neutron as an $(f_{7/2})^1$ configuration. For Pr^{141} the measured spin, the magnetic moment of +3.92 nuclear magnetons, and the quadrupole moment of -0.054 barn are consistent with a mixture[7] of configurations $(g_{7/2})^8(d_{5/2})^1$ and $(g_{7/2})^6(d_{5/2})^3$ for the protons outside the closed shell at 50. With these configurations the ratios of certain nuclear matrix

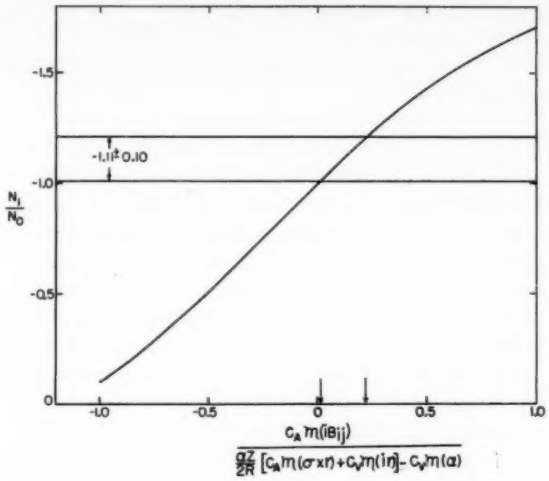

FIG. 1. The quantity N_1/N_0, evaluated at $E=1.85$, as a function of $\{C_A\mathfrak{M}(iB_{ij})\}/\{(\alpha Z)(2R)^{-1}[C_A\mathfrak{M}(\vec{\sigma}\times\vec{r})+C_V\mathfrak{M}(i\vec{r})]-C_V\mathfrak{M}(\vec{\alpha})\}$, using the approximate Coulomb functions described in the text. The range of values allowed by experiment is indicated on the curve.

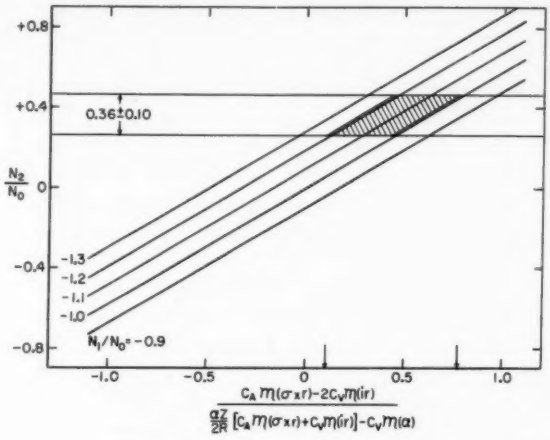

FIG. 2. The quantity N_2/N_0, evaluated at $E=1.85$, as a function of $\{C_A\mathfrak{M}(\vec{\sigma}\times\vec{r})-2C_V\mathfrak{M}(i\vec{r})\}/\{(\alpha Z)(2R)^{-1}\times[C_A\mathfrak{M}(\vec{\sigma}\times\vec{r})+C_V\mathfrak{M}(i\vec{r})]-C_V\mathfrak{M}(\vec{\alpha})\}$, using the approximate Coulomb functions described in the text. The range of values allowed by experiment is indicated on the curve.

elements are predicted uniquely and are, furthermore, completely independent of any details of the nuclear radial wave functions. In addition, admixtures of other configurations such as $(g_{7/2})^4(d_{5/2})^5$, with appropriate initial state proton configurations, do not alter these ratios. Admixtures of higher seniority states involving the rearrangement of the relevant nucleons in the $g_{7/2}$ and $d_{5/2}$ shells will not contribute at all to these matrix element ratios.

We have

$$\mathfrak{M}(i\vec{r})/\mathfrak{M}(\vec{\sigma}\times\vec{r})=-1;\quad \mathfrak{M}(iB_{ij})/\mathfrak{M}(\vec{\sigma}\times\vec{r})=-3(\tfrac{2}{5})^{1/2}.$$

The other ratio $\mathfrak{M}(\vec{\alpha})/\mathfrak{M}(\vec{\sigma}\times\vec{r})$ involves the relativistic operator $\vec{\alpha}$ which normally connects large with small components of relativistic four-component wave functions. Since most nuclear models involve only nonrelativistic wave functions, we must use a nonrelativistic operator as obtained from a canonical transformation[8] yielding $\vec{\alpha}\to i\vec{\nabla}/M$. This ratio is calculated to be

$$\frac{\mathfrak{M}(\vec{\alpha})}{\mathfrak{M}(\vec{\sigma}\times\vec{r})}=-\frac{1}{M}\frac{\int r^2u_f(r)^*\left(\frac{d}{dr}+\frac{4}{r}\right)u_i(r)dr}{\int r^2u_f(r)^*u_i(r)dr},$$

where the value depends on the details of the nuclear radial wave functions.

The radial wave functions are not predicted by the shell model without the introduction of a specific potential, so that we treat $\mathfrak{M}(\vec{\alpha})/\mathfrak{M}(\vec{\sigma}\times\vec{r})$ as a parameter to be determined by the experiment after the theoretical values of $\mathfrak{M}(i\vec{r})/\mathfrak{M}(\vec{\sigma}\times\vec{r})$ and $\mathfrak{M}(iB_{ij})/\mathfrak{M}(\vec{\sigma}\times\vec{r})$ have been introduced. In the evaluation of this parameter, we use the exact lepton radial wave functions referred to above. In Fig. 3 we show the theoretical predictions for N_1/N_0 and N_2/N_0 as functions of $[C_V\mathfrak{M}(\vec{\alpha})]/[C_A\mathfrak{M}(\vec{\sigma}\times\vec{r})]$. In this figure we have assumed nuclear radii $R=1.2A^{1/3}\times10^{-13}$ cm and $R=1.3A^{1/3}\times10^{-13}$ cm, and that $C_A=-1.21C_V$. The value of $\mathfrak{M}(\vec{\alpha})/\mathfrak{M}(\vec{\sigma}\times\vec{r})$ allowed by experiment is also given in Table I for the two values of the nuclear radius.

For comparison we have also included the conventional approximation[1,2] for the radial functions

Table I. Experimental values of $\mathfrak{M}(\vec{\alpha})/\mathfrak{M}(\vec{\sigma}\times\vec{r})$ for several evaluations of the lepton radial wave functions.

Lepton radial wave functions employed	
"Exact," $R=1.3A^{1/3}\times10^{-13}$ cm	-29.4 ± 1.4
"Exact," $R=1.2A^{1/3}\times10^{-13}$ cm	-29.5 ± 2.3
"Approx.," $R=1.3A^{1/3}\times10^{-13}$ cm	-36.6 ± 1.0

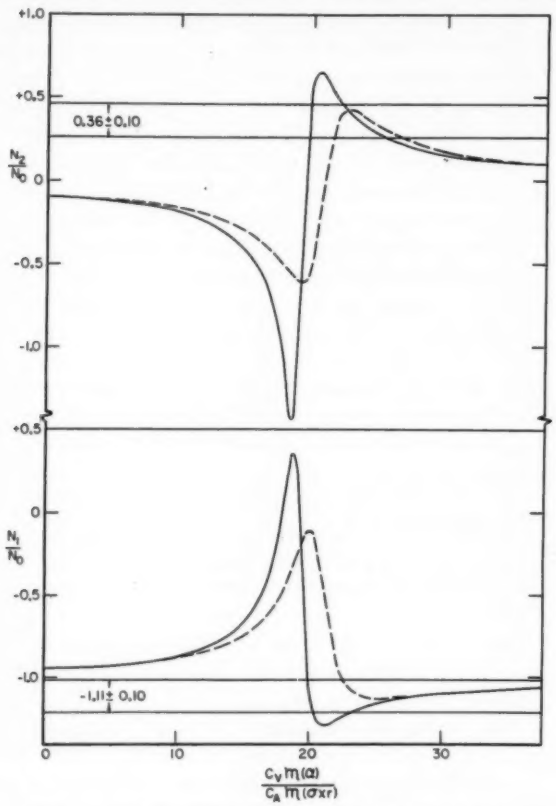

FIG. 3. The quantities N_1/N_0 and N_2/N_0 as functions of $[C_V\mathfrak{M}(\vec{\alpha})]/[C_A\mathfrak{M}(\vec{\sigma}\times\vec{r})]$, using exact Coulomb radial functions. The values of $[C_V\mathfrak{M}(i\vec{r})]/[C_A\mathfrak{M}(\vec{\sigma}\times\vec{r})]$ and $[C_A\mathfrak{M}(iB_{ij})]/[C_A\mathfrak{M}(\vec{\sigma}\times\vec{r})]$ have been fixed by adopting the single-particle values and $C_A=-1.21C_V$. The solid line corresponds to $R=1.3A^{1/3}\times10^{-13}$ cm, and the dashed line corresponds to $R=1.2A^{1/3}\times10^{-13}$ cm.

expanded in powers of ξ for a point nucleus but evaluated at $R=1.3A^{1/3}\times10^{-13}$ cm. It is instructive to see how poor the approximation is compared to the more exact treatment.

Figure 3 indicates that for certain choices of the radius $\mathfrak{M}(\vec{\alpha})/\mathfrak{M}(\vec{\sigma}\times\vec{r})$ may be double valued. The lower value can be rejected as being incompatible with the observed spectrum shape. It is interesting to note that the large coefficient for the P_2 term is consistent with the measured shape. The errors quoted in Table I do not include any uncertainty in the correct ratio for C_A/C_V in this particular transition. It is also interesting to note that a radius much smaller than $R=1.2A^{1/3}\times10^{-13}$ cm would be incompatible with the experimental results.

Several theoretical estimates of $\mathfrak{M}(\vec{\alpha})/\mathfrak{M}(i\vec{r})$ based on various models have been discussed by Rose and Osborn,[8] Ahrens and Feenberg,[9] and Pursey,[10] and our value for $\mathfrak{M}(\vec{\alpha})/\mathfrak{M}(\vec{\sigma}\times\vec{r})$ lies at about the negative mean of these estimates.

The absolute magnitude of the nuclear matrix elements may be fixed by fitting the calculated total transition probability to the observed *ft* value, viz., $\log ft=7.7$. Information on the radial integrals and configurational mixing is thereby obtained. The observed *ft* is several orders of magnitude greater than the lower limit that is predicted using our matrix-element values when one assumes a pure single-particle configuration with complete overlap of the radial functions.

Finally, we have also a preliminary determination of the β-correlation function calculated by Morita and Morita[11] for the 435-kev, $\Delta J=0$, transition to the excited state. However, the six contributing matrix elements cannot be uniquely defined by the limited number of parameters thus far determined. We are not presenting our results on this transition until further work is completed, at which time we shall present a more complete exposition of the experimental results.

[1]M. Morita and R. S. Morita, Phys. Rev. 109, 2048 (1958).
[2]A. M. Bincer, Phys. Rev. 112, 244 (1958).
[3]C. S. Wu, E. Ambler, R. W. Hayward, D. D. Hoppes, and R. P. Hudson, Phys. Rev. 105, 1413 (1957).
[4]C. P. Bhalla and M. E. Rose, Oak Ridge National Laboratory Report ORNL-2924 (unpublished).
[5]M. S. Freedman and D. W. Engelkemier, Phys. Rev. 79, 897 (1950).
[6]J. T. Jones, Jr., and E. N. Jensen, Phys. Rev. 97, 1031 (1955).
[7]H. Noya, A. Arima, and H. Horie, Progr. Theoret. Phys. (Kyoto) Suppl. No. 8, 33 (1959).
[8]M. E. Rose and R. K. Osborn, Phys. Rev. 93, 1326 (1954).
[9]T. Ahrens and E. Feenberg, Phys. Rev. 86, 64 (1952).
[10]D. L. Pursey, Phil. Mag. 42, 1193 (1950).
[11]M. Morita and R. S. Morita, Phys. Rev. 110, 461 (1958).

ISOTOPIC SPIN ADMIXTURES IN $Ge^{66} \rightarrow Ga^{66} \rightarrow Zn^{66}$ β TRANSITIONS*

W. P. Alford and J. B. French
Department of Physics and Astronomy, University of Rochester, Rochester, New York
(Received January 9, 1961)

There has been recent discussion,[1] stimulated by the theory of the conserved vector interaction,[2] concerning the goodness of the isotopic spin quantum number T in low-lying states of intermediate-weight nuclei. Isotopic spin admixtures have been measured by determining the Fermi contribution to a $\Delta J = 0$ ($J \neq 0$), $\Delta T = 1$ β transition which proceeds mainly via a Gamow-Teller interaction.

The fact that the odd-odd nucleus Ga^{66} has spin zero[3,4] implies that both of the transitions $_{32}Ge^{66} \rightarrow _{31}Ga^{66} \rightarrow _{30}Zn^{66}$ involve a $\Delta J = 0$ ($J = 0$) isotopic-spin-forbidden pure Fermi transition. It then follows that the ft values[5] ($\log ft \geq 6.8$ for the first, $\log ft = 7.88$ for the second) supply rather precise determinations of isotopic-spin admixtures. The three ground states must have different T values (since otherwise one or both of the transitions would be superallowed) and we can assume, without affecting the argument, that $T = 1, 2, 3$, respectively, which is most probable. We note first that the relativistic correction to the vector β decay interaction does not contribute in a $0^+ \rightarrow 0^+$ decay.[6] Then if mesonic effects are negligible or conserve isotopic spin, we see that the Ge^{66} β decay proceeds via an admixture in its own ground state of the $T = 2$ level which is the analog of the Ga^{66} ground state. Similarly Ga^{66} decays via an admixture in its ground state of the analog of the Zn^{66} ground state. We label these amplitudes as α_{21} and α_{32}, respectively. For a transition of this variety with T, $T_z = T$, $T_z + 1$ the ft value is given by

$$(ft)^{-1} = C |\alpha|^2 (T - T_z)(T + T_z + 1),$$

where the constant C is determined by the O^{14} decay[7] ($T = 1$, $T_z = 0$, $\alpha = 1$, $ft \simeq 3100$). We then find immediately that

$$|\alpha_{21}|^2 \leq 3 \times 10^{-4}; \quad |\alpha_{32}|^2 = 1.4 \times 10^{-5}.$$

These small values do not of course give the total admixture since other 0^+ states, which do not contribute to the β decay, should be admixed. But the admixtures determined here are of exactly the same nature as those determined less accurately in the (β, γ) experiments: and, besides that, there are no experiments which determine the total T impurity. It is likely too that the total impurity is quite comparable with the values given for a single component since the density of low-lying 0^+ states which may be admixed should be quite small.[8] Small values would also be expected from the calculations of MacDonald,[9] of Bouchiat,[10] and of Iwao.[11]

It is probable that the $_{31}Ga^{64} \rightarrow _{30}Zn^{64}$ decay supplies an analogous example since the Ga^{64} ground-state spin is probably[12] 0^+. In this case $\log ft = 6.6$ which would give, for Ga^{64}, $|\alpha_{21}|^2 = 4 \times 10^{-4}$. A more certain determination of the Ga^{64} spin would be worthwhile. It would also be of interest to measure more accurately the ft value for Ge^{66} and to locate the contributing 0^+ state in Ge^{66}, Ga^{66}, and Ga^{64}.

We acknowledge a useful conversation concerning the $(\beta\gamma)$ experiments with Dr. S. D. Bloom.

---

*Supported in part by the U. S. Atomic Energy Commission.

[1]S. D. Bloom, L. G. Mann, and J. A. Miskel, Phys. Rev. Letters 5, 326 (1960), and references therein to earlier work.

[2]R. P. Feynman and M. Gell-Mann, Phys. Rev. 109, 193 (1958); R. P. Feynman, Proceedings of the Tenth Annual International Conference on High-Energy Physics, 1960 (Interscience Publishers, New York, 1960), p. 501.

[3]J. C. Hubbs, W. A. Nierenberg, H. A. Shugart, and J. L. Worcester, Phys. Rev. 107, 723 (1957); J. L. Worcester, W. A. Nierenberg, R. Marrus, and J. C. Hubbs, Bull. Am. Phys. Soc. 2, 383 (1957).

[4]A. Schwarzschild and L. Grodzins, Phys. Rev. 119, 276 (1960).

[5]K. Way, F. Everling, G. H. Fuller, N. B. Gove, C. L. McGinnis, and R. Nakasima, Nuclear Data Sheets (National Research Council, Washington, D. C.).

[6]A. Altman and W. M. MacDonald, Phys. Rev. Letters 1, 456 (1958).

[7]R. K. Bardin, C. A. Barnes, W. A. Fowler, and P. A. Seeger, Phys. Rev. Letters 5, 323 (1960).

[8]The argument could fail if the other 0^+ states were much more strongly admixed. On the other hand, the admixing Coulomb matrix element corresponding to α_{32} is $4 \times 10^{-3} \Delta E$, where ΔE is the excitation energy of the first 0^+, $T = 3$ state in Ga^{66}, and, assuming that ΔE is a few Mev, this is probably not an anomalously small value.

[9]W. M. MacDonald, Phys. Rev. 110, 1420 (1958).

[10]C. C. Bouchiat, Phys. Rev. 118, 540 (1960).

[11]S. Iwao, University of Rochester thesis, 1960 (unpublished).

[12]T. H. Jacobi, H. A. Howe, and J. R. Richardson, Phys. Rev. 117, 1086 (1960).

DEUTERON ELECTRIC QUADRUPOLE MOMENT*

J. P. Auffray
Institute of Mathematical Sciences, New York University, New York, New York
(Received December 19, 1960)

The nuclear radio-frequency spectra of molecular hydrogen and deuterium, first observed by Rabi et al.,[1] were reinvestigated by Ramsey et al.[2] From these experiments the value of the quadrupole coupling constant eQq, in the $v=0$, $J=1$ vibrational-rotational level of the electronic ground state of D_2, was determined with an estimated accuracy of better than 1 part in 10^3.

An accurate value for the deuteron electric quadrupole moment Q can be derived from this result if q, the electric field gradient along the molecular axis at one deuteron, is evaluated theoretically. This was done by Nordsieck[3] and later by Newell[4] using a trial molecular wave function which gave a molecular binding energy D_e of 4.566 ev.[5]

The present author has calculated q from a trial function which gives $D_e = 4.728$ ev. This is much closer to the experimental value[6] of 4.747 ev. The trial function was constructed in the framework of the Born-Oppenheimer approximation. Its electronic part consisted of an expansion in the electronic coordinates and the interelectronic distance, of the type first investigated by James and Coolidge,[7] and recently by Kolos and Roothaan.[8]

The value of q obtained from this function yields $Q = 2.82 \times 10^{-27}$ cm^2. This is about 3% larger than the currently accepted value based on Newell's result.

The discrepancy is larger than the estimate given by Newell.[4] Newell, however, obtained this estimate by an admittedly crude procedure. In addition it should be noted that q, in these calculations, is not stationary. Consequently no rigorous estimate of the error in q can actually be made.

The details of this calculation will be given in a forthcoming publication.

---

*The work presented in this paper is supported by the AEC Computing and Applied Mathematics Center, Institute of Mathematical Sciences, New York University, under contract with the U. S. Atomic Energy Commission.

[1] J. M. B. Kellogg, I. I. Rabi, N. F. Ramsey, Jr., and J. R. Zacharias, Phys. Rev. 57, 677 (1940).

[2] H. G. Kolsky, T. E. Phipps, Jr., N. F. Ramsey, and H. B. Silsbee, Phys. Rev. 87, 395 (1952).

[3] A. Nordsieck, Phys. Rev. 58, 310 (1940).

[4] G. F. Newell, Phys. Rev. 78, 711 (1950).

[5] Converted in electron volts from Newell's value in atomic units (see reference 4), using 1 a.u. = 27.210 ev.

[6] G. Herzberg, Spectra of Diatomic Molecules (D. Van Nostrand and Company, Inc., Princeton, New Jersey, 1950).

[7] H. M. James and A. S. Coolidge, J. Chem. Phys. 1, 825 (1933).

[8] W. Kolos and C. C. J. Roothaan, Revs. Modern Phys. 32, 219 (1960).

POSSIBLE EXISTENCE OF A NEW K' MESON*

J. Tiomno, A. L. L. Videira, and N. Zagury
Centro Brasileiro de Pesquisas Físicas and Faculdade Nacional de Filosofia, Rio de Janeiro, Brazil
(Received December 15, 1960)

It has been experimentally established that the Λ particles produced in the reaction

$$p + \pi^- \rightarrow K^0 + \Lambda \qquad (1)$$

are strongly peaked backward in the c.m. system. Pais[1] has tried to explain this result by assuming the existence of a $KK\pi$ interaction and that the main contribution to reaction (1) comes from the Feynman graph of Fig. 1, assuming χ^+ to be a K^+ meson. He has obtained a reasonable qualitative agreement with the available experimental data at 1.1 Bev. However, his scheme, supposing opposite parities for K^+ and K^0, leads to many problems of difficult solution, arising from the failure of charge independence of the π interaction. One such difficulty results from the lack of a $KK\pi^0$ interaction, which gives rise to a mass of charged π's smaller than that of π^0.[2]

In the present paper we shall try, maintaining the convenient features of the Pais scheme, to

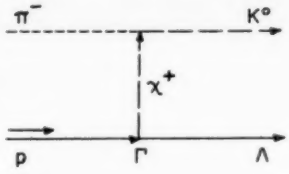

FIG. 1. Feynman diagram of the assumed predominant contribution to $K^0\Lambda$ production.

overcome such difficulties by assuming the existence of another K' meson of the same hypercharge and isospin (1/2) as those of the ordinary K meson but of opposite parity.[3]

Reaction (1) proceeds now mainly via the same graph as in Fig. 1 but with the intermediate χ^+ being a K'^+ meson instead of K^+.

In order to compute the differential cross sections of reaction (1) we add to the usual d'Espagnat Prentki interaction Hamiltonian density a $KK'\pi$ and a $\Lambda K'N$ term:

$$2m_K f(\bar{K}\vec{\tau}K' + \bar{K}'\vec{\tau}K)\cdot\vec{\pi} + g(\bar{K}'\bar{\Lambda}\Gamma N + \text{H.c.}), \quad (2)$$

where m_K is the mass of the K meson and Γ is 1 or γ_5 according to the parity of K'.

Using the Born approximation, we get for the differential cross section:

$$d\sigma/d\Omega = A\frac{1 + v_p v_\Lambda \cos\theta \pm m_\Lambda m_p/E_\Lambda E_p}{[m_\pi^2 + m_K^2 - \mu^2 - 2E_\pi E_K(1 + v_\pi v_K\cos\theta)]^2}, \quad (3a)$$

$$A = 4m_K^2(f^2/4\pi)(g^2/4\pi)p_K E_p E_\Lambda/(E_p + E_\pi)^2 p_\pi, \quad (3b)$$

where μ is the mass of the K' meson and θ is the angle between π and Λ in the c.m. system. The plus sign corresponds to $\Gamma = 1$ (K' scalar), and the minus to $\Gamma = \gamma_5$ (K' pseudoscalar).

Although the use of the Born approximation is not well justified, we compared (3) with the available experimental distributions at several values of the energy with the best statistics.[4,5] In this way we determined in each case the value of μ which gave the best fit. These values of μ (or μ^2) are given in Table I, for both scalar and pseudoscalar K'. The values of $fg/4\pi$ are also indicated for the cases where total cross sections were available. The most probable value was found to be

$$\mu = 605 \pm 49 \text{ Mev} \quad (K' \text{ scalar}), \quad (4a)$$

$$\mu = 176 \pm 46 \text{ Mev} \quad (K' \text{ pseudoscalar}). \quad (4b)$$

The last possibility can be immediately excluded since it would lead to a fast decay of K into $K' + \pi$. Thus we conclude that the K' (if it exists) is scalar, K being pseudoscalar in agreement with other experimental indications.[6]

In Fig. 2 all experimental data are plotted together to give an idea of the goodness of fit with a unique mass in the case of scalar K'. In order to do this we introduce the notation (c.m. system):

$$x(\theta, E) = 2E_\pi E_K(1 + v_\pi v_K\cos\theta) - (m_\pi^2 + m_K^2), \quad (5a)$$

$$z^{-2}(\theta, E) = \frac{d\sigma/d\Omega}{\sigma(E)L(\theta, E)} \int \frac{L(\theta, E)d\Omega}{[\mu^2 + x(\theta, E)]^2}, \quad (5b)$$

$$L(\theta, E) = 1 + v_p v_\Lambda \cos\theta + m_\Lambda m_p/E_\Lambda E_p. \quad (5c)$$

Thus Eqs. (3) imply that

$$z(\theta, E) = \mu^2 + x(\theta, E), \quad (6)$$

for all energies ($E = E_\pi^{\text{lab}}$) and angles.

The x and z coordinates for each experimental point plotted were obtained from (5) using $\mu = 605$ Mev. The values of $(1/\sigma)d\sigma/d\Omega$ and $\cos\theta$ used were average values in the intervals in which the angular distribution histograms, represented as functions of $\cos\theta$, were divided. The straight

Table I. Values of the mass of the hypothetical K' meson and the product of the coupling constants obtained by fitting the experimental data to the theoretical curve.

T_π^{lab} [a] (Bev)	K' scalar		K' pseudoscalar	
	μ (Bev)	$fg/4\pi$	μ^2 (Bev^2)	$fg/4\pi$
0.902[b]	0.90 ±0.20	···	0.048 ±0.034	···
0.907[b]	0.66 ±0.12	···	0.063 ±0.035	···
0.910[c]	0.45 ±0.11	0.33 ±0.07	-0.012 ±0.029	0.70 ±0.10
0.960[c]	0.49 ±0.11	0.43 ±0.09	0.011 ±0.099	0.91 ±0.40
1.200[c]	0.59 ±0.11	0.31 ±0.06	0.034 ±0.039	0.55 ±0.08
1.300[c]	0.80 ±0.12	0.48 ±0.09	0.103 ±0.085	0.69 ±0.08

[a] T_π^{lab} is the kinetic energy of the pion in the lab system.
[b] See reference 4.
[c] See reference 5.

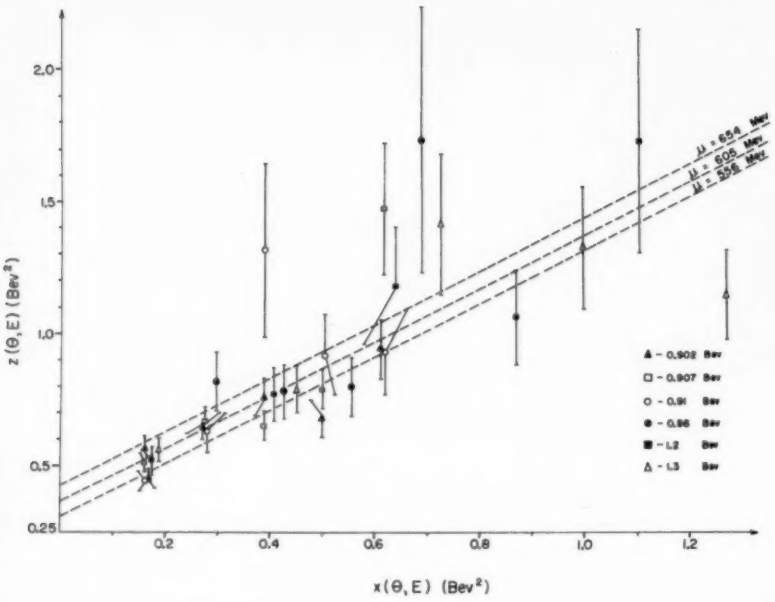

FIG. 2. Comparison of the experimental data on the angular distribution of Λ at several energies with theoretical curves (dashed lines). The values of the mass of the hypothetical K' meson are indicated. The coordinates x and z are defined by Eqs. (6).

lines indicated correspond to Eq. (6) for values of $\mu = 605$, and 605 ± 49 Mev. The fit of the experimental points in Fig. 2 with these theoretical lines seems to be very good except for the points to the right which correspond to $\cos\theta \sim 1$, as should be expected. These points also have poorer statistics. The fit in the case of pseudoscalar K' was not so good.

Actually the experimental points plotted are only appropriate for the comparison with the theoretical line for $\mu = 605$ Mev since z_{exp} depends on μ. However, for the two other values (605 ± 49 Mev) the experimental points would be only slightly shifted. If we interpret these results as indicating the existence of the K' meson, this meson should have a mass $\mu \geq m_K + m_\pi$ for otherwise it would have been already observed. Then K' should be very short-lived since the interaction leading to $K' \to K + \pi$ is strong. However, it cannot be excluded that the K' meson does not exist, representing only a pair of π and K, which are exchanged between the baryons and a $KK\pi\pi$ vertex. The existence of the K' can be tested indirectly by the study of the reaction

$$\pi + N \to K + \pi + \Lambda \text{ (or } \Sigma), \tag{7}$$

if the graph of Fig. 3(a) gives a significant contribution. Thus there should be a characteristic peaking in the energy distribution of Λ (or Σ) in the c.m. system at a point depending on the mass of K'. The values (4a) should not, however, be taken very seriously due to the approximations made which are more satisfactory for higher π energies. As seen from Table I, larger values of μ are obtained at higher energies. Also in this peak the Λ (and Σ) should have some backward preference and strong $K\pi$ angular correlations should be observed. The most spectacular effects of similar kind would occur, however, in the reaction

$$K + N \to K + \pi + N, \tag{8}$$

due to the graph of Fig. 3(b).

A more detailed version of the present paper will appear in Anais da Academia Brasileira de Ciências.

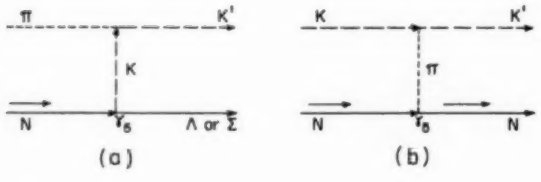

FIG. 3. Diagrams of (a) π production of K'; (b) scattering of K producing a K'.

*The essential results of this paper were reported by J. Tiomno at the 1960 Rochester Conference during

the discussion of Gell-Mann's paper. This work was supported in part by the Conselho Nacional de Pesquisas, Rio de Janeiro.

[1]A. Pais, Phys. Rev. 112, 624 (1958).

[2]J. Tiomno (unpublished).

[3]See also M. Gell-Mann, Proceedings of the 1960 Annual International Conference on High-Energy Physics at Rochester (Interscience Publishers, New York, 1960).

[4]M. Schwartz, Proceedings of the 1960 Annual International Conference on High-Energy Physics at Rochester (Interscience Publishers, New York, 1960). We are thankful to Dr. Schwartz who kindly supplied us with the data.

[5]F. Eisler et al., Nuovo cimento 10, 468 (1958).

[6]M. Moravcsik, Phys. Rev. Letters 2, 352 (1959); C. M. Meltzer, Ph. D. thesis, Duke University, 1960 (unpublished).

SOLAR-PRODUCED COSMIC RAYS NEAR THE NORTH AND SOUTH POLES*

M. A. Pomerantz, S. P. Duggal, and K. Nagashima
Bartol Research Foundation of The Franklin Institute, Swarthmore, Pennsylvania
(Received January 16, 1961)

The sudden arrival of solar-produced cosmic radiation of sufficient energy to be detectable at ground stations, a relatively rare phenomenon, has for the first time been observed simultaneously by the two neutron monitors which are currently closest to the North and South geomagnetic poles. Two events, each of which appeared to be associated with a solar flare of Importance 3+, occurred on November 12 and 15, 1960, respectively, the former displaying some remarkable features.

The locations of the Arctic and Antarctic stations operated by the Bartol Research Foundation are listed in Table I, and the relevant data are plotted in Fig. 1. The intensity is expressed in terms of percent deviation from the preflare mean (0000 to 1200 U. T. on November 12) of barometric pressure-corrected counts, recorded during 15-minute intervals. It is apparent that, on November 12, the increase at both stations manifested an unusual double-hump structure, whereas the November 15 event is similar to previous flare-associated intensity enhancements.

It is interesting to note that, on November 12, greater increases in intensity were recorded at the Antarctic station during the period of the first hump. On the contrary, the increases at both stations were approximately equal thereafter, although there is some uncertainty in the comparison of the amplitudes of the second maximum on this date, owing to a 45-minute gap in the record during the weekly routine Ra-Be source runs.

As a quantitative measure of the relative intensity enhancement at the two polar stations, the ratios of the increases, ΔI(McMurdo)/ΔI(Thule), are also plotted in Fig. 1. The 12-hour preflare mean counting rate on each of the two respective dates is selected as reference level for the percent deviation, ΔI. This ratio attains a maximum about 30 minutes after onset, and approaches unity after approximately 5 hours on November 12. The first peak in the ratio ΔI(McMurdo)/ΔI(Thule) occurs during the rising portion of the first hump, while the second peak occurs between the two humps. A single peak of shorter duration also occurs during the rising portion of the event of November 15.

The onset times, and times and amplitudes of maxima, are listed in Table II. Onset is defined as the first 2-minute interval during which, together with five consecutive equal intervals, the

Table I. Locations of the polar neutron monitor stations.

Station	Geographic coordinates Latitude	Longitude	Altitude (meters)	Geomagnetic coordinates Latitude	Longitude
Thule	N 76.6°	W 68.8°	260	+88.0°	1.1°
McMurdo	S 77.9°	E 166.6°	48	-79.0°	294.3°

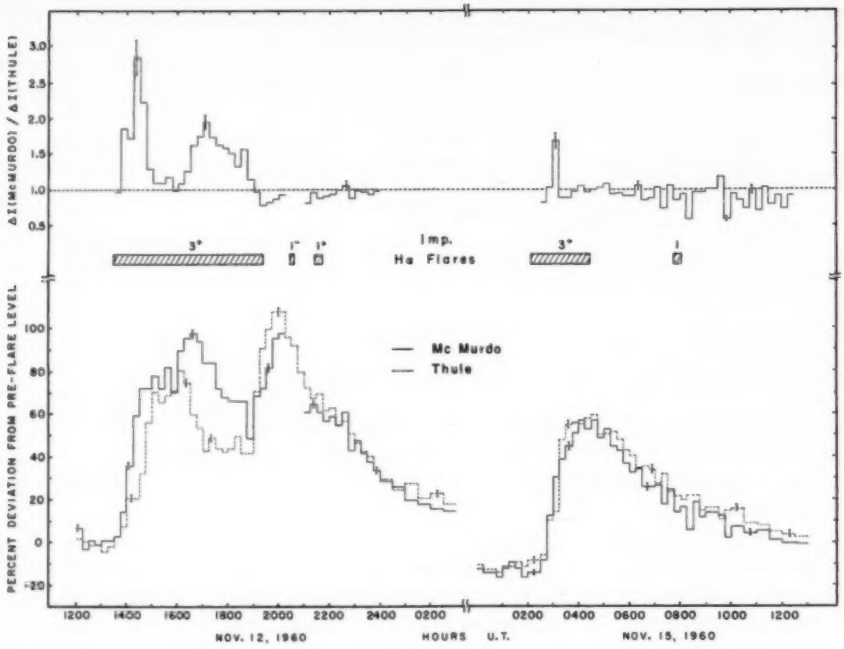

FIG. 1. Lower histograms: percent deviation from the preflare level of the intensity of the nucleonic component at Thule and McMurdo during the events of November 12 and 15, 1960. Upper histograms: ratio of percent deviation at McMurdo to that at Thule.

intensity exceeds by 2σ that which prevailed during one hour immediately preceding the flare. Maximum is defined as the 2-minute interval during which the intensity exceeds by 2σ that during the intervals on either side. Recorded counts uncorrected for pressure were selected for these time determinations. The indicated uncertainties arise solely from statistical considerations. Since, in the case of McMurdo, three equal maxima satisfying the above conditions occurred on November 12, the total period including all of these has been designated as the time of maximum. The amplitudes of the maxima are intensities expressed as percent deviations from the mean preflare intensity on November 12, pressure corrections having been applied.

Table II reveals that, within the experimental uncertainties, the onset times of the November 12 and 15 events are the same at both stations. However, in the former case, the initial intensity maximum is attained somewhat later, and is greater, at McMurdo than at Thule, in contrast with the November 15 increase.

The observation of these increases at polar stations is incompatible with simple impact zone theory.[1] Magnetized clouds in the interplanetary space, perhaps associated with the magnetic storm which commenced at 1350 U. T.

Table II. Comparison of the two events as observed at the polar stations.

Date	Hump	Times and amplitudes	Thule	McMurdo
November 12, 1960		Onset time, U. T.	1357 ±1	1355 ±1
	I	Time of maximum, U. T.	1608-1610	1624-1640
		Amplitude of maximum	103%	118%
	II	Time of maximum, U. T.	1958-2000	...
		Amplitude of maximum	135%	...
November 15, 1960		Onset time, U. T.	0239 ±1	0239 ±1
		Time of maximum, U. T.	0436-0438	0436-0438
		Amplitude of maximum	83%	85%

on November 12,[2] may have been responsible for the deflection of the solar-produced particles into the polar regions.

The double-hump structure of the increase in the intensity of the nucleonic component has not been observed previously. The most remarkable feature is the difference in the ratio, ΔI(McMurdo)/ΔI(Thule), in the first hump as compared with the second. For an isotropic distribution of cosmic-ray intensity, the ratio is approximately unity. Hence, a value of the ratio exceeding unity is indicative of an anisotropy in the intensity distribution of the solar-produced cosmic rays in the vicinity of the earth. As is seen in Fig. 1, the anisotropy prevailed during the first hump and isotropy has been almost established near the beginning of the second hump. A possible interpretation may be that, during the first hump, the earth was located near the boundary of the modulating region, which later completely surrounded the earth.

It is interesting to note that the anistropy was evident only during the exceptionally long duration (about 6 hours) of the Hα flare. However, the significance of this coincidence is not clear, especially since a Forbush-type decrease commenced[3] at approximately the same time as the termination of the optical flare.

It is a pleasure to acknowledge the important contributions to the program by Hugo A. C. Neuburg and Jamie Chapman who are in charge of the stations at McMurdo and Thule, respectively. Appreciation is expressed to the Geophysics Research Directorate for maintaining the Arctic Station at its Polar Research Facility, operated by the American Geographical Society under contract with the U. S. Air Force. The Antarctic Station is part of the U. S. Antarctic Research Program.

---

*This work was supported in part by grants from the National Science Foundation, and was also assisted by the Office of Naval Research.

[1]A. Schlüter, Z. Naturforsch. 6a, 613 (1951).

[2]We are grateful to Mr. Robert Clements for tracings of the magnetograms recorded at the New Zealand Station at Scott Base.

[3]K. G. McCracken, D. C. Rose, G. Schwachheim, R. Palmeira, and T. Thambyahpillai (private communications).

CLOUD-CHAMBER OBSERVATIONS OF PRIMARY COSMIC-RAY ELECTRONS*

James A. Earl
School of Physics, University of Minnesota, Minneapolis, Minnesota
(Received December 16, 1960)

This Letter reports new measurements of the flux of high-energy (0.3 Bev to 3.0 Bev) electrons and gamma rays at the top of the atmosphere. In 1949, an experiment using essentially identical equipment (a multiplate cloud chamber carried to high altitudes by a balloon) was performed by Critchfield, Ney, and Oleksa.[1] While no evidence for primary cosmic-ray electrons was found in that experiment, improvements in cloud-chamber technique and higher balloon altitude capability now make it possible to demonstrate the existence of a small flux of primary electrons.

Table I summarizes the data pertaining to the balloon flight and to the characteristics of the cloud chamber. Electrons and gamma rays were identified by the characteristic electron-photon cascade showers which they produced in the lead plates of the cloud chamber. These showers, which appear as a sequence of cones of minimum-ionizing nonpenetrating tracks emerging from the lower surfaces of the lead plates, are readily distinguished from events produced by nuclear interactions. The selection criterion that the axis of accepted showers had to pass through the illuminated areas of both the top and the bottom of the cloud chamber ensured that the axis passed through all five plates. In passing through this thickness of material a nuclear shower would almost certainly reveal its nature through the presence of penetrating particles and/or heavily ionizing evaporation tracks. Figure 1 shows a typical example of a shower produced by an electron. The incident electron appears in the top section of the chamber as a single minimum-ionizing track which lies on the axis of the shower. Since it is very unlikely that a background track or a back-scattered track from the shower would coincide accurately with the shower axis, it appears certain that events such as the one shown in Fig. 1 are initiated by high-energy electrons.

Table I. Data on the balloon flight and the cloud chamber.

Balloon flight	
Date:	May 12, 1960
Location:	Minneapolis, Minnesota (geomagnetic latitude 55°N)
Time at ceiling:	12 hours
Pressure altitude:	4 to 6.5 g cm^{-2}. Average: 4.5 g cm^{-2}
Multiplate cloud chamber	
Number of lead plates:	5
Thickness of plates:	0.6 cm - 7.5 g cm^{-2} (1.1 radiation lengths)
Sensitive time per picture:	(0.19 ±0.01) sec
Geometric factor for region bounded by illuminated areas of top and bottom:	(33.5 ±1.5) cm^2 sr

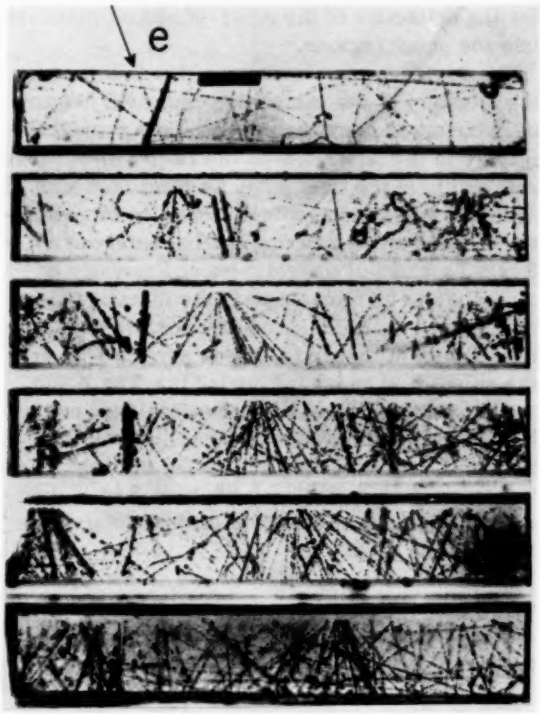

FIG. 1. A cloud-chamber picture of a shower produced by a high-energy electron. The incident electron is visible in the top section of the cloud chamber.

Shower events in which there was no trace of a track in the top section even though the axis was well illuminated were assumed to be initiated by gamma rays. There is no reason to believe that the upper section was insensitive at any time during the flight. The procedure used to determine the energies of the electrons and gamma rays is identical to that used by Roe and Ozaki[2] and is based on the Monte-Carlo calculations of Wilson.[3]

Figure 2 and Table II summarize the data taken while the balloon was at ceiling altitude. Figure 2 shows the differential energy spectra for the electrons and gamma rays. While it is certain that some electrons were incident upon the chamber, it is not possible to estimate the number of primary electrons without first knowing the number of secondary electrons produced in the atmosphere above the chamber. An upper limit for the number of secondaries can be computed from the observed number of gamma rays under the assumption that all the gamma rays arise from nuclear interactions above the chamber. The dashed histogram in Fig. 2 shows the energy spectrum of secondary electrons computed from the observed gamma-ray spectrum under the following assumptions: (a) The gamma rays arise only as decay products of π^0 mesons; (b) two charged π mesons are produced for every π^0 meson; (c) the charged π mesons and the π^0 mesons are produced with the same energy spectrum; and (d) the Michel parameter which describes the μ-meson decay spectrum has the value $\rho m = 0.75$.[4] Under these assumptions, most of the secondary electrons come from the decay of μ mesons created when the charged π mesons decay (a small contribution from pair production by the gamma rays has also been included). In the simplest approximation, the number of gamma rays and secondary electrons should be equal because there are two gamma rays per π^0 meson and two charged π mesons (each of which should ultimately give an electron) per π^0 meson. A more detailed analysis shows that less than half of the μ mesons decay before they reach the level of the balloon and that many of the electrons from these have energies so low that they could not be primary cosmic rays arriving at the latitude of Minneapolis. The net result is that, in the energy region accessible to primary cosmic rays (above 0.5 Bev), only 1.5 ± 0.4 secondary electrons are expected, while the total number of electrons observed was 11. There-

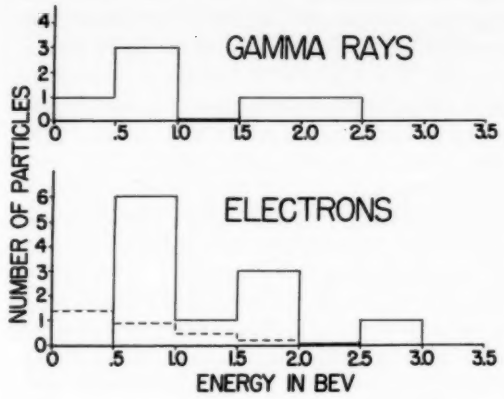

FIG. 2. Differential energy spectra for electrons and gamma rays. The dashed spectrum represents the secondary electrons that would be expected under the assumption that all the gamma rays are secondaries.

fore, most of the observed electrons must be primary cosmic rays. The pronounced peak in the electron energy spectrum between 0.5 Bev and 1.0 Bev is further evidence in favor of this conclusion because such a peak would appear if primary cosmic rays were excluded below the geomagnetic cutoff energy. (The cutoff energy for electrons at Minneapolis is about 0.7 Bev.)[5] While there is a low-energy (about 0.25 Bev) instrumental cutoff arising from the fact that very small showers are not easily recognized, more electrons than are observed would appear in the interval from 0 to 0.5 Bev if the spectrum of the observed electrons had the monotonic increase with decreasing energy which seems to be a characteristic of the spectrum of secondary electrons. A reasonable upper limit on the geomagnetic albedo (upward moving particles produced in the atmosphere which are returned to the earth by the geomagnetic field) is the upward flux at the point of observation. Since no upward moving electrons with energies greater than 0.5 Bev were recorded during the flight, it is very unlikely that the observed electrons arise from this source. (Most of the μ mesons whose decay electrons constitute the upward albedo would be expected to decay before they reach the level of the balloon.)

The value computed from the data in Tables I and II for the flux of electrons incident on the cloud chamber with more than 0.5-Bev energy is

$$I_e = (32 \pm 10) \text{ particles m}^{-2} \text{ sec}^{-1} \text{ sr}^{-1}.$$

No more than $(13 \pm 10)\%$ of this flux is due to

Table II. Tabulation of particles whose paths passed through illuminated areas of both top and bottom of cloud chamber.

Total number of electrons	11
Total number of gamma rays	6
Number of minimum-ionizing particles which penetrated all 5 plates	284
Number of penetrating particles corrected for nuclear interactions	380
Total number of pictures at ceiling	541

secondaries if the assumptions given earlier are correct. Since the correction for secondaries is small and since it is partially offset by absorption of the primary electrons, this flux is a close approximation to the true flux of primary electrons at the top of the atmosphere. The flux of protons determined from the number of minimum-ionizing penetrating particles selected by the same geometric criterion that was applied to shower axes is

$$I_p = (1100 \pm 100) \text{ particles m}^{-2} \text{ sec}^{-1} \text{ sr}^{-1}.$$

A correction based on a mean free path for nuclear interactions of protons in lead of 140 g cm^{-2} has been applied in computing this flux. The ratio of the electron flux to the proton flux is

$$I_e/I_p = (3 \pm 1)\%.$$

In 1949 Critchfield, Ney, and Oleksa set an upper limit on this ratio of 0.6%. The reasons that the above-measured value is larger than this upper limit are the following: (1) The minimum energy of the accepted showers was larger in the earlier experiment (1.0 Bev vs 0.5 Bev); (2) the proton flux was higher in 1949 than in 1960 (2200 p m^{-2} sec^{-1} vs 1100 p m^{-2} sec^{-1}); and (3) the thickness of the air above the balloon was less in the present experiment (4.5 g cm^{-2} vs 15 g cm^{-2}). The conclusion that primary electrons exist was made possible in the present experiment by (1) a clear separation of electrons and gamma rays which enabled a rigorous calculation of background effects to be made, and (2) the high altitude obtained which ensured that the flux of secondary electrons would be small.

Calculations by Ginzburg[6] indicate that synchrotron radiation from high-energy electrons would account for the observed intensity of galactic

radio emission if the density of electrons with energy greater than 1 Bev is on the order of 3×10^{-13} cm^{-3}. The density computed from the measured electron flux is 1.3×10^{-12} cm^{-3}, which appears to be more than enough to account for the observations of galactic radio noise.

An upper limit for the flux of electrons arising from nuclear interactions of cosmic rays with interstellar hydrogen gas can be obtained from the data which were used earlier to determine the number of secondary electrons produced in the atmosphere. Although the average thickness of matter traversed by a cosmic ray within the galaxy is about 1 g cm^{-2} (this thickness is suggested as an upper limit by considerations based on the relative abundances of protons and heavy nuclei in the cosmic-ray beam), the number of electrons produced in this thickness of interstellar hydrogen is about the same as the number produced in the 4 g cm^{-2} of air above the balloon. This occurs because the interaction probability per g cm^{-2} for hydrogen is about twice that for air and because all of the μ mesons produced in space decay while only half of those produced in the atmosphere above the balloon do so. (The flux of gamma rays from interstellar nuclear collisions is very small compared to the electron flux because the time that the electrons are trapped by galactic magnetic fields is large compared to the time required for the gamma rays to leave the galaxy on straight paths.) If the mean distances traversed in the galaxy by protons and electrons are equal, the electron flux arising from nuclear interactions in interstellar space is no larger than the flux arising from nuclear interactions in the atmosphere above the balloon. Since this flux was estimated to be only 13% of the total electron flux, it appears unlikely that all of the observed electrons arise from nuclear interactions of cosmic rays with interstellar hydrogen.

The author would like to thank Professor E. P. Ney for his interest in this investigation and Professor J. R. Winckler for his comments on the manuscript.

---

*Supported by the joint program of the U. S. Atomic Energy Commission and the Office of Naval Research.

[1]C. L. Critchfield, E. P. Ney, and Sophie Oleksa, Phys. Rev. 85, 461 (1952).

[2]B. P. Roe and S. Ozaki, Phys. Rev. 116, 1022 (1959).

[3]R. R. Wilson, Phys. Rev. 79, 204 (1950).

[4]W. F. Dudziak, R. Sagane, and J. Vedder, Phys. Rev. 114, 336 (1959).

[5]F. B. McDonald and W. R. Webber, Phys. Rev. 115, 194 (1959).

[6]V. L. Ginzburg, Progress in Elementary and Cosmic Ray Physics, edited by J. G. Wilson and S. A. Wouthuysen (North Holland Publishing Company, Amsterdam, 1958); Vol. 4, Sec. 5.

MEASUREMENT OF THE ANOMALOUS MAGNETIC MOMENT OF THE MUON

G. Charpak, F. J. M. Farley, R. L. Garwin,* T. Muller, J. C. Sens, V. L. Telegdi,† and A. Zichichi
CERN, Geneva, Switzerland
(Received January 16, 1961)

By storing polarized μ mesons in a magnetic field for as long as 1000 cyclotron periods it has been possible to measure directly the anomalous magnetic moment. We find the anomaly in agreement to within 2% (that is, 2×10^{-3} accuracy on the total magnetic moment) with that expected from the quantum electrodynamics of a Dirac particle.

At present the muon appears to be a heavy electron with no interactions except the electromagnetic and the weak. This concept gives no explanation for the muon-electron mass difference, but allows the muon magnetic moment to be calculated from the Dirac equation and quantum electrodynamics as[1-6]

$$\mu = g(e/2Mc) \times (\hbar/2), \tag{1}$$

with $g \equiv 2(1+a)$, the anomalous part of the moment, a, being

$$a_{\text{th}} \equiv (g-2)/2 = (\alpha/2\pi) + 0.75(\alpha^2/\pi^2) + \cdots = 0.001165, \tag{2}$$

with $\alpha^{-1} \equiv \hbar c/e^2 = 137.04$, the fine-structure constant of atomic physics. The first term in Eq. (2), $\alpha/2\pi$, arises from the emission and reabsorption of single photons, which alter the Dirac moment in two distinct ways, by the muon recoil, and by the muon spin-flip during the period of

existence of the virtual photon.

A "breakdown of quantum electrodynamics," for instance a cutoff on the photon propagator at energy $\Lambda m_\mu c^2$, will modify Eq. (2) to (approximately)[7]

$$a = (\alpha/2\pi)(1 - \tfrac{2}{3}\Lambda^{-2}) + \cdots, \qquad (3)$$

while the existence of a "fundamental length" L, which might be expected to introduce cutoffs on the muon form factor and muon propagator, as well as on the photon propagator, will also introduce[8] a correction of form Eq. (3), but with $\Lambda \sim \hbar(4McL)^{-1}$.

Thus an experiment to a precision of 10^{-5} on g, or 1% of the a to be expected from Eq. (2), is sensitive to the behavior of the electromagnetic field alone to a distance of $\sim 3\times10^{-14}$ cm, and to the existence of a fundamental length as small as 7.5×10^{-15} cm. Since there is nothing special about a photon, other fields with which the muon interacts would contribute in just the same way to the anomalous moment, scalar fields giving only the recoil effect while vector fields yield also the spin-flip term. Thus a 1% experiment is sensitive to the existence of a coupling constant of order of magnitude 10^{-4} to a field of mass equal to that of the muon, or 10^{-3} for a field of mass equal to that of the nucleon. Of course, these coupling constants depend on the type of coupling assumed.

The magnetic moment of the muon has been measured[9] to high accuracy in absolute units, as has the muon mass[10,11] (needed for computing the muon magneton in order to calculate g). But to determine a to 1% of the expected value would require the mass to $<10^{-5}$ accuracy, which seems impossible even with the advanced techniques employed so far.

Fortunately there exists a direct way to compare the magnetic moment with the muon magneton using the principle employed for the electron by Louisell, Pidd, and Crane[12] and already applied very roughly to the muon by Garwin et al.[13] If muons are made to circle in a magnetic field, the spin turns $(1+\gamma a)$ times as fast as the momentum vector, with the result that after time t in a magnetic field B the relative angle between spin and momentum is changed by the amount $\theta = aB\omega_0 t$, where ω_0 is the cyclotron frequency for zero-energy muons in unit magnetic field.[14,15] We wish to report here the first precision measurement of the muon anomalous moment by this method.[16]

The muon mean life, 2.2 microseconds for a muon at rest, sets a limit to the storage time t which may be used. In fact, if the only loss is due to decay, the optimum storage time is two mean lives. In such an experiment the problems are therefore to know the direction of the polarization of the muons (relative to the momentum) before and after the precession time t, to know the mean field B, and to know the time t spent in the field, all to an accuracy considerably better than 1%. In fact, we record the polarization angle θ as a function of storage time t, since in our method muons have a range of storage times from 2.0 μsec to about 6.5 μsec.

In our scheme shown in Fig. 1, longitudinally polarized muons, formed by forward decay of pions in flight inside the cyclotron, are focused by a bending magnet and quadrupole pair into the

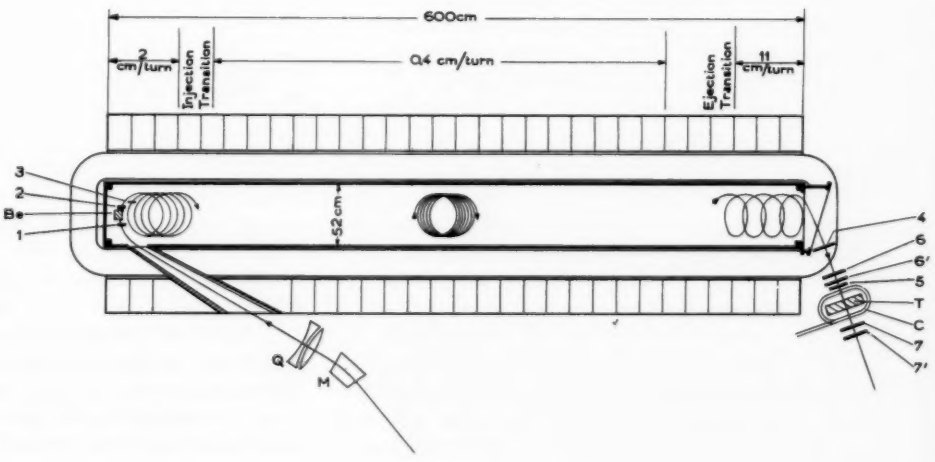

FIG. 1. General plan of the 6-meter magnet. M: bending magnet; Q: pair of quadrupoles; 1, Be, 2, 3: injection assembly consisting of Be-moderator and counters 1, 2, 3; T: methylene-iodide target; counters 66', 77': "backward" and "forward" electron telescopes. A stored and ejected muon is registered as a coincidence 4, 5, 66' $\overline{7}$, gated by a 1, 2, 3 and by either a forward or backward electron signal.

entrance channel of the "6-meter magnet" and cross the center line ($y=0$) at roughly 90°. At this point the muons are moderated by a beryllium block to a mean energy corresponding to a radius of curvature R of 19 cm in the magnetic field B_0 of 15.8 kgauss. The field is not uniform but has at any x in the horizontal median plane the form

$$B(y)=B_0(1+ay+by^2+cy^3), \quad (4)$$

in which the term ay produces a walking towards $+x$ with a "step-size" per turn, $S=\pi R^2 a$, where R is the orbit radius. The term by^2 with $b<0$ adds vertical focusing, and the term cy^3 changes the step-size to

$$S=\pi R^2(a+0.75cR^2), \quad (5)$$

allowing one to choose c to give constant S for all R in the neighborhood of the mean radius. Such a field with $c=0$ and with a and b constant in x has been used at this laboratory with a smaller magnet to store muons for 25 turns and to measure their electric dipole moment.[17]

In the injection region, $S\sim 2$ cm/turn to allow considerable tolerance in alignment. A slow transition is then made to a weaker gradient giving a storage region with $S=4$ mm/turn, while in the ejection region the step-size is 10 cm/turn to allow the particle to cross the exit face of the magnet nonadiabatically and so to be ejected from the field. In practice the desired field shapes were obtained by shimming a magnet with flat pole faces with many layers of 0.5-mm steel shims. About 300 kg of shim is inside the magnet vacuum chamber.

Hall plate measurements showed that the necessary field form had been obtained, and the desired motion of the orbits was verified by studying the flux through a search coil of 18-cm radius, the flux through the walking orbit being an adiabatic invariant. The field is calibrated by proton resonance. A change of field of 0.1% from one end of the storage region to the other would produce a 2.5-cm sidewise displacement of the orbit and would lead to a considerable loss in intensity. By correcting local inhomogeneities by shims as thin as 0.03 mm, we achieved a field in which the orbits do not wander by more than ±1 cm laterally.

The timing to ~0.1% accuracy is done with a "digitron" developed from that of Swanson and Lundy.[18] Additional dead-time circuits are incorporated to remedy some minor defects in the original instrument and the timing is now referred to a 10-Mc/sec crystal oscillator. It is of great importance not only to time every muon to 1%, but also to reduce below 0.1% the probability of assigning the wrong injection count to an emerging μ, etc. The electronics which accomplishes this is too complex to discuss in full here, but it has a timing accuracy of 10^{-9} sec and a flat spectrum between random events to $\ll 1\%$; and it rejects completely all cases of doubtful parentage or progeny of no matter how high order.

The muons emerging from the magnet are stopped in a field-free region (<0.1 gauss) in a nondepolarizing, nonconductive target (methylene iodide). The electronics stores events associated with "backward decay electrons" (6-6′ coincidences with appropriate gating) in channels 1-50 of a CDC "pulse-height analyzer," as a function of the storage time t of the parent muon in the magnet (2.0-6.5 μsec); similarly events associated with forward decay electrons in telescope 7-7′ are classified according to storage time in channels 51-100. The muon spin direction is flipped in successive runs through ±90° in the 1.0 μsec following its arrival by means of a pulsed vertical magnetic field produced by an aluminum-tape coil wound on the target. From the counts c_{n+} and c_{n-} in the nth channel for ±90° flipping, one can compute independently for each channel an asymmetry

$$A_n=(c_{n+}-c_{n-})/(c_{n+}+c_{n-})=A\sin(aB\omega_0 t_n), \quad (6)$$

where A is proportional to the polarization of the incident beam and t_n is the storage time corresponding to the nth and $(n+50)$th channel.

Figure 2 shows the observed data as well as the computed curve of the form (6) which fits it best. In actual practice the muons available for injection are not exactly longitudinally polarized. There is a transverse component which varies with range ($\sim 5°/\text{g cm}^{-2}$), crossing zero at the peak of the range curve. This has been measured and included in the calculation, as has the angular distribution of decaying muons with respect to the normal to the polarization analyzer. The parameter $(g-2)/2$ for this best fit is

$$a_{\text{exp}}=a_{\text{th}}(0.983\pm 0.019)=0.001145\pm 0.000022, \quad (7)$$

and the χ^2 for this fit is 13.5, in comparison with 9.7 expected.[19]

Of the 1.9% error quoted in Eq. (7), 1.7% is statistics, 0.6% comes from the uncertainty in the measured direction of the ejected beam, 0.6% from uncertainty in the part of the range spectrum (and hence transverse polarization) of the

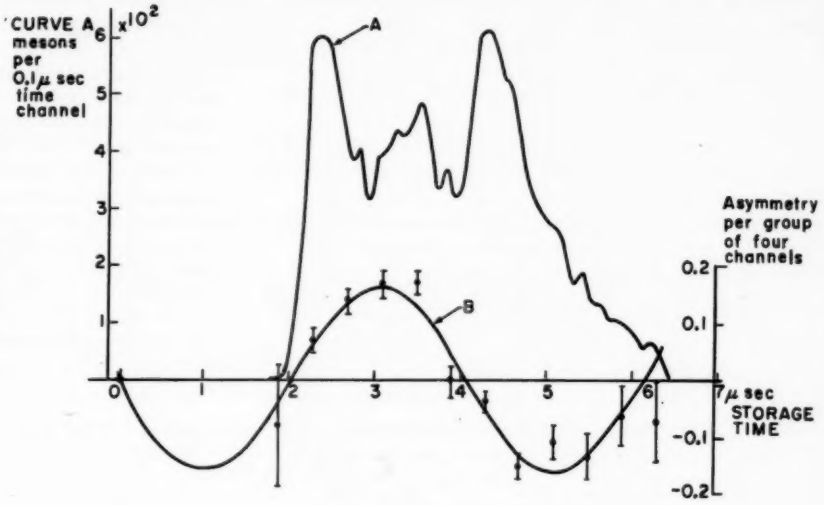

FIG. 2. Curve *A* (left-hand scale for ordinate): Storage-time distribution of muons that stop in the polarization analyzer and give rise to decay electrons. Curve *B* (right-hand scale for ordinate): The sinusoidal curve [see formula (6)] represents the best fit to the measured variation of the asymmetry with storage time. The curve must pass through the point near zero time, which is a very important datum for the fitting.

injected beam, and 0.3% from the statistical uncertainty in the initial polarization measurement.

We conclude that, using the available theoretical estimates,[1-8] and barring accidental cancellation of the effects on the muon moment, the following assertions can be made with 95% confidence:

(1) Conventional quantum electrodynamics is applicable to distances as small as 7×10^{-14} cm.

(2) The "radius" of the muon is less than 4.5×10^{-14} cm.

(3) No fundamental length exists with magnitude larger than 2×10^{-14} cm.

(4) The coupling constant $G^2/4\pi$ of the muon to an unknown field of nucleonic mass is less than $\sim3\times10^{-3}$, this limit varying approximately as $\lambda^2(\ln\lambda)^{-1}$, with $\lambda\equiv M/m_\mu$.

Combining our result with the muon precession measurement,[9] we obtain for the mass of the muon 206.77 ± 0.01 electron masses.

We wish to thank Professor G. Bernardini in particular for several decisions which were essential to the successful conclusion of this experiment, and Professor C. M. York for his close collaboration. Mr. B. Nicolai was of great technical assistance, as were R. Bouclier and L. Magnani. Professor W. K. H. Panofsky contributed very significantly during the fall of 1959. We are grateful to several physicists in this laboratory, in particular Dr. A. Petermann, for clarification of theoretical questions.

A more complete report, with details of the experimental techniques, of orbit theorems, etc., will be published.

---

*Ford Foundation Fellow from IBM Watson Laboratory, Columbia University, New York, New York.

†National Science Foundation Senior Postdoctoral Fellow from Department of Physics and Enrico Fermi Institute for Nuclear Studies, University of Chicago, Chicago, Illinois.

[1]J. Schwinger, Phys. Rev. 73, 416 (1948).

[2]R. Karplus and N. M. Kroll, Phys. Rev. 77, 536 (1950).

[3]H. Suura and E. H. Wichmann, Phys. Rev. 105, 1930 (1957).

[4]A. Petermann, Phys. Rev. 105, 1931 (1957).

[5]C. M. Sommerfield, Phys. Rev. 107, 328 (1957).

[6]A. Petermann, Helv. Phys. Acta 30, 407 (1957).

[7]V. B. Berestetskii, O. N. Krokhin, and A. K. Khlebnikov, J. Exptl. Theoret. Phys. (U.S.S.R.) 30, 788 (1956) [translation: Soviet Phys.—JETP 3, 761 (1956)].

[8]B. de Tollis, Nuovo cimento 16, 203 (1960).

[9]R. L. Garwin, D. P. Hutchinson, S. Penman, and G. Shapiro, Phys. Rev. 118, 271 (1960); also more recent results of D. P. Hutchinson, J. Menes, A. M. Patlach, S. Penman, and G. Shapiro [Proceedings of the 1960 Annual International Conference on High-Energy Physics at Rochester (Interscience Publishers, New York, 1960), p. 778].

[10]J. F. Lathrop, R. A. Lundy, V. L. Telegdi, R. Winston, and D. D. Yovanovitch, Nuovo cimento 17, 109 (1960). J. F. Lathrop, R. A. Lundy, S. Penman, V. L. Telegdi, R. Winston, and D. D. Yovanovitch, Nuovo cimento 17, 114 (1960).

[11]S. Devons, G. Gidal, L. M. Lederman, and

G. Shapiro, Phys. Rev. Letters 5, 330 (1960).
[12]W. H. Louisell, R. W. Pidd, and H. R. Crane, Phys. Rev. 94, 7 (1954); A. A. Schupp, R. W. Pidd, and H. R. Crane, Phys. Rev. 121, 1 (1961).
[13]R. L. Garwin, L. M. Lederman, and M. Weinrich, Phys. Rev. 105, 1415 (1957).
[14]H. Mendlowitz and K. M. Case, Phys. Rev. 97, 33 (1955).
[15]V. Bargmann, L. Michel, and V. L. Telegdi, Phys. Rev. Letters 2, 435 (1959); M. Fierz and V. L. Telegdi (to be published).
[16]A preliminary measurement by a somewhat different method was presented by us at the Rochester Conference [G. Charpak et al., Proceedings of the 1960 Annual International Conference at Rochester (Interscience Publishers, New York, 1960), p. 778].
[17]G. Charpak, L. M. Lederman, J. C. Sens, and A. Zichichi, Nuovo cimento 17, 288 (1960).
[18]R. A. Swanson, Rev. Sci. Instr. 31, 149 (1960); R. A. Lundy (private communication).
[19]The result (7) is the best least-squares fit to the data grouped in time channels 0.400 μsec wide. A maximum-likelihood solution for the anomaly has also been made on the IBM 709. The result is $a_{exp} = 0.001144 \pm 0.000022$. The individual fits for forward electron telescopes and back are (with the full 0.100-μsec digitron resolution): $a_{exp} = 0.001147$ (forward), $a_{exp} = 0.001142$ (backward). To allow A in (6) to be an arbitrary linear function of the time changes a_{exp} by $\sim 1 \times 10^{-6}$.

ELASTIC SCATTERING OF LOW-ENERGY K^- MESONS ON PROTONS

D. H. Davis and R. D. Hill*
University College, London, England

B. D. Jones, B. Sanjeevaiah,† and J. Zakrzewski‡
H. H. Wills Physics Laboratory,‖ University of Bristol, Bristol, England

and

J. P. Lagnaux
Laboratoire de Physique Nucléaire, Université Libre de Bruxelles, Brussels, Belgium
(Received January 3, 1961)

Following the CERN Conference in 1958[1] there was considerable interest shown in the possibility of a peak at ~30-Mev K^--meson laboratory energy in the elastic scattering cross section of K^- mesons on protons. Matthews and Salam[2] proposed an interpretation of the peak in terms of a $J = 1/2$ resonance of the K^--p system. However, Jackson and Wyld[3] pointed out that the peak could also be satisfactorily understood on the basis of S-wave zero-range K^--p scattering theory and a repulsive K^--p nuclear interaction. The resonance proposal has also been discounted by Dalitz and Tuan[4] who pointed out that the effective range of the K^--p interaction would have to be unreasonably large in order to exhibit the observed elastic scattering cross sections at the low-energy values in the region of the so-called resonance.

At the Kiev Conference in 1959, bubble chamber results[5] were presented which no longer exhibited a peak in the low-energy elastic K^--p scattering cross section. However, further emulsion results[6] by the combined Bologna-Munich-Paris-Parma laboratories still tended to show the elastic cross-section flattening off at the lowest energies.

Emulsion data from the European K^- Collaboration groups[7] have now been carefully scrutinized for low-energy K^--proton elastic scattering events. All two-pronged events which could possibly be attributed to K^--p elastic scattering have been analyzed. Low-energy elastic scattering events on free protons can be readily recognized because these only will show coplanarity with complete balance of momentum and energy. Moreover, since the fraction of inelastic scattering events in which the K^- meson re-emerges from emulsion nuclei is known[8] to be only a few percent for energies in the range 30-100 Mev, there is a negligibly small chance of an apparent K^--p scattering occurring on an internal proton of an emulsion nucleus, especially for K^- meson energies below 10 Mev.

The results of our investigations, based on a study of 10 850 K^- mesons coming to rest and 2060 K^- mesons decaying or interacting in flight, are shown in Table I. Our results, which are shown with others of the bubble chamber[5] and emulsion[6] groups in Fig. 1, appear to indicate that the elastic K^--p scattering cross section is

Table I. Summary of low-energy K^--p elastic scattering events.

p (Mev/c)	53	93	133	173	213	253
Number of events	4	6	14	15	17	
Track lengths (cm)	659	1769	3977	6804	10497	
$\sigma_{el}(K^-p)$ (mb)	187	105	108	68	50	

increasing in the region of lowest K^--meson momentum. Although the statistics are still quite poor, on the basis of our observations, there is only an approximate 10% probability that the K^--p elastic scattering cross-section curve flattens off at momenta lower than 120 Mev/c.

There are possibly two explanations of the observed flattening in the earlier emulsion experiments. One could possibly be that because the track lengths in the lowest energy intervals were so small, different experimental groups probably made energy cutoffs at different values. In our present investigation we have consistently worked down to a K-meson momentum of 53 Mev/c, for which the residual range is 100 microns.

The other possible reason that many low-energy scattering events may not have been recorded is that they were classified as "double stars," i.e., they were regarded as K-meson capture stars and secondary stars resulting from interactions or decays of hyperons or hyperfragments. Photographs of two very low energy K^--p scattering events are shown in Fig. 2.

There is, of course, a third possibility: that the differences are largely statistical.

At the very low K^--meson energies considered in these experiments there may be, in point of fact, a significant contribution to the elastic scattering from the Coulomb field of the proton. The Coulomb effect on the total elastic scattering cross section has already been calculated, for the conditions of our experiment, by Jackson and

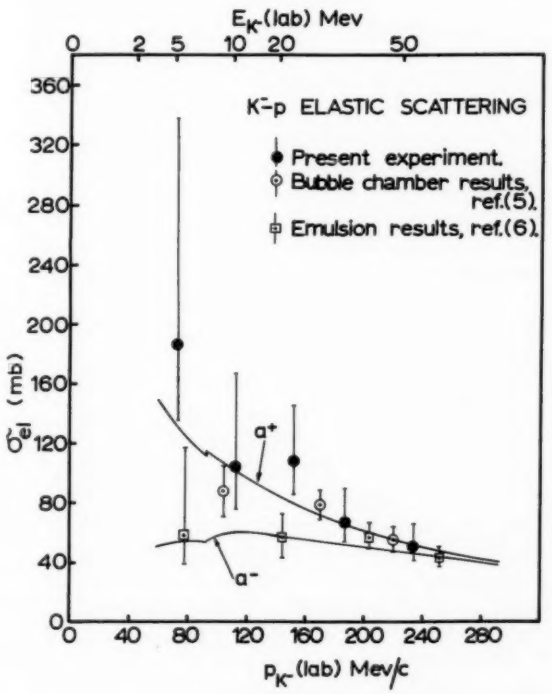

FIG. 1. Total elastic K^--p scattering cross sections versus K^--meson momentum. The curves, which were taken from the theory of Jackson and Wyld,[3] show the σ_{el} variation to be expected from constructive interference a+ and destructive interference a- between the Coulomb and nuclear parts of the K^--p scattering.

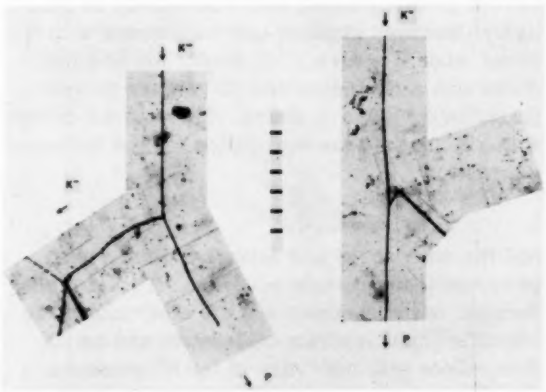

FIG. 2. Two examples of low-energy K^--p elastic scattering events. The energies of the incident K^- mesons are 5.5 and 5.3 Mev. Scale divisions (between photographs) are 10 microns apart.

Wyld.[3] They considered two cases, $a+$ and $a-$, of the nuclear K^--p scattering phase shifts, and these two curves are shown in Fig. 1. It is seen that our results, as also those of the Berkeley bubble chamber group, suggest the attractive $a+$ set of K^--p nuclear phase shifts.

---

*Fulbright and Guggenheim scholar on leave from University of Illinois, Urbana, Illinois.

†On leave from University of Mysore, Mysore, India.

‡On leave from University of Warsaw, Warsaw, Poland.

‖Miss V. Mayes and Mr. M. G. Bowler assisted in the early part of the work.

[1]M. F. Kaplon, 1958 Annual International Conference on High-Energy Physics at CERN, edited by B. Ferretti (CERN Scientific Information Service, Geneva, 1958), p. 171. Both the Berkeley Bubble Chamber data, Fig. 8, and the collected emulsion data, Fig. 13, showed essentially the same feature of a broad peak at $E_K \approx 30$ Mev or $p_K \approx 150$ Mev/c.

[2]P. T. Matthews and A. Salam, Phys. Rev. Letters 2, 226 (1959).

[3]J. D. Jackson and H. W. Wyld, Phys. Rev. Letters 2, 355 (1959). Their interpretation of a flattening in the elastic K^--p scattering cross section has been questioned by F. Ferrari, G. Frye, and M. Pusterla, Phys. Rev. Letters 4, 615 (1960), who suggested that at very low energies the flattening could be due to an interference between a two-pion exchange interaction and a short-range core-part nuclear interaction.

[4]R. H. Dalitz and S. F. Tuan, Phys. Rev. Letters 2, 425 (1959), footnote 2.

[5]L. W. Alvarez, University of California Radiation Laboratory Report UCRL-9354 (unpublished), Fig. 7; and Report of Kiev Conference, 1959 (unpublished).

[6]W. Alles, N. N. Biswas, M. Ceccarelli, R. Gessaroli, G. Quareni, M. Göing, K. Gottstein, W. Püschel, J. Tietge, G. T. Zorn, J. Crussard, J. Hennessy, G. Dascola, and S. Mora, Nuovo cimento 11, 771 (1959).

[7]K^- European Collaboration $K5$ stack, Nuovo cimento (to be published).

[8]W. Alles, N. N. Biswas, M. Ceccarelli, and J. Crussard, Nuovo cimento 6, 571 (1957); D. F. Davis, N. Kwak, and M. F. Kaplon, Phys. Rev. 117, 850 (1960); etc.

Ξ^- PRODUCTION BY K^- MESONS

William B. Fowler,* Robert W. Birge,† Philippe Eberhard,‡ Robert Ely, Myron L. Good,‖ Wilson M. Powell, and Harold K. Ticho**
Lawrence Radiation Laboratory, University of California, Berkeley, California
(Received January 6, 1961)

The Berkeley 30-inch propane chamber was operated in a 1.17-Bev/c K^- beam[1] at the Bevatron to produce cascade particles. Out of the 100 000 pictures taken, there have been 18 positively identified negative cascade decays with the decay mode $\Xi^- \to \Lambda + \pi^-$. Of these, six were produced with a K^+ meson and three were accompanied by a visible θ_1 decay. Three of the events with a K^+ satisfy the kinematics for the hydrogen interaction

$$K^- + p \to \Xi^- + K^+,$$

and the other three are assumed to have been produced from protons in carbon. Two of the K^+ decayed in the chamber and the other four were identified by comparing momentum and ionization. Since only one-third of the K^0 produced in the interaction

$$K^- + n \to \Xi^- + K^0$$

decay into a visible mode, it is quite consistent to attribute the nine events in which no positive-strangeness K particle was observed to the neutral mode of the θ_1 decay, to the θ_2 decay, or to a K^+ that could not be distinguished from a proton.

The 18 events were selected from a sample of 47 in which a V particle was thought to come from a prong of a K^- interaction which appeared to decay into a π^-. The selection consisted of a series of two single-origin constraints on an IBM-704 calculator: (a) the Q of the V particle was required to be consistent with that of a Λ, 37 Mev, and its line of flight consistent with the assumed Ξ^- decay origin; (b) the Λ and the π^- were required to be coplanar with the assumed Ξ^- and to balance transverse momentum. Revised estimates of the momentum and angles of the Λ and π^- were obtained from the constraint program, and the average mass of the Ξ^- for the 18 surviving events, weighted by the estimated probable error of each event, was found to be

$$M_{\Xi^-} = 1317.9 \pm 1.9 \text{ Mev}.$$

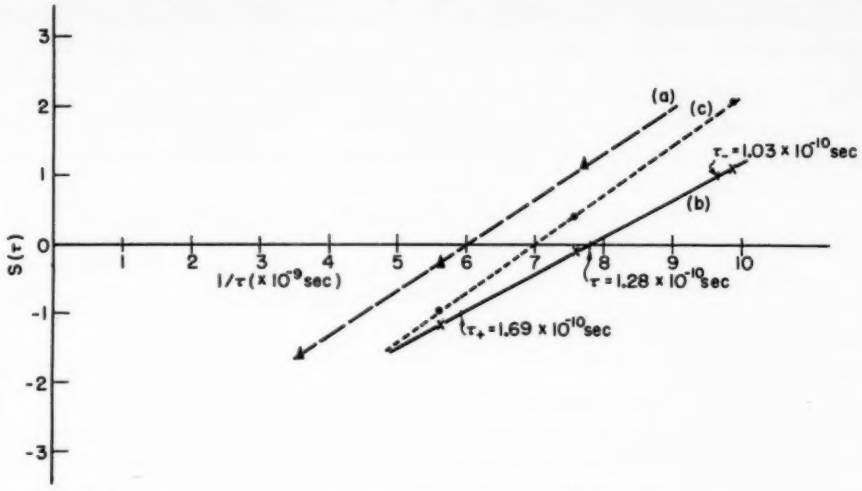

FIG. 1. Bartlett's $S(\tau)$ function with a Λ lifetime correction for (a) the 18 observed Ξ^- from this experiment, (b) this experiment corrected for scanning bias, and (c) the corrected data of this experiment combined with six events from Trilling and Neugebauer.[3]

The mean life of the Ξ^- has been determined by means of a modification of the statistical method of Bartlett[2] which accounts for the necessity of seeing the Λ decay before the Ξ^- leaves the chamber. The possible time for decay was determined by calculating the time of flight to the boundary of the fiducial region, which was chosen to allow a minimum of 4 cm for the measurement of the Λ decay. In all cases the correction due to finite chamber size is small, and the total correction amounts to less than 10% of the uncorrected mean of the actual flight times. The flight times include dE/dx corrections and the possible times were modified for those cases in which the Ξ^- would have come to rest before leaving the chamber. Figure 1 shows a plot of Bartlett's S function as a function of $1/\tau$. This function is zero at the most probable lifetime and ± 1 at the best estimate of the standard error. Figure 2 is a cumulative histogram of the calculated times of flight, t_i, and indicates a considerable scanning bias against flight times less than 0.5×10^{-10} sec. An estimate of the total number of events was obtained by fitting those events with a time of flight greater than 0.5×10^{-10} sec to the exponential $N_0 e^{-t/\tau}$. The revised mean life consistent with this procedure required the addition of seven events in the interval from zero to 0.5×10^{-10} sec, and was found to be

$$\tau = (1.28^{+0.41}_{-0.25})\times10^{-10} \text{ sec}.$$

The S function corrected for scanning bias is shown as the solid line b in Fig. 1. This mean life is considerably shorter than that found by Trilling and Neugebauer.[3] However, their events at high cascade momentum required much greater corrections for chamber size. The dashed line c in Fig. 1 shows the S function for their six events combined with our 25 (including corrections for scanning bias), and it is seen that the combined mean life falls within our error.

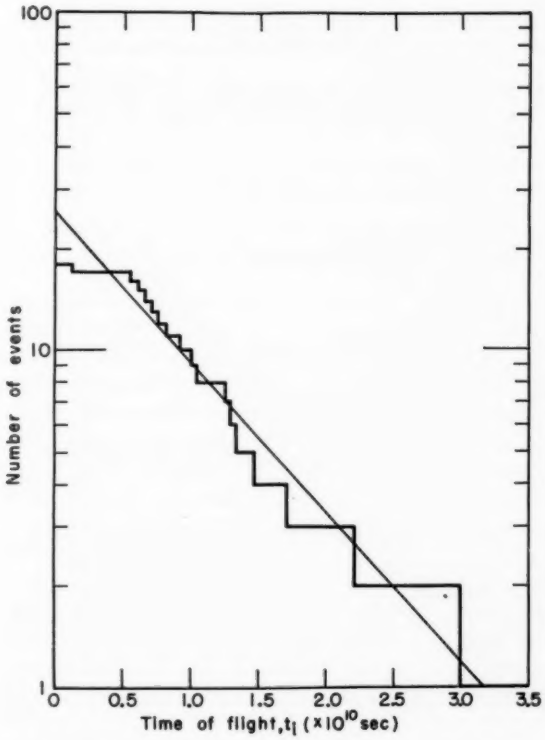

FIG. 2. A cumulative histogram of the times of flight of the Ξ^-. The solid line is the best fit of those events with $t_i > 0.5\times10^{-10}$ sec to an exponential.

A violation of parity conservation in the cascade decay will manifest itself as a fore-aft asymmetry in the Λ decay, the Ξ^- serving to polarize the Λ with the strength α_{Ξ} which is then analyzed by the Λ decay. Denoting a unit vector in the direction of the Λ in the Ξ^- rest frame as $\hat{u}$ and a unit vector in the direction of the proton in the Λ center-of-mass system as $\hat{p}$, the distribution of $\hat{u}\cdot\hat{p}$ is[4]

$$P(\hat{u}\cdot\hat{p})\,d(\hat{u}\cdot\hat{p}) = \tfrac{1}{2}[1+(\alpha_{\Xi}\alpha_{\Lambda})(\hat{u}\cdot\hat{p})]\,d(\hat{u}\cdot\hat{p}).$$

We have found, on the basis of the above 18 events,

$$(\alpha_{\Xi}\alpha_{\Lambda}) = -0.65\pm 0.35,$$

using $(\alpha_{\Xi}\alpha_{\Lambda}) = (3/N)\sum_i(\hat{u}\cdot\hat{p})_i$ as the best method of estimation. The negative sign shows the helicity of the Λ from the Ξ^- to be opposite to that of the proton from Λ decay. Birge and Fowler[5] find the helicity of the proton to be positive, implying that the helicity of the Λ is negative. Using the best estimate of the magnitude of $|\alpha_{\Lambda}|$ as 0.95 ± 0.07,[6] and the sign of α_{Λ} as determined by Birge and Fowler, we find

$$\alpha_{\Xi} = 0.69\pm 0.36.$$

The possibility of an up-down asymmetry of the decay π^- from $\Xi^-\to\Lambda+\pi^-$ produced in the reaction

$$K^-+N\to\Xi^-+K$$

has been examined, and $(\alpha_{\Xi}\bar{P})$ is -0.28 ± 0.40, where $\bar{P}$ is the polarization of the Ξ^- in production and α_{Ξ} the decay asymmetry parameter. There seems to be no indication that the Ξ^- produced in this manner from carbon are polarized.

In the 100 000 pictures we had a total of $(1.5\pm 0.2)\times 10^7$ cm of K^- track length. After adding seven events to correct for scanning bias and then 50% to correct for the unobserved neutral decay mode of the Λ, we estimate the total number of Ξ^- to be 37.5. On this basis the Ξ^- production cross section in the reaction $K^-+N\to\Xi^-+K$ is

$$\sigma_{\Xi^-} = 18\pm 5\ \mu\text{b/nucleon},$$

assuming an $A^{2/3}$ correction for shielding in the carbon nucleus.

*Brookhaven National Laboratory, Upton, New York.
†Laboratoire de Physique, Ecole Polytechnique, Paris, France.
‡Laboratoire de Physique, Collège de France, Berthelot, Paris, France.
‖Physics Department, University of Wisconsin, Madison, Wisconsin.
**Physics Department, University of California, Los Angeles, California.

[1]P. Eberhard, M. L. Good, and H. K. Ticho, University of California Radiation Laboratory Report UCRL-8878, August, 1959 (unpublished).
[2]M. S. Bartlett, Phil. Mag. 44, 249 (1953).
[3]G. H. Trilling and G. Neugebauer, Phys. Rev. 104, 1688 (1956).
[4]W. B. Teutsch, S. Okubo, and E. C. G. Sudarshan, Phys. Rev. 114, 1148 (1959).
[5]R. W. Birge and W. B. Fowler, Phys. Rev. Letters 5, 254 (1960).
[6]Frank S. Crawford, Jr., Lawrence Radiation Laboratory (private communication).

TEST FOR PION-PION RESONANCE

G. Pinski
Department of Physics and Astronomy, University of Rochester, Rochester, New York
(Received January 9, 1961)

It has been suggested[1] that the two-pion effective mass squared distribution in antinucleon annihilation could serve as an efficient test for the proposed pion-pion resonance. This currently fashionable resonance has been investigated on several fronts.[2-4] In this note, we would like to suggest a particular decay mode for study, in which the effects of a pion-pion resonance would be most easily detected.

The relative transition probability for annihilation into n mesons is given, according to the covariant statistical theory,[5] by

$$W_n = \int\prod_i^n [d^4p_i\ \theta(p_i^0)\delta(p_i^2-1)]f(P_N,P_{\bar{N}},p_i)\delta^4(P_N+P_{\bar{N}}-\sum_i^n p_i).$$

In this formalism the invariant function f is taken to be independent of the nucleon and pion four-momenta. A pion-pion resonance may be incorporated into the statistical theory by choosing f to be a resonant function in the effective mass of pairs of particles, peaked at the "resonant mass":

$$f = 1 + \lambda^2 \sum_{i>j} \mathfrak{F}[(p_i + p_j)^2 - M^2],$$

where $(p_i + p_j)^2 = (p_i^0 + p_j^0)^2 - (\vec{p}_i + \vec{p}_j)^2$ and λ^2, M^2 are two constants with the dimensions of the square of a mass. The effective mass squared distribution, ${}_nP_{12}(\mu^2)$, where $\int {}_nP_{12}(\mu^2)d(\mu^2) = W_n$, is given by

$${}_nP_{12}(\mu^2) = \int \prod_i^n [d^4p_i\, \theta(p_i^0)\delta(p^2 - 1)] \{1 + \lambda^2 \sum_{i>j} \mathfrak{F}[(p_i + p_j)^2 - M^2]\} \delta[(p_1 + p_2)^2 - \mu^2]\, \delta^4[P_N + P_{\bar{N}} - \sum_i^n p_i],$$

in units of the pion mass $|p_i| \equiv [(p_i^0)^2 - |\vec{p}_i|^2]^{1/2} = 1$.

This quantity is as useful as the angular correlation, but being covariant, is incomparably easier to evaluate. Since the effective mass $(p_1 + p_2)^2$ is equal to $2 + 2p_1 \cdot p_2$, it can be thought of as a measure of "covariant angle":

$$\theta_{\text{cov}} = \frac{p_1 \cdot p_2}{|p_1|\,|p_2|} = p_1 \cdot p_2.$$

This distribution has been calculated in the two extreme cases:

(1) $\lambda = 0$. ${}_nP^0$ is the distribution for no resonant term.

(2) $\lambda = \infty$. ${}_nP'$ is the distribution for resonant term only.

For case 2 there are three contributions:

(a) ${}_nP_{\gamma\gamma'}$ if the correlation is between the two particles which are in resonance.

(b) ${}_nP_{\gamma f}'$ if the correlation is between one resonant and one nonresonant particle.

(c) ${}_nP_{ff}'$ if the correlation is between nonresonant particles.

If one considers a pion-pion resonance in the $T = 1$ state, there will be a decided difference between the $\lambda = 0$ and $\lambda = \infty$ terms. In the $T = 1$ state, like pions cannot be in resonance and the like-pion correlation will not contain the term ${}_nP_{\gamma\gamma'}(\mu^2)$ which equals ${}_nP^0(\mu^2)\mathfrak{F}(\mu^2 - M^2)$. This term contains the effect of the resonance explicitly and is sharply peaked while the other terms are relatively broad. One therefore expects a marked difference between (++) or (--) and (+-) correlations.

For unlike pions, the $\lambda = \infty$ term is of the form $a\,{}_nP_{\gamma\gamma'} + b\,{}_nP_{\gamma f'} + c\,{}_nP_{ff'}$, while for like pions it is $b'{}_nP_{\gamma f}' + c'{}_nP_{ff}'$, the coefficients depending on the particular charge complexion of the annihilation. Only the ratios b/a, c/a, and c'/b' are important here. As n increases, b and c increase relative to a, since there remains only one way for the pair being correlated to be the resonant pair, while the total number of ways of choosing the resonant pair increases. Therefore the effect of a pion-pion resonance is more prominent for n small. The annihilation $\bar{p} + n \to \pi^- + \pi^- + \pi^+$ should be ideal. Here the $\lambda = \infty$ term for (--) is ${}_3P_{\gamma f}'$ and for (+-) is ${}_3P_{\gamma\gamma'} + {}_3P_{\gamma f}'$.

In Fig. 1 these distributions are plotted along with the $\lambda = 0$ distribution, normalized to the same area against μ. Most of the area under the (+-) curve is concentrated around the resonant mass so that the difference between (--) and (+-) curves is unmistakable.

These distributions have been calculated for annihilation at rest, $E = 1.874$ Bev or 13.4 pion masses, using $M = 4$ as resonant mass. For resonant function the smeared-out δ function,

$$\bar{\delta}(\mu^2 - M^2) = \frac{1}{2M} \frac{\epsilon/\pi}{(\mu - M)^2 + \epsilon^2},$$

was used, with half-width ϵ taken as 1/2 pion mass.

This result assumes that there are no π^0's present in the annihilation. In approximately 20% of the observed[6] $\bar{p} + n$ events, the charged pions are (--+) but there is an estimated average of 1.4 π^0's. If the experiment were performed in a deuterium bubble chamber, it would be easier to verify by momentum balance those events in which no π^0 is present.

The (+-) correlation is quite sensitive to the position of the resonance, and so should serve to fix the resonant mass. If sufficiently detailed experimental information is available, it may be possible to determine the details of the resonance function. There has been speculation[7] on the nonoccurrence of the two-pion annihilation. If the annihilation proceeds through the resonant ($\lambda = \infty$) channel, a sharp resonance will reduce the phase

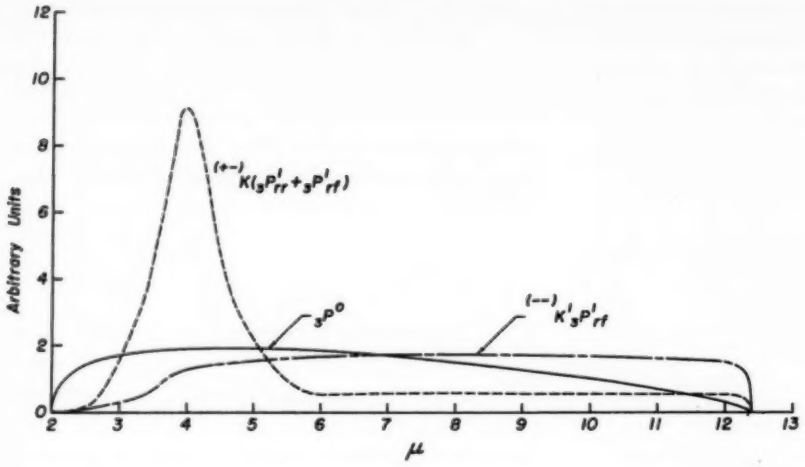

FIG. 1. Pion mass squared distributions for $\bar{p}+n \rightarrow \pi^- + \pi^- + \pi^+$.

space sufficiently to account for the suppression of this mode.

Even if the number of such annihilations is small compared to the number of events with one and two neutral pions, the poorer statistics should be compensated for by the pronounced peaking of the effective mass, which would tend to be suppressed for higher multiplicities.

The author would like to thank Professor E. C. G. Sudarshan for his continued interest and guidance in this work, Dr. T. Yamanouchi and Dr. S. Iwao for useful discussions, and Mr. K. T. Mahantappa for assistance with calculations.

[1]G. Pinski, E. C. G. Sudarshan, and K. T. Mahantappa, Proceedings of the Tenth Annual International Rochester Conference on High-Energy Physics, 1960 (Interscience Publishers, New York, 1960).

[2]T. Goto, Nuovo cimento 8, 625 (1958).

[3]W. R. Frazer and J. R. Fulco, Phys. Rev. Letters 2, 365 (1959).

[4]G. Goldhaber et al., Phys. Rev. Letters 3, 181 (1959).

[5]P. P. Srivastava and E. C. G. Sudarshan, Phys. Rev. 110, 765 (1958).

[6]R. Silverberg, University of California Radiation Laboratory Report UCRL-9183 (unpublished).

[7]E. O. Okunov, Dubna Report No. 534 (unpublished).

TWO-PION EXCHANGE INTERACTION*

G. Breit, K. E. Lassila, H. M. Ruppel, and M. H. Hull, Jr.
Yale University, New Haven, Connecticut
(Received January 12, 1961)

There is evidence for the one-pion exchange (OPE) interaction in nucleon-nucleon scattering.[1-3] The agreement of the coupling constant g with that from pion physics is satisfactory, and tests of the form of the OPE potential (OPEP) performed by adding a central field term and by varying proportions of spin-spin and tensor force terms have not indicated[4] a significant deviation from expectation for angular momentum $L>4$. The inclusion of phase shift K_4 indicated[4] a statistically significant coefficient of a central force addition to OPEP and it has been stated[4] that this probably indicates the setting in of two-pion exchange (TPE) effects. The statement was based on comparisons of Gupta's TPE potential[5] (TPEP) with the OPEP at the classical turning point for $L=4$. Results of further comparisons and of employing dispersion relations[6] are reported below.

Gupta's potential has a direct relationship to Dyson's scattering matrix S in terms of free-particle wave functions. In this respect the employment of field theory is similar to that of dispersion relations. The location of singularities does not enter the application of field theory, but unknown contributions[7] of higher powers of g^2 interfere with applicability of theory except at high L. The numerical values[5] of the TPEP use

nonrelativistic approximation and do not include some additional effects.[8]

Since the TPE as well as the sum of OPE and TPE effects on phase shifts in states with $L>1$ is in most cases <0.2, accurate distinctions between a phase shift δ, and $\sin\delta$ or $\tan\delta$ do not enter and effects of second and fourth order potentials V_2 and V_4 were added employing Taylor's formula for each.[9] Effects of the order of a percent corresponding to $\delta=0.2$ are of no interest here. The effect of V_4 was obtained with the aid of numerical values in Table I of reference 5. The integrand of the phase shift formula has a maximum close to the classical turning point, and for V_4 the relative importance of small r is higher than for V_2. The effect of V_2 was calculated as in reference 9. On account of the meaning of V_4, questions of wave function distortion do not arise and the integral converges.

According to Grashin,[10] in triplet states with total angular momentum $J=L+1$ the energy dependence of the OPE phase shift is anomalously rapid at small energies, E. This may be seen as a cancellation of dominant terms employing the formulas in reference 9. These states are thus especially suitable for TPE detection. The $^3P_2$ phase parameter θ^{P}_{2} is higher than its OPE value for all recently published fits[11] which fall in a band narrow compared with the distance from OPE. For $^3F_4$ only the rather improbable fit YRB3 crosses the OPE curve and falls below it above 180 Mev. All other fits give values of θ^{F}_{4} greater than those for OPE. Similarly for the n-p phase parameter[12] θ^{D}_{3} the OPE value is below all empirical fits and has the wrong sign. An exception to these relationships is θ^{G}_{5} for which most fits give values below those of OPE. But one of the empirically probable fits falls above OPE at low E, crosses it at 180 Mev, and differs from the sum of OPE and TPE at 274 Mev on the limit of error.

In Table I the contributions of V_2 and V_4 are shown for T=1. For θ^{P}_{2}, V_4 definitely overcorrects the difference between OPE and the fits, the standard deviation being small and all searches giving nearly the same values at the energies considered. Evidence below shows that this is probably due to short-distance effects. The disagreement of calculation with YLAM values of δ^{P}_{0} and δ^{P}_{1} is more marked and similarly in the case of K_1. For K_2 the agreement of calculated and YLAM values is good at the two lower energies and is much better than between OPE and YLAM. At 274 Mev, V_4 overcorrects OPE, presumably because of short-distance effects. For θ^{F}_{2} the accuracy of YLAM and the agreement among searches are poor.[11] At the two higher energies calculation and YLAM disagree markedly, but on account of the poor accuracy, a conclusion is difficult. An additional uncertainty may enter on account of coupling of P_2 to F_2. The disagreement is therefore not

Table I. Comparison of combined effect of V_2+V_4 (in radians) with fit YLAM (T=1).

Phase parameter	E (Mev)	V_2	V_4	V_2+V_4-YLAM	Standard deviation
θ^{P}_{2}	68.5	0.026	0.23	0.12	0.011
	137	0.05	0.48	0.30	0.009
K_2	68.5	0.025	0.018	0.000	0.006
	137	0.035	0.067	0.006	0.003
	274	0.044	0.176	0.055	0.007
θ^{F}_{2}	68.5	0.0096	0.0014	0.0040	0.009 (0.0025)
δ^{F}_{3}	68.5	-0.020	0.001	0.002	
	137	-0.043	0.011	0.011	
	274	-0.073	0.043	0.035	0.006
θ^{F}_{4}	68.5	0.002	0.001	0.002	
	137	0.006	0.011	0.011	
	274	0.015	0.043	0.031	0.006

Table II. Comparison of combined effect of V_2+V_4 (in radians) with fit YLAN3M (T = 0).

Phase parameter	E (Mev)	V_2	V_4	V_2+V_4 - YLAN3M	Standard deviation
θ^D_1	68.5	-0.132	0.025	0.066	0.011
	137	-0.265	0.094	0.084	0.010
	274	-0.467	0.252	0.164	0.03
δ^D_2	68.5	0.183	0.025	-0.07	0.018
	137	0.33	0.09	0.04	0.013
θ^D_3	68.5	-0.021	0.025	-0.010	0.010
	137	-0.050	0.094	0.010	0.006
	274	-0.10	0.25	0.07	0.022
K_3	68.5	-0.031	0.002	0.002	
	137	-0.056	0.014	0.015	
	274	-0.073	0.059	0.045	0.030

surprising. The F_3 search YLAM used the OPE value below 160 Mev. The disagreement at 137 Mev is, therefore, not significant and δ^F_3 was probably forced towards small values by the enforcement of OPE. This view is supported by the almost exact agreement of the calculated value with fit YLA at 137 Mev and the location of YLA nearly halfway between YLAM and YRB1. Similarly for θ^F_4, the 137-Mev value falls on YRB2 and overshoots YRB1 only slightly. Possibly in both cases YLAM has underestimated the values at 137 Mev.

In Table II similar comparisons are made with fit YLAN3M to T = 0 states.[12] Effects of V_4 are in the wrong direction to give agreement for $^3D_1$. Since $^3D_1$ is coupled to $^3S_1$ to which the application of V_2+V_4 is inadequate, this disagreement is in the same class as that for θ^P_2. For δ^D_2 the addition of the V_4 effects is helpful at 68.5 Mev and overshoots YLAN3M at 137 Mev. A number of other fits fall in between the calculated value and YLAN3M, however. There appears to be agreement on the whole in this case. For θ^D_3 the OPE value has the wrong sign but TPE brings about agreement at 68.5 and 137 Mev on the limit of error. At 274 Mev the TPE overshoots again. For K_3 the YLAN3M used OPE values in $0<E<175$ Mev. The calculated value exceeds YLAN3M by half the standard deviation but YLAN3M would be higher had OPE not been enforced below 175 Mev. There is agreement on the whole and deviations from V_2+V_4 follow similar patterns for T = 0 and T = 1.

Tables III and IV show comparisons of phase parameters for T = 1 and T = 0, respectively, according to the dispersion relations (DR) treatment of Galanin et al.[5] and of Grashin and Kobsarev[6] employing their tabulated ratios of values of TPE to OPE. The TPE gives improvement for $^3P_1$ and $^3P_2$, but not for $^3P_0$. The critical quantity $(L/k)(m_\pi c/\hbar) = L\mu/k$ is only 1.5 at 100 Mev and is hardly large enough to expect agreement. For K_2, i.e., $^1D_2$, the potential gives by far the better agreement; for F_2 the DR are somewhat the better; for F_3 and F_4 the DR give the better fit to YLAM but the potential is conceivably the better taking YRB1, YLA into account. For T = 0 the DR are much the better for K_1, i.e., $^1P_1$, and also for $^3D_1$, but the potential is the better below 200 Mev for $^3D_2$ and much the better up to 300 Mev for $^3D_3$. For K_3 the DR agree best with YLAN3 but considering the enforcement of OPE below 175 Mev for this fit the potential may be actually the better. For G_3, G_4, G_5 the two ways of treating TPE do not appear significantly different considering the uncertainties of the fits to data.

In the calculations of the effect of V_4, the maximum of the integrand falls at $x_m > 1$ ($x = rm_\pi c/\hbar$) only for $L \geq 2$ at the three energies used. At 274 Mev, $x_m > 1$ only for $L > 2.2$, and for $L = 2$ this criterion is barely satisfied at 137 Mev. The disagreement of the potential with the empirical fits for P terms is thus understandable and so are the poorer values for $L = 3$ at 274 Mev. The reasonableness of this situation combined with

Table III. Comparison of combined effect YLAM+Δ of one-pion and two-pion exchange effects (in radians) according to Galanin et al. and Grashin and Kobsarev,[a] with fit YLAM for T = 1.

State	E (Mev)	OP	TP	Δ
$^3P_1$	10	-0.052	0.004	0.002
	40	-0.176	0.018	-0.016
	100	-0.341	0.051	-0.056
$^3P_2$	10	0.002	0.002	-0.009
	40	0.014	0.028	-0.045
	100	0.040	0.080	-0.071
$^1D_2$	40	0.016	0.0002	-0.007
	100	0.032	0.008	-0.033
	200	0.041	0.020	-0.071
$^3F_2$	40	0.0042	0.0002	0.0013
	100	0.0160	0.0010	0.16
$^3F_3$	40	-0.094	0.002	0.002
	100	-0.031	0.0012	0.0012
	200	-0.059	0.005	0.0026
$^3F_4$	40	0.0008	0.0002	0.0002
	100	0.0041	0.0016	0.0016
	200	0.0104	0.0073	0.0049
	300	0.0158	0.0158	-0.0008

[a]See reference 6.

Table IV. Comparison of combined effect YLAN3M +Δ of one-pion and two-pion exchange effects (in radians) according to Galanin et al. and Grashin and Kobsarev, [a] with fit YLAN3M for T = 0.

State	E (Mev)	OP	TP	Δ
$^1P_1$	10	-0.060	0.009	-0.033
	40	-0.158	0.032	-0.034
	100	-0.215	0.043	0.034
$^3D_1$	40	-0.070	0.001	0.035
	100	-0.197	-0.010	0.010
	200	-0.364	-0.026	-0.078
$^3D_2$	40	0.103	0.003	-0.061
	100	0.258	0.008	-0.074
	200	0.445	0.018	0.063
$^3D_3$	40	-0.009	0.005	-0.010
	100	-0.034	0.028	-0.029
	200	-0.075	0.060	-0.067
$^1F_3$	100	-0.0424	0.0017	0.0015
	200	-0.065	0.0046	0.0032
	300	-0.076	0.0076	-0.014
$^3G_3$	100	-0.149	-0.0001	0.0000
	200	-0.038	-0.0011	0.0067
	300	-0.059	-0.003	0.054
$^3G_4$	100	0.037	0.0004	0.0005
	200	0.082	0.0016	0.0077
	300	0.120	0.0024	0.044
$^3G_5$	100	-0.0044	0.0009	0.0009
	200	-0.0135	0.0041	0.0047
	300	-0.0226	0.0068	0.0103

[a]See reference 6.

the striking improvements for K_2, D_2, D_3 caused by V_4 indicate the reality of the TPE. This conclusion is strengthened by the DR calculations. The disagreements of the potential with data at low L and the higher E indicate the presence of additional effects in the general region $x < 1$ and closer examination shows the presence of spin-orbit like effects with an "inverted" order.

*This research was supported by the U. S. Atomic Energy Commission and by the Office of Ordnance Research, U. S. Army.

[1]M. Taketani, S. Nakamura, and M. Sasaki, Progr. Theoret. Phys. (Kyoto) 6, 581 (1951); J. Iwadare, S. Otsuki, R. Tamagaki, and M. Watari, Progr. Theoret. Phys. (Kyoto) 16, 455 (1956). In the present note the potential has a different meaning from that used by the above workers and in other publications of the Taketani school.

[2]P. Cziffra, M. H. MacGregor, M. J. Moravcsik, and H. P. Stapp, Phys. Rev. 114, 880 (1959); M. J. Moravcsik, P. Cziffra, M. H. MacGregor, and H. P. Stapp, Bull. Am. Phys. Soc. 4, 49 (1959).

[3]G. Breit and M. H. Hull, Jr., Nuclear Phys. 15, 216 (1960).

[4]G. Breit, M. H. Hull, Jr., K. Lassila, and H. M. Ruppel, Phys. Rev. Letters 5, 274 (1960). G. Breit, M. H. Hull, Jr., K. Lassila, and H. M. Ruppel, Proc. Natl. Acad. Sci. U. S. (to be published).

[5]Suraj N. Gupta, Phys. Rev. 117, 1146 (1960).

[6]A. D. Galanin, A. F. Grashin, B. L. Ioffe, and I. Ya. Pomeranchuk, Nuclear Phys. 17, 181 (1960); A. F. Grashin and I. Yu. Kobsarev, Nuclear Phys. 17, 218 (1960).

[7]According to reference 5, calculations in the literature illegitimately assume the possibility of expansion in the pion mass to nucleon mass ratio.

[8]Professor Gupta has kindly informed the writers of unpublished results in which there appear additional spin-orbit and velocity-dependent contributions.

[9]Equation (A8) of reference 3.

[10]A. F. Grashin, J. Exptl. Theoret. Phys. (U.S.S.R.) 36, 1717 (1959) [translation: Soviet Phys.-JETP 36(9), 1223 (1959)].

[11]G. Breit, M. H. Hull, Jr., K. E. Lassila, and K. D. Pyatt, Jr., Phys. Rev. 120, 2227 (1960).

[12]M. H. Hull, Jr., K. E. Lassila, H. M. Ruppel, F. A. McDonald, and G. Breit (to be published).

INFLUENCE OF THE $\Lambda\pi$ RESONANCE ON CORRELATIONS IN THE REACTION $K^- + d \to \Lambda + \pi^- + p$†

Orin I. Dahl, Nahmin Horwitz,* Donald H. Miller, Joseph J. Murray, and Paul G. White
Lawrence Radiation Laboratory, University of California, Berkeley, California
(Received January 9, 1961)

When K^- mesons are absorbed in deuterium, two possible reactions are

$$K^- + d \to \Lambda + \pi^- + p, \qquad (1a)$$

$$K^- + d \to \Sigma^0 + \pi^- + p \quad (\Sigma^0 \to \Lambda + \gamma). \qquad (1b)$$

We have examined in detail a group of events of types (1a) and (1b) obtained in an exposure of the 15-in. deuterium bubble chamber to a 450-Mev/c separated K^- beam.[1] Application of an energy-momentum balance at the interaction vertex leads to an unambiguous separation of the Λ and Σ^0 events except for a small fraction of those cases in which the recoil proton is too short for measurement.[2] The fitting constraints also ensure a high degree of accuracy (~1%) in the determination of the momenta of the reaction products. Figure 1 shows the distribution of the kinematic variables T_p and T_{π^-} (proton and pion kinetic energy, respectively) for 282 events which (a) were produced by absorption of stopped K^-'s as determined by the fitting procedure and (b) did not result from the decay of a Σ^0 [reaction (1b)]. In addition, the pion and proton spectra for these events are plotted separately in Figs. 2 and 3.

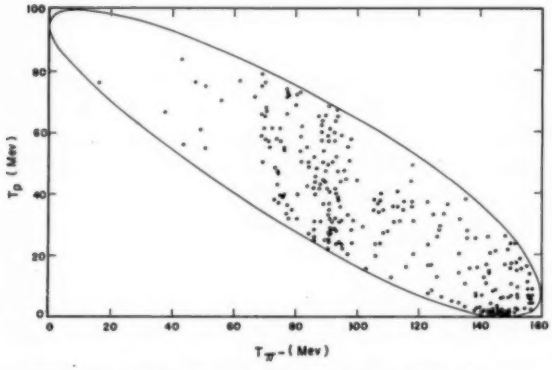

FIG. 1. Distribution of proton and pion kinetic energies in the reaction $K^- + d \to \Lambda + \pi^- + p$ (282 events).

Two prominent features of this absorption reaction are reflected in the pion peaks at $T_{\pi^-} = 92$ and 147 Mev. We consider the higher momentum peak first. Because of the loose structure of the deuteron, it is expected that a group of Λ's will appear as a result of K^- absorptions on single nucleons. This group of events may be described by an impulse model which includes the effects of interactions in the final state. In reaction (1a) the situation is particularly favorable: since the pion-nucleon system is produced in the weakly interacting isotopic spin $I = 1/2$ state, only the Λp interaction need be taken into account. The appropriate modifications of the impulse model have been developed by several authors.[3,4] They point out that for stopped K^-'s captured from

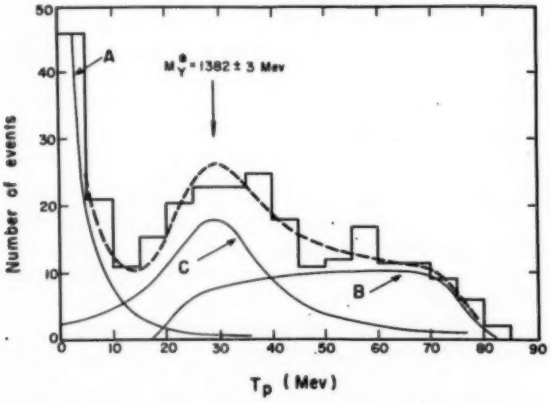

FIG. 2. Proton energy spectrum for the reaction $K^- + d \to \Lambda + \pi^- + p$. A: direct production. B: Σ-Λ conversion. C: resonance events (half-width ± 20 Mev).

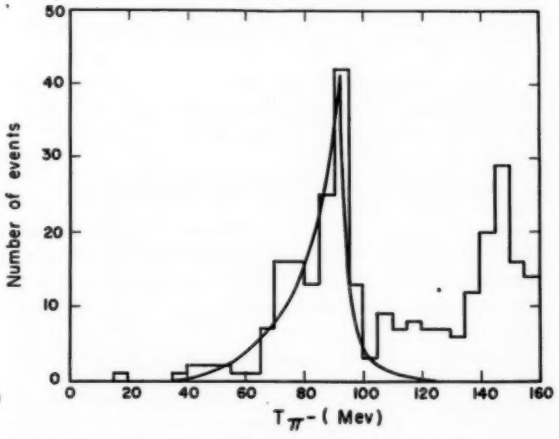

FIG. 3. Pion energy spectrum for the reaction $K^- + d \to \Lambda + \pi^- + p$.

atomic S orbitals,[5] the YN (hyperon-nucleon) system is produced predominantly with relative angular momentum $L=0$, so that interactions in other than S waves of the YN system may be neglected. Using the formulas given by Kotani and Ross,[4] we find that while the angular correlations in the final stage depend sensitively on the strength of the Λp interaction, the total production rate for given T_p is only slightly affected. It is apparent from Fig. 2 that this model qualitatively accounts for absorptions with $T_p<10$ Mev; however, it predicts that less than 20% of the directly produced events will have $T_p>10$ Mev.

The lower energy peak occurs at pion energies expected for production of Σ's in the K^- absorption reaction. Since a Λ rather than a Σ emerges from the absorption vertex, a two-step process is suggested: the K^- interacts with one nucleon to form a Σ and π^-, and then the Σ interacts with the other nucleon and converts to a Λ via the reaction $\Sigma+N\rightarrow\Lambda+p$.[3,4,6] For K^- capture from atomic S orbitals, it may be shown that the observed conversion rate is readily accounted for by reasonable choice of parameters in the zero-effective-range theory for the S-wave ΣN interaction. A typical prediction of the theory for the conversion-pion spectrum is shown in Fig. 3.[7] Since conversion occurs predominantly in the S wave of the ΣN system, the angular distribution of the Λp relative momentum will be isotropic with respect to the direction of the recoil π^-. For such a distribution, the frequency of events along lines of constant T_{π^-} in Fig. 1 will be independent of T_p. The calculated proton spectrum is shown in Fig. 2. Again, although the theory accounts qualitatively for the main features of the conversion process, there remains a group of events with $T_p>10$ Mev and $T_{\pi^-}>100$ Mev which are not readily associated with either direct absorption or internal conversion.

Alston et al. have recently presented strong evidence for the existence of a resonance in the $\Lambda\pi$ system (hereafter called Y^*) at a total mass of $M_{Y^*}=1380\pm5$ Mev and with a half-width less than ±32 Mev.[8] More recent data support the existence of this resonance and suggest that the width may be as little as ±15 Mev.[9] Production of this state in the K^-d absorption reaction would result in a peak in the proton spectrum in the region near $T_p=30.5$ Mev. Examination of Figs. 1 and 2 indicates that the anomalous events may readily be attributed to production of the resonant $\Lambda\pi$ system.[10] Under this assumption, we have attempted to estimate the relative importance of the processes contributing to this reaction by folding together the three distributions in Fig. 2 appropriately normalized to reproduce the observed proton spectrum. Possible interference effects have been neglected. The resonance curve used corresponds to $M_{Y^*}=1382$ Mev, with a half-width of ±20 Mev. From this we estimate that of the 282 events examined, roughly 87 are direct Λ's, 102 are internal conversions, and 93 are associated with the resonant channel.[11]

The spin of the resonant $\Lambda\pi$ state has not yet been established definitely. In the absence of final-state interactions, the resonant channel will result in the $\Lambda\pi$ being produced in a pure angular-momentum state. For $J=1/2$, the distribution of the c.m. $\Lambda\pi$ relative momentum will be spatially isotropic. For $J=3/2$, the distribution is not uniquely determined by conservation of angular momentum alone, but must still be symmetric about a plane perpendicular to the direction of the recoil proton.[12] However, in the region (large T_p) where the effect of the Λp interaction is likely to be small, the angular distribution is distorted by overlap with the internal-conversion events.

A region of particular interest is $5<T_p<20$ Mev, where both the Y^* and direct production are important, while the contribution from internal conversion is negligible. The observed events show a marked tendency for the Λp system to be produced with low relative momentum (large T_{π^-} on Fig. 1). In particular, for the 48 events in this group we obtain

$$(N_f-N_b)/(N_f+N_b)=0.44\pm0.13,$$

where N_f (N_b) is the number of events for which the c.m. angle of the $\Lambda\pi$ system is less than (greater than) 90 deg with respect to the recoil proton direction. If the quantum numbers of the Y^* are the same as those of the zero-energy K^-p system ($S^{1/2}$ for odd $K\Lambda$ parity, $P^{1/2}$ for even), so that this is the resonance suggested by Dalitz and Tuan,[13] the distribution of events for $T_p<20$ Mev is readily understood in terms of an attractive S-wave Λp interaction. In using the final-state interaction theory, the $\Lambda\pi$ resonance was taken into account through an enhancement of the single-nucleon transition operator, $\langle K^-n|T|\Lambda\pi^-\rangle$, as the energy of the $\Lambda\pi$ system was decreased below the K^-n threshold. For a Λp potential of Gaussian form and range corresponding to two-pion exchange, the data suggest that the volume

integral of the average potential is 280 ± 90 Mev-fermi³.[14] A strong S-wave Λp interaction could also be present if the resonant state were $P^{3/2}$ and the $K\Lambda$ parity even. If J is one-half, but the parity of the Y^* differs from that of the zero-energy K^-p system, or if the Y^* state is $P^{3/2}$ and the $K^-\Lambda$ parity is odd, the recoil proton must be produced in an odd angular-momentum state with respect to the Y^*. Since the effect of S-wave Λp scattering will then be small, the angular distribution can probably be accounted for by an interference between the two production modes. In this case, the Λ will in general be polarized with respect to the production plane; however, the data are statistically inadequate to determine whether a significant effect is present.

It is of interest to compare the rate for Y^* production with the rate for the nonmesonic processes

$$K^- + d \rightarrow \Sigma^- + p;\ \Sigma^0 + n;\ \Lambda + n,$$

which occur with a combined frequency of ~1.2% when stopped K^-'s are absorbed.[15] Since reaction (1a) constitutes 21.5% of all zero-energy K^- absorption events,[15] we estimate that ~6% of the absorptions proceed through the resonant $\Lambda\pi^-$ channel. By charge independence, an additional 3% proceeds through the $\Lambda\pi^0$ channel. The suppression of nonmesonic absorption reflects the much smaller volume of the deuteron in which these events may occur because of the large momentum (> 500 Mev/c) present in the final state.

It is a pleasure to thank Professor Luis Alvarez for his advice and encouragement throughout this work, and the assistance of the bubble-chamber and scanning staffs of the Lawrence Radiation Laboratory.

†Work done under the auspices of the U. S. Atomic Energy Commission.

*Present address: Department of Physics, University of Syracuse, Syracuse, New York.

[1]A preliminary analysis of this reaction was presented in Bull. Am. Phys. Soc. 3, 363 (1958).

[2]The few ambiguous events with $T_p < 3$ Mev were assigned to the Σ^0 and Λ categories in proportion to the number observed in each group with $3 < T_p < 10$ Mev.

[3]R. Karplus and L. Rodberg, Phys. Rev. 115, 1058 (1959).

[4]T. Kotani and M. Ross, Nuovo cimento 14, 1282 (1959), Eqs. (50), (51), and (52).

[5]T. Day, G. Snow, and J. Sucher, Phys. Rev. Letters 3, 61 (1959).

[6]The existence of this reaction was first inferred from a study of K^- absorption stars in nuclear emulsion. See F. Webb, E. Iloff, F. Featherston, W. W. Chupp, G. Goldhaber, and S. Goldhaber, Nuovo cimento 8, 899 (1958).

[7]The presence of a cusp in the π^- rate as T_{π^-} is decreased through the threshold for the reaction $\Sigma + N \rightarrow \Lambda + p$ was emphasized in reference 4. [See also L. Fonda and R. Newton, Phys. Rev. 119, 1394 (1960).] The theoretical curve was calculated using Eqs. (59 through 62) of reference 4 and the S-wave effective-range parameters: complex scattering length $A_0 + iB_0 = (-0.005 + i\,0.005)$ Mev/c^{-1}; cutoff $\epsilon = 200$ Mev/c. Though the predictions are somewhat sensitive to ϵ, the data remain in disagreement with the choice of positive A_0, which would correspond to a diagonal $J = 1/2$, ΣN potential strong enough to produce a bound state. This was first noted in reference 3.

[8]M. Alston, L. W. Alvarez, P. Eberhard, M. L. Good, W. Graziano, H. Ticho, and S. Wojcicki, Phys. Rev. Letters 5, 520 (1960).

[9]M. Ferro-Luzzi, J. Berge, J. Kirz, J. Murray, A. Rosenfeld, and M. Watson, Bull. Am. Phys. Soc. 5, 509 (1960).

[10]R. Adair has suggested that part of the effect observed by Alston et al. (reference 4) may result from general constraints imposed on the reaction amplitudes by conservation of angular momentum and centrifugal barrier effects. [See Proceedings of the Conference on Strong Interactions, Berkeley, California, 1960; Bull. Am. Phys. Soc. 5, 516 (1960).] It is difficult to see how the mechanisms pointed out by Adair can be operative in the present reaction.

[11]The observed width of the resonance may be expected to vary, depending upon the reaction in which it is produced. The number of events attributed to the individual mechanisms depends somewhat upon the width assumed for the resonance. A sharper resonance leads to more events being assigned to the internal-conversion process, and conversely.

[12]We are indebted to T. Day, L. Rodberg, G. Snow, J. Sucher, and S. Claus for clarification of this point. See also L. C. Biedenharn, in Nuclear Spectroscopy, edited by Fay Ajzenberg-Selove (Academic Press, New York, 1960), Sec. Vc.

[13]R. H. Dalitz and S. F. Tuan, Ann. Phys. 3, 307 (1960).

[14]For odd $K\Lambda$ parity, the Λp system will be produced in the ^3S state. This potential is then directly comparable to that calculated by R. Downs and R. Dalitz [Phys. Rev. 114, 593 (1959)] from data on lambda-hypernuclear binding energies. Neglecting three-body forces they find 174 Mev-fermi³ for the same volume integral. For even $K\Lambda$ parity, the potential is an appropriate average of both the ^1S and ^3S interactions.

[15]Data of O. I. Dahl, N. Horwitz, D. H. Miller, J. J. Murray, and P. G. White, reported by L. Alvarez at the Ninth International Conference on High-Energy Physics, Kiev, U.S.S.R., 1959 (unpublished); L. Alvarez, Lawrence Radiation Laboratory Report UCRL-9354, September, 1959 (unpublished).

K-π RESONANCE AND LIFETIME OF THE K' PARTICLE*

Mirza A. Baqi Bég and Paul C. De Celles
Brookhaven National Laboratory, Upton, New York
(Received January 12, 1961)

Recent experimental data[1] seem to indicate a resonance in the $\pi+K$ system at an energy of 878 Mev and full width at half maximum of $23\pm20\%$ Mev. The spin and isobaric spin of the resonance have not yet been determined[2]; however, it is certainly attractive to consider the possibility that it might be due to the conjectured K' particle,[3] a scalar isobaric doublet. The theoretical reasons for postulating this particle have been discussed recently by Gell-Mann,[3] Tiomno,[4] and Bernstein and Weinberg.[5] On the other hand, it has been suggested[6] that the small width of the experimental πK resonance might be an indication that it is a P-wave resonance[7] (possibly due to a vector particle, say, K_V).

In this Letter we wish to point out that the cross section for K' (or K_V) production in K-p scattering can be simply related to its lifetime and spin. The relations we derive may then be used to distinguish between the possibilities K' and K_V, and provide a method for measuring the lifetime of the particle involved.[8]

For the scalar case we have, on using Lorentz invariance and parity conservation,

$$(4k_0k_0')^{1/2}\langle K|J_\pi|K'\rangle=\lambda_S(q^2), \tag{1}$$

where J_π is the pion current, $q=k-k'$ is the difference of K, K' 4-momenta, and $\lambda_S(q^2)$ is a scalar function of q^2. The lifetime is simply[9]

$$\tau_S=\frac{8\pi}{\lambda^2(m_\pi^2)}\frac{m_{K'}^2}{\alpha}, \tag{2}$$

where, with an obvious notation for particle masses,

$$\alpha=\frac{1}{2m_{K'}}[(m_{K'}^2-m_K^2-m_\pi^2)^2-4m_\pi^2m_K^2]^{1/2}. \tag{3}$$

The cross section for $K+p\to K'+p$, when calculated in the one-pion approximation in the barycentric frame, is

$$\left(\frac{d\sigma}{d\Omega}\right)_S=-\frac{f^2(q^2)\lambda^2(q^2)}{64\pi^2E^2}\frac{|\vec{k}'|}{|\vec{k}|}\frac{q^2}{|q^2-m_\pi^2|^2}, \tag{4}$$

where E is the total energy of the system, and $if(q^2)\bar{N}'\gamma_5N=\langle N'|J_\pi|N\rangle(\epsilon\epsilon'/m^2)^{1/2}$, $q^2=(k'-k)^2$, with k' and k the 4-momenta of K' and K, respectively, and with ϵ and ϵ' the initial and final proton energies, respectively. Providing q^2 is such that $\lambda(q^2)\cong\lambda(m_\pi^2)$ and $f(q^2)\cong f(m_\pi^2)=G$, the renormalized pion-nucleon coupling constant $(G^2/4\pi=14.5)$, then

$$\left(\frac{d\sigma}{d\Omega}\right)_S=\left(\frac{G^2}{4\pi}\right)\frac{1}{2\tau\alpha}\frac{m_{K'}^2}{E^2}\frac{|\vec{k}'|}{|\vec{k}|}\frac{-q^2}{|q^2-m_\pi^2|^2}. \tag{5}$$

Using the experimental values of $m_{K'}=878$ Mev and E corresponding to the data of reference 1, one finds for the total cross section

$$\sigma(\text{mb})=1.9/(\tau_S\times10^{23}),\quad(\tau_S\text{ in sec}). \tag{6}$$

For the vector case, the analog of Eq. (1) is

$$(4k_0k_{V_0})^{1/2}\langle K|J_\pi|K_V\rangle=\lambda_V(q^2)(\xi\cdot k), \tag{7}$$

where ξ is the "polarization" vector of K_V and we have used the usual subsidiary condition for a Proca field, viz., $k_V\cdot\xi=0$. $\lambda_V(q^2)$ is the appropriate form factor. The lifetime of the K_V is then

$$\tau_V=\frac{8\pi}{\lambda_V^2(m_\pi^2)}\frac{3m_{K'}^2}{\alpha^3}, \tag{8}$$

where we assume that $m_{K_V}=m_{K'}=878$ Mev. Corresponding to Eq. (5), we now have for the differential cross section

$$\left(\frac{d\sigma}{d\Omega}\right)_V=\left(\frac{G^2}{4\pi}\right)\frac{3}{2\tau\alpha^3}\frac{1}{E^2}\frac{|\vec{k}'|}{|\vec{k}|}\frac{-q^2}{|q^2-m_\pi^2|^2}\times\tfrac{1}{4}[4m_K^2m_{K'}^2-(q^2-m_{K'}^2-m_K^2)^2]. \tag{9}$$

The total cross section, corresponding to Eq. (6), is now

$$\sigma(\text{mb})=24/(\tau_V\times10^{23}),\quad(\tau_V\text{ in sec}). \tag{10}$$

The angular distributions of the recoil protons in the c.m. frame is plotted in Fig. 1. A measurement of the backward to forward ratio possibly could decide whether the resonance is to be identified with K' or K_V. Although the angular

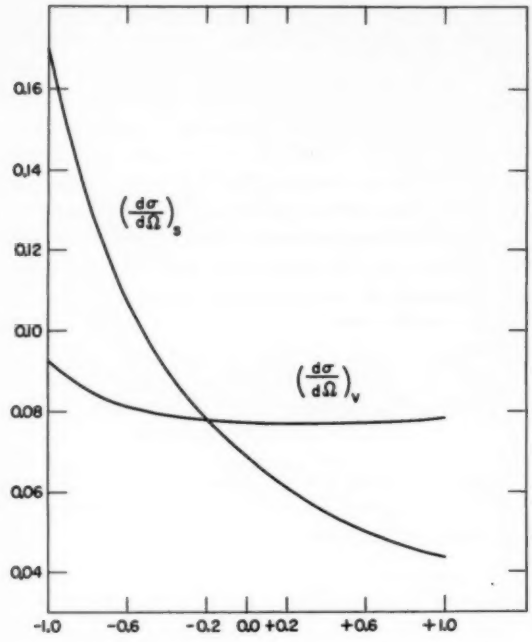

FIG. 1. Angular distribution of recoil protons, in barycentric frame, for the process $K+p \rightarrow K'(K_V)+p$. Both curves are normalized to the same total cross section of 1 mb.

distributions plotted in Fig. 1 are clearly distinguishable, these theoretical cross sections are due to single-pion-exchange graphs only. It is improbable that such terms dominate the cross section over the entire range of $\cos\theta$. A pronounced backward peaking of the protons, however, would be strong evidence for the K', but lack of it would not rule out the same possibility.

Alternatively, a precise knowledge of σ and the resonance width, Γ, could distinguish between the two alternatives. With the available data, $\sigma \cong (1 \pm 0.42)$ mb and thus

$$1.34 < \tau_S \times 10^{23} < 3.28,$$

$$16.9 < \tau_V \times 10^{23} < 41.4, \qquad (11)$$

whereas $2.38 < (1/\Gamma_{\text{exp}}) \times 10^{23} < 3.58$. Therefore, present experimental evidence supports the K' alternative. However, it has been said that the present experimental width Γ_{exp} could be entirely due to experimental uncertainties. Hence, one cannot yet exclude the possibility that the resonance is due to a vector particle.

It should be remarked that the experimental values of E and q^2 used above are not optimal for this kind of analysis. The use of the one-meson approximation in Eqs. (5) and (9) is best when the momentum transfer to the proton is smallest. The q^2 in the data of reference 1 is -0.12 (Bev/c)^2 for protons scattered in the forward direction, which is to be compared with $m_\pi{}^2 = +0.0196$ (Bev)^2. One should therefore consider the inequalities (11) as rather crude estimates until more data corresponding to smaller q^2 and larger E are taken.

We wish to thank J. Bernstein and R. Marr for useful discussions of this work and I. Cole for assistance with the computations.

---

*Work performed under the auspices of the U. S. Atomic Energy Commission.

[1]M. Alston, L. W. Alvarez, P. Eberhard, M. L. Good, W. Graziano, H. K. Ticho, and S. G. Wojcicki, Phys. Rev. Letters 5, 11, 520 (1960); also M. L. Good [private communication to one of the authors (P. C. D.)].

[2]From parity considerations one rules out a pseudoscalar or pseudovector particle as the possible cause of the resonance.

[3]M. Gell-Mann named such a particle K' [Proceedings of the Tenth Annual International Rochester Conference on High-Energy Physics, 1960 (Interscience Publishers, New York, 1960), p. 509].

[4]J. Tiomno, reference 3, pp. 466, 467, and 513.

[5]J. Bernstein and S. Weinberg, Phys. Rev. Letters 5, 10, 481 (1960).

[6]M. Gell-Mann (private communication to J. Bernstein).

[7]Previous theoretical calculations using dispersion relation techniques have indicated a possible P-wave resonance in the πK scattering. B. W. Lee, Phys. Rev. 120, 325 (1960); and M. Gourdin, Y. Noirot, and Ph. Salin, Nuovo cimento 18, 651 (1960). These analyses cannot rule out "kinematical" S-wave resonance [a phrase used by G. F. Chew and S. Mandelstam, Phys. Rev. 119, 467 (1960)]. For our present purpose, it makes no difference whether or not we associate a particle with the observed resonance as long as the resonance exists in a pure state of spin and isobaric spin.

[8]Essentially similar techniques were employed by H. Primakoff [Phys. Rev. 81, 899 (1951)] in his discussion of the π^0 lifetime.

[9]This is similar to what one obtains in lowest order perturbation theory from a three-field interaction $L_{\text{int}} = \lambda \pi K K'$, but questions of renormalization and the inapplicability of perturbation theory do not arise in our approach.

NONCLASSICAL STRUCTURE OF THE ENERGY-MOMENTUM TENSOR OF A POINT MASS SOURCE FOR THE SCHWARZSCHILD FIELD*

Frank R. Tangherlini
Institute of Field Physics, University of North Carolina, Chapel Hill, North Carolina
(Received November 28, 1960; revised manuscript received December 22, 1960)

Although the Schwarzschild solution to the field equations has been known for many years, because of the complicated nonlinear character of the equations, there is still no generally accepted form for the structure of the energy-momentum tensor $T_\nu{}^\mu$ when the latter is that of a point mass source. From a classical standpoint, one would surmise that $T_\nu{}^\mu$ in a static coordinate system reduces to $T_0{}^0$, with $T_0{}^0$ proportional to a delta function, but from the structure of the field equations it is by no means obvious that other components are not also present.

Indeed, as we shall now show, and briefly discuss, this tensor does not have only one nonvanishing component, i.e., $T_0{}^0$ (as one might expect classically for a point particle at rest), but four: $T_0{}^0 = T_1{}^1$, $T_2{}^2 = T_3{}^3 = -\frac{1}{2}T_0{}^0$, with $T_0{}^0 = m\delta(r)/2\pi r^2$; the notation is described below.

In order to arrive at this result, we shall first show that, for systems with static spherical symmetry, when a certain condition is satisfied by the $g_{\mu\nu}$ (as is the case for the Schwarzschild solution), the field equations reduce to a pair of dependent linear equations, most simply expressed in terms of the scalar potential U (defined by $g_{00} = 1 + 2U$). Using these equations, the above structure for $T_\nu{}^\mu$ may be immediately inferred.

Upon introducing the coordinate system associated with the following standard line element for systems with static spherical symmetry,

$$ds^2 = g_{00}(r)\,dt^2 + g_{11}(r)\,dr^2 - r^2(d\theta^2 + \sin^2\theta\, d\phi^2), \quad (1)$$

one finds for the nonvanishing components of the field equations[1,2]:

$$G_0{}^0 = -r^{-2}[1 + (rg^{11})_{,r}] = -\kappa T_0{}^0,$$

$$G_1{}^1 = G_0{}^0 + r^{-1}(g^{11}{}_{,r} - g^{00}g^{11}g_{00,r}) = -\kappa T_1{}^1,$$

$$G_2{}^2 = -g^{00}g^{11}(\tfrac{1}{2}\nabla^2 g_{00}) - [\tfrac{1}{2} + \tfrac{1}{4}r(\ln g_{00})_{,r}](G_1{}^1 - G_0{}^0) = -\kappa T_2{}^2, \quad (2)$$

and by spherical symmetry, $G_3{}^3 = G_2{}^2$. We note the following about the equations: (a) The first equation is already linear in g^{11}; (b) the other two equations would be linear if $g^{00}g^{11}$ were a constant,[3] since this is equivalent to $g^{11}{}_{,r} - g^{00}g^{11}g_{00,r} = 0$; by the asymptotic condition[4] this constant may be set equal to -1; (c) if $g^{00}g^{11} = -1$, the transverse equation reduces to a Newtonian one, relating $\nabla^2 g_{00}$ to the transverse stresses; (d) in order for $g^{00}g^{11}$ to be constant, it is necessary and sufficient that $T_0{}^0 = T_1{}^1$. When the latter is the case, the requirement that $T_\nu{}^\mu{}_{;\mu} = 0$ reduces to

$$(r^2 T_1{}^1)_{,r} - 2rT_2{}^2 = 0, \quad (3)$$

and it follows that there is only one independent component for the $T_\nu{}^\mu$ which most conveniently may be replaced by the trace, T. One then has in terms of T for the components

$$T_0{}^0 = T_1{}^1 = r^{-4}\int Tr^3\,dr + C/r^4,$$

$$T_2{}^2 = T_3{}^3 = \tfrac{1}{2}T - T_0{}^0, \quad (4)$$

where C is a constant of integration.[5]

Let us now consider the Schwarzschild field, i.e., $g_{00} = 1 - 2Gm/r$, $g^{11} = -g_{00}$. This field is derived under the assumption that outside the source $T_\nu{}^\mu = 0$; hence in this region, the requirements on $T_\nu{}^\mu$ for linearity are satisfied. We shall continue the solution down to the source point at $r = 0$, noting that $g_{00}(= -g^{11})$ is finite and differentiable even when passing through the Schwarzschild singularity, and the regularity of the field equations is not altered by the fact that $g_{00} = 0$ (or $g_{11} = \infty$) at $r = 2Gm$, since this is not a singularity in the differential equations themselves.[6]

Upon introducing the scalar potential, $-g^{11} = g_{00} = 1 + 2U$, the field equations reduce to the following pair of dependent linear equations[7]:

$$-2r^{-2}(rU)_{,r} = \kappa T_0{}^0 (= \kappa T_1{}^1),$$

$$-\nabla^2 U = \kappa T_2{}^2 (= \kappa T_3{}^3), \quad (5)$$

where, for the case of a point particle, the source terms are singular distributions which vanish for $r > 0$. For the Schwarzschild solution, i.e., $U = -Gm/r$, one readily obtains the following

values for the T_ν^μ which may be conveniently summarized as

$$T_\nu^\mu = \text{diag}\,(1, 1, -\tfrac{1}{2}, -\tfrac{1}{2})\, m\delta(r)/2\pi r^2, \qquad (6)$$

where $\delta(r)$ is the radial delta function $\int_0^\infty \delta(r)\,dr = \frac{1}{2}$. Since $r\delta'(r) = -\delta(r)$, these distributions satisfy the requirement (3).

Although the m appearing in the above equations is up to this point of the discussion to be thought of only as a gravitational mass, it follows directly from the action principle that it is also a dynamical quantity, the rest mass. We have for the gravitational action, A, the expression $\int(-g)^{1/2}\kappa^{-1}R\,d^4x$ which by the field equations may be written $\int(-g)^{1/2}T\,d^4x$. Hence, since $T = T_0^0 = m\delta(r)/2\pi r^2$, the action integrated for a finite time interval over any spatial region ω containing the particle is

$$A(t;\omega) = \int_{t_0}^{t} dt \int_\omega \frac{m\delta(r)}{2\pi r^2}\, d^3r = m(t - t_0). \qquad (7)$$

The surfaces of constant action are therefore parallel to the surfaces of constant time, and for this case, and in general for static coordinate systems,[8] the normal derivative to the action surface is the rest mass, i.e., $dA/dt = m = \int(-g)^{1/2}T\,d^3x$.[9]

The result is therefore quite analogous to special relativity because in the above case $T_1^1 + T_2^2 + T_3^3 = 0$, so that $T_0^0 = T$ as in special relativity for a particle at rest. However, despite this analogy, we encounter a difficulty if we try to describe T_ν^μ classically. We would expect $T_\nu^\mu = \rho(dx^\mu/ds)(dx_\nu/ds)$, where ρ is the trace or proper density $m\delta(r)/2\pi r^2$. However, the previously found values for T_ν^μ would imply, formally, in the limit $r = 0$,

$$g_{00}(dt/ds)^2 = 1, \quad g_{11}(dr/ds)^2 = 1, \quad r^2(d\theta/ds)^2 = \tfrac{1}{2}, \quad r^2\sin^2\theta(d\phi/ds)^2 = \tfrac{1}{2}, \qquad (8)$$

instead of as in special relativity $(dt/ds)^2 = 1$, with the other terms vanishing. Moreover, again formally, we have (since $|g_{00}| = \infty$, $g_{11} = 0$, at $r = 0$) $dt/ds = 0$, $|dr/ds| = \infty$, in contrast with the classical result $dt/ds = 1$, $dr/ds = 0$. The two angular terms may be formally equated to yield $d\theta^2 = \sin^2\theta\, d\phi^2$, which has the particular integral, $\sin\theta \exp|\phi| = \text{constant}$, corresponding to spirals on the unit sphere.[10]

While these results follow because we are no longer working in the classical region of spacetime, and because of the structure of T_ν^μ, it would appear that we have reached a fundamental limitation here in understanding the point particle in general relativity as a purely classical object (i.e., a structureless mass point, with the spatial stresses vanishing).[11] We leave as an open question whether this nonclassical structure has some relation to the nonclassical behavior of particles as exhibited in the quantum domain.

In conclusion, to clarify the physical principle underlying the condition on the T_ν^μ, we note that one may arrive at this condition in the following way: Let a particle be freely falling radially in a gravitational field described by the line element (1); what is the condition on g_{00} and g_{11} that will make the radial acceleration independent of the energy integral $E = g_{00}\,dt/ds$? One readily finds that the condition is $g_{00}g_{11} = \text{constant}$, and upon examining the field equations, one finds $T_0^0 = T_1^1$. In other words, we are dealing here with a consequence of the principle of equivalence as it manifests itself in the field equations.[12] It is certainly remarkable that this condition should also make the equations, for this case, linear and, upon transforming to rectangular coordinates, make the coordinate system "proper" (to within a normalization constant). We hope to discuss these results further in a subsequent publication.

---

*This research was supported by the United States Navy under a contract monitored by the Office of Naval Research.

[1]Because of the final linearity in g_{00} and g^{11}, it will not be convenient to make the customary substitution $g_{00} = \exp\mu(r)$, $g_{11} = -\exp\nu(r)$. However, if one adopts static cylindrical coordinates, one obtains an equation linear in $\ln g_{00}$, as first shown by H. Weyl, Ann. Physik 54, 117 (1917); 59, 185 (1919). See also T. Levi-Civita, Rend. Accad. nazl. Lincei, (1917-1919); R. Bach and H. Weyl, Math. Zeit. 13, 134 (1922). We should like to emphasize the restricted character of our results, i.e., to systems with static spherical symmetry, and to call attention to the more general problem of finding rigorous linearizing conditions for the field equations, and determining, by experiment, whether or not they do occur.

[2]We set $c = 1$, $\kappa = 8\pi G$, where G is the Newtonian gravitational constant, also $f_{,r} \equiv df/dr$, $\nabla^2 f \equiv r^{-2}(r^2 f_{,r})_{,r}$.

[3]This condition is not, however, necessary for linearity, e.g., $g_{00} = \text{constant}$ yields equations linear in g^{11}, although it, of course, requires a different structure for the T_ν^μ than the Schwarzschild solution.

[4]That is, as $r \to \infty$, $g_{\mu\nu} \to \eta_{\mu\nu} = \text{diag}\,(1, -1, -1, -1)$, to the extent that we may neglect cosmological effects.

[5]The term C/r^4, with $C = e^2/2$, where e is the charge of the electron in Heaviside units, occurs in the Reissner-Nordstrom solution, for which the T_ν^μ also

satisfy the above linearity condition, as does also the cosmological term $\Lambda\delta_\nu{}^\mu$.

[6]Moreover, we note that the Schwarzschild solution for g_{00} is linear in m; hence we could alternatively reflect m and obtain a solution for which $g_{00} \geq 1$ for $0 < r \leq \infty$. One should therefore draw a clear distinction between singular points or regions in the field equations, and singularities or "unphysical" behavior in $ds^2 = g_{\mu\nu}dx^\mu dx^\nu$ due to the values of the $g_{\mu\nu}$.

[7]Note that upon substituting the expressions for $T_\nu{}^\mu$ in (5) into the requirement (3), it is satisfied identically, so that a reduced version of the Bianchi identities has been preserved.

[8]If one adopts the isotropic coordinates by setting $r = (1 + Gm/2\bar{r})^2\bar{r}$, one finds the interesting result that the particle cannot be located at $\bar{r} = 0$ in the isotropic system, and that rather $\bar{r} = -Gm/2$ corresponds to the particle's location. Moreover, the isotropic system for the range $0 \leq \bar{r} \leq \infty$ covers the space outside the Schwarzschild radius twice, so that $\bar{r} = 0$ actually corresponds to spatial infinity, as may be seen from the above transformation or by observing that the isotropic line element is form-invariant under the substitution $q = G^2m^2/4\bar{r}$. Compare the results, different from ours, obtained by R. Arnowitt, S. Deser, and C. W. Misner, Phys. Rev. Letters 4, 375 (1960), who assume the particle to be located at $\bar{r} = 0$.

[9]We have also calculated the surfaces of constant action for Lemaître's nonstatic coordinate system [G. E. Lemaître, Ann. soc. sci. Bruxelles, Ser. A. 53, 51 (1933)], and find $A = m(t' + r')/2$. The original static observers satisfy $t' - r' =$ constant. Differentiating A in the direction $dt' = dr'$, we have again m.

[10]An alternative classical representation for the $T_\nu{}^\mu$ is given by $T_\nu{}^\mu = (\rho + p)(dx^\mu/ds)(dx_\nu/ds) - p\delta_\nu{}^\mu$, where p is a scalar "pressure." One then has $p = \rho/2$ and again, formally, $g_{00}(dt/ds)^2 = g_{11}(dr/ds)^2 = 1$, with the angular "motion" vanishing.

[11]One is perhaps reminded here of Einstein's feeling that one should not assume a priori a classical representation for the singularities of the gravitational field in connection with deriving the equations of motion from the field equations. See the interesting accounts in L. Infeld, Helv. Phys. Acta. Suppl. IV, 206 (1956); Revs. Modern Phys. 29, 398 (1957). The above results bring out the urgency of finding exact solutions to the two-body problem.

[12]The question of the relationship of this condition to the principle of equivalence has been raised recently by H. Bondi and S. Kilmister, Am. J. Phys. 28, 508 (1960), in their Letter commenting on the recent application of the principle by L. I. Schiff, Am. J. Phys. 28, 340 (1960). Note, however, that Schwarzschild's interior solutions do not in general satisfy this condition, in contrast with the interior solutions that would be obtained from (5).

ABSTRACTS

In this section are printed the abstracts of Articles that have been forwarded to The American Institute of Physics for publication in THE PHYSICAL REVIEW. In quoting information obtained from this section before the appearance of the corresponding Article, reference should be made to "Physical Review (to be published)" rather than to this Journal.

DYNAMICS OF ATOMIC MOTIONS IN LIQUIDS AND COLD NEUTRON SCATTERING. A Rahman, K. S. Singwi, and A. Sjölander, Argonne National Laboratory, Argonne, Illinois (Received November 16, 1960).

The self-correlation function for the motion of an atom in a liquid has been constructed in a manner which simulates the behavior of this function between the two extreme cases: viz., that in a solid and that in a simple diffusive model. Using this function, the differential scattering cross section for cold neutrons has been calculated for liquid lead and compared with available experimental results. It appears that even in a simple liquid like lead the solid-like behavior of atomic motions persists for a considerable time.

SOLUTION FOR THE TWO-ELECTRON CORRELATION FUNCTION IN A PLASMA. Burton D. Fried, Space Technology Laboratories, Incorporated, Los Angeles, California, and H. W. Wyld, Jr., University of Illinois, Urbana, Illinois (Received November 23, 1960).

The two-electron correlation function, g, responsible for "collisional" corrections to the correlationless (or Vlasov) description of a plasma, is investigated. It is shown that an exact solution of the integral equation for g can be found for a fairly wide class of spatially homogeneous, one-electron distribution functions, f (the ion dynamics being neglected). This is carried out in detail for the simplest member of the class (the resonance shape), and the Landau damping of g to its asymptotic ($t\to\infty$) form is exhibited explicitly. It is shown that correlations between particles separated by more than the Debye length are damped in a time which exceeds the period of plasma oscillations, ω_p^{-1}, and that these make an appreciable contribution to the "collisional" rate of change of f. It is concluded that for rapidly varying f (as in problems involving plasma oscillations) conventional treatments of the "collision" term should be replaced by a self-consistent solution of the coupled equations for f and g.

FINE STRUCTURE AND MAGNETO-OPTIC EFFECTS IN THE EXCITON SPECTRUM OF CADMIUM SULFIDE. J. J. Hopfield,* Bell Telephone Laboratories, Murray Hill, New Jersey and Laboratoire de Physique, École Normale Supérieure, Paris, France, and D. G. Thomas, Bell Telephone Laboratories, Murray Hill, New Jersey (Received November 15, 1960).

The valence band of cadmium sulfide is split by spin-orbit and crystal field effects into three nearly degenerate bands at $\vec{k}=0$. The magneto-optic absorption spectrum of direct excitons formed from the top valence band and the conduction band has been studied in detail. Most of the experiments reported have been performed in light polarized parallel to the hexagonal axis. In this geometry, the exciton series consists of weak lines amenable to magneto-optic experiments. When the magnetic field and the wave vector of the light are perpendicular to each other and to the hexagonal axis, the reversal of the magnetic field produces large changes in the absorption spectrum. This effect can be quantitatively understood as an interference effect between allowed exciton transitions (optical matrix elements independent of the wave vector of the light) and forbidden exciton transitions (optical matrix elements proportional to the wave vector of the light). It is shown that in CdS the forbidden processes having a principal quantum number 2 are somewhat stronger than allowed processes of the same quantum number. By using group theory and the effective-mass approximation, the electron and hole anisotropic g values and masses are determined from an analysis of the exciton spectrum. The electron mass, $0.20_3 m$ (almost isotropic), determined in this analysis is compatible with the assumption that the $\vec{k}=0$ conduction band valley is the lowest conduction band valley. The hole masses for the top valence band are $m_{h\perp}=0.7m$ and $m_{h\parallel}\approx 5m$. An experimental upper limit on the slope of the conduction band at $\vec{k}=0$ is obtained.

*Now at the École Normale Supérieure, Laboratoire de Physique, Paris, France.

LORENTZ FORCE ON SCREW DISLOCATIONS AND RELATED PROBLEMS. Jens Lothe,* Metals Research Laboratory, Carnegie Institute of Technology, Pittsburgh, Pennsylvania (Received October 14, 1960; revised manuscript received December 15, 1960).

The concept of a Lorentz force on screw dislocations, first introduced by Nabarro, is analyzed. It is concluded that the Nabarro Lorentz force on screws and the Lorentz force of electromagnetism are not analogous, and that the term "a Lorentz force on screws" should be dropped in order to avoid confusion. Only when the screw is constrained to move on one slip plane is the analogy with electromagnetism complete. Total quasi-momentum is not generally conserved when screw dislocations interact with elastic waves.

*On leave from Universitetets Fysiske Institutt, Blindern, Oslo, Norway.

PHOTOCHEMICALLY PRODUCED COLOR CENTERS IN KCl AND KBr. John A. Cape,* Department of Physics, University of Illinois, Urbana, Illinois (Received September 26, 1960).

KCl and KBr crystals were exposed to unfiltered mercury arc radiation at 15°K. If an "OH" band was present in the crystals before irradiation, the ultraviolet irradiation produced an optical absorption spectrum similar to that produced by x rays at 15°K. The optical absorption spectrum and the changes in the absorption produced by annealing at higher temperatures were measured and compared with the spectra observed during similar annealing of x-irradiated crystals. In KCl the 335-mμ band, formed by the uv irradiation, bleaches thermally at 56°K as does the 335-mμ H band of x-irradiated KCl. In KBr the 381-mμ band bleaches in steps at 35°, 46°, 56°, and 80°K as compared with the 381-mμ H band in x-irradiated KBr which bleached at 30°, 46°, 56°, and 80°K. In both KCl and KBr the V_1 band appears with the disappearance of the H band. Illumination in the V_1 band causes regeneration of the H band, as occurs in x-irradiated KCl and KBr. In both KCl and KBr the photoproduced H band grows by about 10% at approximately 25°K. It is concluded that the H centers bleach thermally by diffusing to and combining with other color centers. Recombination with F and α centers annihilates the H centers and leads to the formation of V_K centers, while recombination with a third center (possibly a positive-ion vacancy) results in the formation of V_1 centers.

U, U_1, U_2, O^-, and α centers are produced by the uv irradiation as well as F and H centers. The photoproduced F band may be bleached optically with negligible effect on the H band.

*Present address: Atomics International, Division of North American Aviation, Inc., Canoga Park, California.

ENERGY RELEASE IN REACTOR-IRRADIATED COPPER. II. 600 TO 700°K RELEASE. T. H. Blewitt and S. T. Sekula, Solid State Division, Oak Ridge National Laboratory, Oak Ridge, Tennessee and J. Diehl, Max-Planck-Institut für Metallforschung, Stuttgart, Germany (Received October 17, 1960).

The energy release associated with the recovery peak occurring between 600 and 700°K in neutron-irradiated copper was measured utilizing a new technique, that of nuclear heating. Following a bombardment at 40°C of 1.7×10^{20} fast neutrons of a $1/E$ distribution which raised the critical shear stress to 12.8 kg/mm^2 at 4.2°K (5.2 kg/mm^2 at 300°K), a release of 7.7 cal/mole was measured. Using this measured value of the energy release, it is possible to estimate the number of defects annihilated if it is assumed that the annealing is the result of the migration and subsequent annihilation of a single defect. In this way the number of interstitials, vacancies, interstitial-vacancy pairs, and dislocation lines required to account for the measured energy release were estimated. The values were, respectively, 5×10^{19} per mole, 2×10^{20} per mole, 4×10^{19} per mole, and 1×10^{12} cm per mole.

FERROMAGNETIC RESONANCE LINEWIDTH IN COBALT-SUBSTITUTED FERRITES. C. Warren Haas and Herbert B. Callen, Department of Physics, University of Pennsylvania, Philadelphia, Pennsylvania (Received November 14, 1960).

The effect of small concentrations of substitutional ions on the ferromagnetic resonance linewidth of a host ferrite is calculated. The resonance linewidth arises from magnon scattering induced by the variation from ion-to-ion of the spin-orbit interaction. This interaction is uniquely large for cobalt ions because of the orbital

degeneracy of the ground state of the ion in a trigonally-symmetric crystalline field. The resultant contribution to the linewidth is found to be isotropic and of the order of 20-30 oersteds for each percent of cobalt in normal (i.e., noninverse) ferrites or in ferrous ferrite. In other ferrites the effect is diminished by the lifting of the ground-state orbital degeneracy at some of the cobalt sites; this diminution is calculated as a function of the degree of inversion.

DIRECT CURRENT ELECTROLUMINESCENCE AT LOW VOLTAGES. W. A. Thornton, Lamp Division, Westinghouse Electric Corporation, Bloomfield, New Jersey (Received November 29, 1960).

Electroluminescence due to dc excitation occurs in activated ZnS films at 2.0 volts. Since in the dc case no ambiguity is introduced by possible transient potential differences within the phosphor layer, these experiments show that electroluminescence can occur at applied voltages corresponding to about half the band gap (3.8 electron volts) of the ZnS phosphor. The acceleration-collision theory of electroluminescence is thus ruled out at low voltage, and since no appreciable difference is found to be characteristic of the electroluminescence at low voltages, the acceleration-collision mechanism may not be important in any voltage range.

THEORY OF AUGER NEUTRALIZATION OF IONS AT THE SURFACE OF A DIAMOND-TYPE SEMICONDUCTOR. Homer D. Hagstrum, Bell Telephone Laboratories, Murray Hill, New Jersey (Received November 21, 1960).

The two-electron, Auger-type transitions which occur when an ion of sufficiently large ionization energy is neutralized at the atomically clean surface of a diamond-type semiconductor are discussed. Consideration of the basic elements of the problem leads to a computing program which enables one to calculate the total electron yield and kinetic energy distribution of ejected electrons in terms of a number of parameters. It is possible to account for the experimental results for singly-charged noble gas ions incident on the (111) faces of Si and Ge and the (100) face of Si. The fit of theory to experiment is unique in its principal features yielding numerical results concerning (1) the state density function for the valence bands of Si and Ge, (2) the energy dependence of the matrix element as it is determined by symmetry of the valence-band wave functions, (3) the effective ionization energy near the solid surface, (4) energy broadening, and (5) electron escape over the surface barrier. Over-all width of the valence band is found to be 14-16 ev for both Si and Ge. Width of the degenerate p bands is 5.1 ev in Si, 4.3 ev in Ge. The matrix element for p-type valence electrons is 0.3 times that for s-type valence electrons. Effective ionization energy is 2.2 ev less than the free-space value for 10-ev He^+ ions and decreases linearly with ion velocity. Energy broadening is small for 10-ev ions and increases approximately linearly with ion velocity. Probability of electron escape is several times that predicted for an isotropic distribution of excited electrons incident on a plane surface barrier. A general theory of Auger neutralization is given in which the conclusions of the fit to experiment are interpreted. Investigation of the matrix element as a Coulomb interaction integral involving wave functions whose general characteristics are known but which are not explicitly evaluated leads to an understanding of its principal dependences on energy and angle.

VIBRATIONAL SPECTRUM OF GOLD. S. K. Joshi and M. P. Hemkar, Physics Department, The University, Allahabad, India (Received November 28, 1960).

A theoretical lattice vibration spectrum is calculated for gold on the basis of a three-force-constant model as elaborated by Bhatia. The lattice specific heat is calculated and compared with the experimental data.

CYCLOTRON RESONANCE IN INDIUM ANTIMONIDE AT HIGH MAGNETIC FIELDS. B. Lax, J. G. Mavroides, H. J. Zeiger, and R. J. Keyes, Lincoln Laboratory, Massachusetts Institute of Technology, Lexington, Massachusetts (Received November 28, 1960).

The room-temperature pulsed magnetic field infrared cyclotron resonance data of Keyes and co-workers in indium antimonide are interpreted using the $\vec{k}\cdot\vec{p}$ perturbation technique of Kane, which is extended to include the effects of a dc magnetic field. The energy levels are calculated

for a carrier in a band, in the presence of a magnetic field, which is interacting with neighboring bands. From the energy expression, the variation of the apparent effective mass with magnetic field is calculated. The theory is consistent with the room-temperature measurements of Keyes et al. as well as with other cyclotron resonant results obtained at low temperatures.

ANNIHILATION OF POSITRONS IN LiH. A. T. Stewart* and R. H. March,† Dalhousie University, Halifax, Nova Scotia (Received November 23, 1960).

The angular correlation of photons from positron annihilation in LiH and NaH has been measured. The data yield a wave-function product density distribution much wider than the outer-shell electron density around the negative ion. This result is in contrast with the observations for other alkali halides for which these two distributions are much alike.

*Now at the University of North Carolina, Chapel Hill, North Carolina.

†Now at Clarendon Laboratory, Oxford University, Oxford, England.

CURRENT NOISE AND DISTRIBUTED TRAPS IN CADMIUM SULFIDE. James J. Brophy, Physics Division, Armour Research Foundation, Chicago, Illinois (Received November 30, 1960).

The high-frequency portion of the current noise spectrum observed in lightly doped CdS single crystals under uniform 5200A illumination is characteristic of electron trapping transitions to shallow levels. In many crystals the noise spectra have a characteristic $1/f$ trend when the electron quasi-Fermi level is not located near a discrete trap. The $1/f$ trapping noise observed in one crystal at temperatures of 10, 27, and 52°C and for 20 different positions of the electron quasi-Fermi level between 0.5 and 0.3 ev below the conduction band can be represented by a single expression of the form $(1/\omega)\tan^{-1}\omega\tau$, where τ is determined by the low-frequency turnover of the $1/f$ trapping noise. From these experimental values of τ, trap depths are calculated which are in good agreement with the positions of discrete trapping levels determined from other measurements. Since the low-frequency turnovers of the $1/f$ spectra are thus related to the discrete traps, rather than to the position of the electron quasi-Fermi level directly, it appears that the $1/f$ noise may not be associated with a postulated continuous distribution of traps in energy, but rather with a dispersion of capture and release times into the discrete traps.

PARAMAGNETIC BEHAVIOR OF METALLIC CERIUM AND EUROPIUM. R. V. Colvin, Sigurds Arajs, and J. M. Peck, Edgar C. Bain Laboratory for Fundamental Research, United States Steel Corporation Research Center, Monroeville, Pennsylvania (Received November 28, 1960).

The magnetic behavior of metallic polycrystalline cerium and europium has been studied above room temperatures. The measured paramagnetic behavior of cerium can be explained using the interacting Ce^{+++} ion model ($\theta = -50°K$) and the Van Vleck theory of paramagnetism with an additional temperature-independent paramagnetic term $\chi_c = 1.00\times10^{-6}$ g^{-1} cm^3 resulting from the conduction electrons. Europium metal has an unusual magnetic behavior. Its paramagnetic properties in the solid state definitely cannot be explained on the basis of the Eu^{++} model. Near the melting point metallic europium behaves as a collection of weakly interacting Eu^{+} ions. The Bohr magneton number of liquid europium is very close to that of Eu^{++} ions.

ABSOLUTE MEASUREMENT OF THE ATOMIC SCATTERING FACTORS OF IRON, COPPER, AND ALUMINUM. Boris W. Batterman, Bell Telephone Laboratories, Murray Hill, New Jersey, and David R. Chipman and John J. DeMarco, Ordnance Materials Research Office, Watertown, Massachusetts (Received November 16, 1960).

The x-ray atomic scattering factors of iron, copper, and aluminum were carefully remeasured to obtain more reliable information on the outer electron charge densities in these elements. The scattering factors were obtained from measurements of the integrated Bragg intensities of powder samples using monochromatic Mo $K\alpha$ radiation. The intensities were put on an absolute scale by direct measurements of the power in the primary x-ray beam. Extinction, surface roughness, and preferred orientation effects were shown to be negligible in the samples used.

The ratios of the measured scattering factors of the three elements agree with those calculated from Hartree-Fock theory to within 1%. This substantiates the findings of Batterman, and, in contrast with the previous results of Weiss and DeMarco, indicates that there is no large discrepancy between the electronic structures of copper and iron. The absolute values of the measured scattering factors, however, lie about 4% below theory in the region of low $\sin\theta/\lambda$. It is pointed out that the high theoretical values for iron and copper could result from known differences in electronic structure between a free atom and one in the solid, but that present theory probably cannot account for the discrepancy in the case of aluminum.

CLUSTER SIZE IN RANDOM MIXTURES AND PERCOLATION PROCESSES. C. Domb and M. F. Sykes, Wheatstone Laboratory, King's College, London, England (Received November 30, 1960).

It is pointed out that the topological problem which arises in the theory of critical concentration in ferromagnetic crystals, and discussed recently by Elliott et al., is identical with a problem arising in the statistical theory of random mixtures. Additional terms of series expansions are given, and these enable improved estimates of the critical concentration to be made. A distinction is drawn between "site mixtures" and "bond mixtures," the latter having been previously considered under the heading of "percolation processes." The critical concentrations for the two problems are usually different. Some rigorous results regarding the critical concentrations are quoted.

MICROWAVE ZEEMAN EFFECT OF FREE HYDROXYL RADICALS. H. E. Radford, National Bureau of Standards, Washington, D. C. (Received November 7, 1960).

Paramagnetic resonance absorption at 3-cm wavelength has been observed in the products of an electric discharge in low-pressure H_2O and D_2O vapor. The spectra are of the electric dipole type, and arise from Λ-type doubling transitions in low-lying rotational levels of the free $O^{16}H$ and $O^{16}D$ radicals. The theory of the Zeeman effect in $^2\Pi$ levels of light diatomic radicals is extended to the general intermediate-coupling case, and is used for a detailed analysis of the observed spectra. Numerical results of this analysis include molecular g factors precise to within 3 parts in 10^5, and magnitudes of the Λ-type doubling intervals in several low rotational levels. The measured g factors are compared with theory, including small corrections for molecular rotation, the anomalous spin magnetic moment of the electron, and estimated relativistic effects. This comparison yields the value 0.66 ± 0.01 for the molecular matrix element $(\Pi | L_y | \Sigma)$, and also brings to light serious discrepancies between the present experimental results and earlier measurements of the Λ-type doubling in OH and OD. The paramagnetic resonance spectra also exhibit hyperfine structure, from which are derived the following molecular constants:

$$\langle 1/r^3 \rangle_{av} = (0.616 \pm 0.006) \times 10^{24} \text{ cm}^{-3},$$

$$\langle (3\cos^2\chi - 1)/r^3 \rangle_{av} = -(0.21 \pm 0.04) \times 10^{24} \text{ cm}^{-3},$$

$$\psi^2(0) = (0.184 \pm 0.004) \times 10^{24} \text{ cm}^{-3},$$

which describe the distribution of unpaired electrons about the H or D nucleus.

ANALYTICAL METHODS IN HARTREE-FOCK SELF-CONSISTENT FIELD THEORY. S. Huzinaga,* Laboratory of Molecular Structure and Spectra, Department of Physics, University of Chicago, Chicago, Illinois (Received November 7, 1960).

Two alternative schemes are proposed for the determination of electronic self-consistent field (SCF) orbitals in atoms and molecules. They are designed to be applied principally to electronic configurations consisting of two open shells. Both schemes are based upon the idea that the SCF orbitals are expanded in terms of adequate basis functions but they are different in the way of solving the SCF problem. An attempt is made to rate relative merits of both schemes, though they have not yet received any actual application.

*Permanent address: General Education Department, Kyushu University, Fukuoka, Japan.

DETERMINATION OF ELECTRON AND POSITRON HELICITY WITH MØLLER AND BHABHA SCATTERING. J. D. Ullman,* H. Frauenfelder, H. J. Lipkin,† and A. Rossi,‡ University of Illinois, Urbana, Illinois (Received November 16, 1960).

The determination of the helicity of electrons and positrons from beta decay by means of electron-electron (Møller) and positron-electron (Bhabha) scattering is discussed. The theoretical background, the apparatus, and the experimental procedure are treated in detail. The apparatus included, in addition to the conventional parts, a beta monochromator with a momentum resolution of 16% for the investigation of the energy dependence of the helicity. Experiments were performed with P^{32}, Au^{198}, RaE, and Ga^{68}. In all cases, the helicities P were found to be proportional to v/c. The measured helicities, in units of v/c and averaged over the observed range of energies, are summarized as follows. (The errors given are statistical only; systematic errors are estimated to be less than ±3%.)

Radioisotope	P^{32}	Au^{198}	RaE	Ga^{68}
Particles	e^-	e^-	e^-	e^+
Energy interval in kev	660 - 990	460 - 810	520 - 950	1030 - 1300
Helicity $P/(v/c)$	-1.00 ±0.02	-0.98 ±0.03	-0.75 ±0.03	+0.99 ±0.09

*Present address: Centre de Recherche Nucléaire, Department de Physique Nucléaire, Université de Strasbourg, Strasbourg, France.

†Present address: Weizmann Institute of Science, Rehovoth, Israel.

‡Present address: Centro Ricerche Nucleari, Sorin, Saluggia, Vercelli, Italy.

SOME CONSIDERATIONS CONCERNING THE NUCLEAR MATRIX ELEMENT $\sum|B_{ij}|^2$ IN BETA DECAY. Don S. Harmer, Engineering Experiment Station, Georgia Institute of Technology, Atlanta, Georgia, and Morris L. Perlman, Chemistry Department, Brookhaven National Laboratory, Upton, New York (Received November 29, 1960).

Evidence that the nuclear matrix element $\sum|B_{ij}|^2$ contributes to first-forbidden transitions may be deduced from the electron capture-positron emission ratios observed in these transitions and from an analysis of the energy and Z dependence of the coefficients of all the nuclear matrix elements involved. The analysis of these coefficients for the capture and for the emission processes shows that it is reasonable to expect that, except for $\sum|B_{ij}|^2$, these transitions would be characterized by essentially the same capture-positron ratios as those characteristic of allowed transitions. Consequently the deviations of the observed ratios from the allowed values would be due to contributions from $\sum|B_{ij}|^2$; and the magnitude of the deviation, in a particular case, together with lifetime information may be used to compute values for this matrix element and for the sum of the others. Values are thus computed from available experimental data for three $2- \rightarrow 2+$ transitions, and these are compared with values derived directly from the theory of Rose and Osborne. In each case the value of $\sum|B_{ij}|^2$ computed from experiment is nearly as large as the theoretical $\sum|B_{ij}|^2$ value calculated for nucleon spin change two and is considerably larger than those calculated for spin change zero or one; furthermore, the "observed" value for the sum of the other matrix elements is considerably smaller than the largest single matrix element calculated for spin change zero or one. These results are consistent with the conclusion that the nuclear states involved are of such a nature that the transitions proceed unhindered only via $\sum|B_{ij}|^2$, $\Delta j = 2$. One arrives at the same conclusion on the basis of the shell-model description of these nuclear states. For $2- \rightarrow 0+$ transitions, which can be effected only by $\sum|B_{ij}|^2$, the "observed" and theoretical values of the matrix element are in good agreement; and it is of interest to note that both the theoretical and "observed" values of $\sum|B_{ij}|^2$ in each of these $2- \rightarrow 0+$ transitions are about the same or smaller than the values for the $2- \rightarrow 2+$ transition in the same nucleus.

SPIN-ORBIT SPLITTING IN NUCLEI DUE TO TENSOR INTERACTION. Paul Goldhammer, Physics Department, University of Nebraska, Lincoln, Nebraska (Received October 31, 1960).

The effect of the tensor force in nuclei with closed shells plus one nucleon has been investigated using second-order perturbation theory. It is found that one can explicitly exhibit the spin-orbit splitting due to the tensor force using some simple identities. The spin-orbit splitting in He^5 is computed, and found to be 3.4 Mev compared with an experimental value of 2.6 Mev.

SMALL-ORDER SHAPE FACTORS IN In^{114}, P^{32}, AND Y^{90}. R. T. Nichols,* R. E. McAdams, and E. N. Jensen, Institute for Atomic Research and Department of Physics, Iowa State University, Ames, Iowa (Received November 7, 1960; revised manuscript received January 4, 1961).

The beta spectra of In^{114}, P^{32}, and Y^{90} have been studied closely in an intermediate-image beta-ray spectrometer and compared to theoretical predictions in terms of a linear shape factor of the form $(1+aW)$. The values obtained for a were $(+0.0036\pm0.0021)/mc^2$ for In^{114}, $(-0.0133\pm0.0011)/mc^2$ for P^{32}, and $(-0.0047\pm0.0008)/mc^2$ for Y^{90}, all for electron kinetic energies from about 200 kev up to near the maximum beta energies. Tests were made to give indications for spectrometer fidelity. Because of the linearity of the shape-factor plots and the similarity in energy range, the comparative results from In^{114}, P^{32}, and Y^{90} are taken as a definite indication that for at least two of these activities the shape factors have nonzero slopes, irrespective of questions of instrumental fidelity.

*Present address: Gustavus Adolphus College, St. Peter, Minnesota.

ANALYSIS OF SOME DEUTERON-INDUCED REACTIONS IN OXYGEN-18. J. C. Armstrong* and K. S. Quisenberry, Radiation Laboratory, University of Pittsburgh, Pittsburgh, Pennsylvania (Received November 21, 1960).

The reactions $O^{18}(d,t)O^{17}$, $O^{18}(d,d')O^{18*}$, and $O^{18}(d,p)O^{19}$ are studied using 15-Mev deuterons and magnetic analysis of reaction particles. Absolute cross sections are determined for all reactions studied and the Butler-Born approximation is used to extract reduced widths when possible. Angular distributions of triton groups corresponding to the ground, 0.871-, 3.846-, 4.555-, 5.083-, and 5.378-Mev states of O^{17} are obtained. An estimate of the configuration admixtures in the O^{18} ground state is made from analysis of the reduced widths and indicates the presence of a sizable (about 6%) $(1f_{5/2}{}^2)_0$ component. The experimentally determined admixtures are compared with several theoretical estimates. All O^{18} levels observed in the inelastic deuteron scattering have been previously reported—the known 5.01-Mev state is not observed. The angular distribution of inelastic deuterons corresponding to the 1.982-Mev state of O^{18} is obtained and comparison of the absolute cross section with theory provides an estimate of the O^{18} deformation. Proton groups from $O^{18}(d,p)O^{19}$ reactions are observed corresponding to O^{19} excitations of 0, 1.469, 3.164, 3.948, (4.123), (4.586), (4.706), (5.165), 5.45, 5.707, and 6.279 Mev, where assignment of the levels in parentheses to O^{19} is uncertain. The known 0.096-Mev state is not observed and the proton group corresponding to 5.45-Mev excitation contains contributions from at least two states. Angular distributions leading to the O^{19} ground, 1.469-, 3.164-, 3.948-, 5.707-, and 6.279-Mev states are obtained and reduced widths extracted. The l_n values for these angular distributions are ambiguous except for the ground-state reaction ($l_n=2$) and the 1.469-Mev state reaction ($l_n=0$). Analysis of the data suggests that J^π (ground state) $=5/2^+$ and J^π(0.096-Mev state) $=3/2^+$. Using parameter values estimated from the O^{19} energy level spectrum or obtained from neighboring nuclei, a description of this nucleus in terms of the strong-coupling unified model agrees with the data.

*Now at Physics Department, University of Maryland, College Park, Maryland.

14.4-Mev $(n,2n)$ CROSS SECTIONS. L. A. Rayburn,* Argonne National Laboratory, Argonne, Illinois and Department of Physics and Astronomy, University of Georgia, Athens, Georgia (Received November 14, 1960).

Cross sections for the $(n,2n)$ reaction have been measured at an incident neutron energy of 14.4 ± 0.3 Mev for 27 nuclides. These measurements were made relative to the cross section for the $Cu^{63}(n,2n)Cu^{62}$ reaction. The relative

cross sections were then converted to absolute cross sections by using the weighted mean of several $Cu^{63}(n,2n)Cu^{62}$ reaction-cross-section measurements made by other investigators.

*Present address: Department of Physics and Astronomy, University of Georgia, Athens, Georgia.

AVERAGE RADIATIVE CAPTURE CROSS SECTIONS FOR 7- TO 170-kev NEUTRONS. J. H. Gibbons, R. L. Macklin, P. D. Miller, and J. H. Neiler, Oak Ridge National Laboratory, Oak Ridge, Tennessee (Received August 17, 1960).

Measurements of neutron radiative capture cross sections in the kev region have been made using fast (millimicrosecond) time-of-flight techniques and a large liquid scintillator tank. Two series of measurements have been completed on a number of nuclides. These are determinations of (1) cross sections relative to that of indium at 30 kev and at 65 kev for 49 nuclides, and (2) cross sections as a function of neutron energy for the following nuclei: Br, Nb, Pd, Ag, Cd, In, Sb, I, Pr, Sm, Gd, Tb, Dy, Ho, Er, Tm, Yb, Lu, Ta, W, Pt, and Au. Curve fits, using the statistical model, have been obtained for Br, Nb, Ag, In, Sb, I, Pr, Tb, Ho, Tm, Lu, Ta, and Au. The results demonstrate the presence of the $2p$ giant resonance near $A = 100$ predicted by the optical model. The average nuclear parameters obtained are in good agreement with recent low-energy total cross-section results, but are in poor agreement with earlier results. Possible reasons for these disagreements are discussed.

DECAY OF Na^{26}. E. L. Robinson, B. T. Lucas, and O. E. Johnson, Physics Department, Purdue University, Lafayette, Indiana (Received November 18, 1960).

The bombardment of high-purity natural magnesium targets with fast neutrons from the $Li^7(d,n)Be^8$ reaction ($E_n \lesssim 24$ Mev) yielded, in addition to activities associated with well-known isotopes, an activity having an experimental half-life of 1.03 ± 0.06 sec. Scintillation spectrometer measurements showed a (1.82 ± 0.03)-Mev gamma ray and a (6.7 ± 0.3)-Mev beta group decaying with the 1.03-sec half-life. The 6.7-Mev beta group was found to be in coincidence with the 1.82-Mev gamma ray. The assignment of the (1.03 ± 0.06)-sec half-life to Na^{26} produced in the reaction $Mg^{26}(n,p)Na^{26}$ and the proposed decay scheme are supported by internally consistent arguments based on the known characteristics of the reaction products and their decay modes, the half-life studies using both beta and gamma radiation, the features of experimental beta and gamma spectra, and nuclear systematics. The decay of the ground state of Na^{26} takes place in part by a (6.7 ± 0.3)-Mev beta transition to the (2+) first excited state of Mg^{26}. The intensities of the beta transitions to the (2+) second excited state and the (0+) ground state are less than 0.1 of the intensity of the (6.7 ± 0.3)-Mev transition. The possible ground-state spin and parity assignment for Na^{26} is either 1+, 2+, or 3+. A weak theoretical argument against spin 1 is presented. The present experimental measurements alone will not reduce the ambiguity in the spin assignment. A $Na^{26}-Mg^{26}$ mass difference of 8.5 ± 0.3 Mev is derived from the known level structure of Mg^{26} and the beta transition energy measured in the present investigation.

MECHANISM OF THE REACTION $O^{16}+p \rightarrow p+4\alpha$ AT 29 Mev. Oscar C. Kolar, Lawrence Radiation Laboratory, University of California, Berkeley, California (Received October 26, 1960).

An expansion cloud chamber containing oxygen gas at 1/3 atmosphere pressure was used to study the reaction $O^{16}+p \rightarrow p+4\alpha$ at a bombarding energy of 28.9 Mev. Two hundred and twelve events were obtained that satisfied the criteria of energy and momentum balance. Ninety-one of these had all five outgoing prongs visible, while the remaining 121 had but four prongs visible, the fifth being obscured by the beam. Slightly more than half of all the events showed the presence of the ground state of Be^8. Of these, five events showed the presence of two Be^8 nuclei in the ground state. The events exhibiting the presence of a single ground-state Be^8 were interpreted according to the mechanism $O^{16}+p \rightarrow p+2\alpha+Be^8$; $Be^8 \rightarrow 2\alpha$. The possibility of a compound state was considered. If such an intermediate state did occur, it was such that it did not obey strictly the predictions of the compound nucleus theory. The remaining half of the events did not show evidence for any intermediate nuclei (with the possible exception of the appearance of the 1.4-Mev state of B^9 in

5%, or fewer, of the cases) and could be interpreted only on the basis of the direct quadripartition of the oxygen nucleus.

CLUSTER NATURE OF Li^7 AND Be^7. T. A. Tombrello and G. C. Phillips, Rice University, Houston, Texas (Received November 17, 1960).

Measurements of the capture γ-radiation processes, mass $3+\alpha \rightarrow$ mass $7+\gamma$ and nucleon $+Li^6 \rightarrow$ mass $7+\gamma$, give information about the cluster structure of the mirror nuclei Li^7 and Be^7. The cluster model predicts that the ground state and low excited states of these nuclei should have large reduced widths $\theta_{3+4}{}^2$ for the configuration mass $3+\alpha$ particle and small reduced widths $\theta_{1+6}{}^2$ for the configuration nucleon + Li^6. Scattering experiments provide accurate initial, capturing, wave functions, and an assumption of the cluster nature of the final, bound states allows the electromagnetic capture cross sections to be calculated and compared to experiment. The reduced widths deduced show that $\theta_{3+4}{}^2$ is large, $\theta_{1+6}{}^2$ is small, and that the ground states and first excited states of Li^7 and Be^7 are primarily of the two-body cluster form, mass $3+\alpha$ particle.

ANGULAR YIELD OF NEUTRONS FROM THE $T(d,n)He^4$ REACTION FOR 6- TO 11.5-Mev DEUTERONS. Murrey D. Goldberg and James M. LeBlanc, Lawrence Radiation Laboratory, University of California, Livermore, California (Received November 21, 1960).

The angular yield of monoenergetic neutrons from the $T(d,n)He^4$ reaction has been measured with 6.2-, 7.9-, 9.1-, 10.2-, and 11.4-Mev deuterons. The neutrons were detected with a proton recoil telescope which provided discrimination against neutrons from the $T(d,np)T$ breakup reaction. The yield curves are all peaked forward, with a second maximum at about 65° which becomes more pronounced with increasing energy, and a back-angle rise. A quasi-absolute determination of the 0° cross section for this reaction is described. The measured yield curves are compared to those for the companion $He^3(d,p)He^4$ reaction and a strong similarity in shape and magnitude is noted. A simple stripping model is inadequate to describe these data. A distorted-wave calculation is required.

TWO-NUCLEON INTERACTION FROM DOUBLET SPLITTINGS. F. C. Barker, Australian National University, Canberra, Australia (Received November 8, 1960).

The splitting of closely spaced doublet levels of spin $J+\frac{1}{2}$ and $J-\frac{1}{2}$ is investigated in cases which can be approximated by a core of spin J and an s nucleon. Allowance is made for the Thomas shifts of the levels. Using j-j coupling wave functions, the exchange parameters and strength of the effective interaction between nucleons in the nucleus are determined by a least-squares fit to the doublet splittings, and some improvement is made over results obtained with previously accepted parameters. It is suggested that measurement of the sign of some doublet splittings would clarify the interaction further.

K^--MESON SCATTERING IN NUCLEAR EMULSION. R. D. Hill, J. H. Hetherington, and D. G. Ravenhall, Department of Physics, University of Illinois, Urbana, Illinois (Received October 5, 1960).

Elastic single scatterings of K^- mesons by nuclei of a dilute $G5$ photographic emulsion have been experimentally measured for energies between 30 and 80 Mev. Accurate numerical calculations of the differential scattering cross sections have been carried out by solving a Klein-Gordon wave equation for an optical-model potential of the Woods-Saxon form. Experimental and theoretical results are in good agreement both on an absolute and on a relative-variation basis if the real part of the K^--nuclear potential is attractive. The connection with low-energy K^--nucleon scattering is discussed.

π^- SCATTERING FROM COMPLEX NUCLEI. R. M. Edelstein,* W. F. Baker,† and J. Rainwater, Columbia University, New York, New York (Received November 29, 1960).

Differential cross sections were measured for π^--carbon scattering at 69.5 and 87.5 Mev and π^--oxygen scattering at 87.5 Mev from 20° to 125° extending the technique of Baker, Rainwater, and Williams. The energy resolution was sufficient to measure pure elastic as well as 5- and 10-Mev inelastic cross sections. The modified Kisslinger optical-model equation was used to fit the elastic cross-section data. A χ^2 analysis

for the 69.5-Mev carbon data gave a nuclear radius parameter $r_0 = 1.05 \pm 0.02$ fermis and a fall-off parameter $t = 1.16 \pm 0.07$ fermis. These parameters give good fits to the other data as well. An energy dependence in the strength parameters for carbon is observed in qualitative agreement with prediction.

*Present address: Carnegie Institute of Technology, Pittsburgh, Pennsylvania.

†Present address: Brookhaven National Laboratory, Upton, New York.

STARS PRODUCED BY π^- CAPTURE IN A HYDROGEN BUBBLE CHAMBER CONTAINING DISSOLVED HELIUM. Michel Schiff,* The Enrico Fermi Institute for Nuclear Studies and Department of Physics, University of Chicago, Chicago, Illinois, Roger H. Hildebrand, Argonne National Laboratory, Argonne, Illinois and The Enrico Fermi Institute for Nuclear Studies, University of Chicago, Chicago, Illinois, and Clayton Giese, Department of Physics, University of Chicago, Chicago, Illinois (Received November 28, 1960).

One-pronged stars produced by π^- capture in a hydrogen bubble chamber containing dissolved helium have been investigated. The distribution of prong lengths in the interval 0.029 to 0.64 g/cm^2 is presented. About one third of the prongs in this interval are found to have a unique range corresponding to tritons from the reaction $\pi^- + He^4 \rightarrow H^3 + n$. Some prongs lying beyond the triton peak are identified as protons from the reaction $\pi^- + He^4 \rightarrow H^1 + 3n$. The fraction of pions producing stars is found to be approximately equal to the helium concentration.

*Present address: 7 bis Rue Alexandre Parodi, Paris 10, France.

TOTAL CROSS SECTIONS FOR NEGATIVE PIONS ON PROTONS AT 230, 290, 370, 427, AND 460 Mev. John C. Caris,* Lester K. Goodwin,† Robert W. Kenney, Victor Perez-Mendez, and Walton A. Perkins, III,‡ Lawrence Radiation Laboratory, University of California, Berkeley, California (Received November 21, 1960).

Total cross sections for negative pions on protons were measured at laboratory energies of 230, 290, 370, 427, and 460 Mev. The measurements were made in the same pion beams as, and at energies identical with those of our $\pi^- p$ differential scattering experiments. Comparisons of the total and differential scattering can be made with the dispersion theory at a given energy without introducing the systematic errors that would normally enter due to uncertainties in the parameters of more than one pion beam. The measured total cross sections are found to agree within statistics with other measured values, and with the sums of elastic, inelastic, and charge-exchange cross sections measured at this laboratory. The results are:

E (Mev)	σ_{total} (mb)	E (Mev)	σ_{total} (mb)
230 ±6	58 ±9	427 ±10	27 ±2
290 ±7	33 ±2	460 ±20	28 ±2.
370 ±9	27 ±2		

*Present address: Aeronutronic, Newport Beach, California.

†Present address: Physics Department, Hebrew University, Jerusalem, Israel.

‡Present address: Lawrence Radiation Laboratory, University of California, Livermore, California.

RELATIVISTIC PARTICLE SYSTEMS WITH INTERACTION. Leslie L. Foldy, Case Institute of Technology, Cleveland, Ohio (Received November 17, 1960).

The possibility of covariantly describing a system of a fixed number of particles interacting directly is explored by attempting a direct "integration" of the cummutation relations for the inhomogeneous Lorentz group under restrictions appropriate to the term "system of a fixed number of particles." By direct interaction is meant the fact that interaction between the particles is expressed directly in terms of coordinates, momenta, and spins for the particles rather than through the agency of a mediating field. The integration is carried out in considerable generality with the assumption that the infinitesimal generators of the group have expansions in inverse powers of the square of the velocity of light. The result coincides with that obtained earlier by Bakamjian and Thomas, but the method employed yields greater insight into the generality of the result, as well as into how further conditions beyond covariance, such as the property which is here called "separability of the interaction," can be incorporated in the result. The relationship of the result to the complete reducibility of a representation of the inhomogeneous Lorentz

group is pointed out. Possible generalizations and applications of the procedures here employed are discussed.

TIME-ORDERED GREEN'S FUNCTIONS AND PERTURBATION THEORY. M. Muraskin and K. Nishijima, Department of Physics, University of Illinois, Urbana, Illinois (Received November 16, 1960).

A formulation of field theories based on the generalized unitarity condition and parametric dispersion relations is presented. In the perturbation theory we discuss the connection between the present scheme and the Lagrangian theory and derive the renormalizability condition in our formulation. Finally we show for typical processes in the first, second, third, and fourth orders that our theory can reproduce the renormalized Feynman perturbation theory.

TIME-ORDERED GREEN'S FUNCTIONS AND ELECTROMAGNETIC INTERACTIONS. K. Nishijima, Department of Physics, University of Illinois, Urbana, Illinois (Received November 16, 1960).

In the present paper we study various aspects of the Ward-Takahashi equations. In perturbation theory the equivalence between this set of equations and the requirement of gauge invariance is shown. It is then shown that these equations are valid for composite particles as well as for elementary particles. Based on our new formulation the definition of composite particles is given, and then we show with the aid of the Ward-Takahashi equations that the photon is an elementary particle.

THEORETICAL ASPECTS OF NONLEPTONIC HYPERON DECAYS. A. Pais,* Lawrence Radiation Laboratory, University of California, Berkeley, California (Received November 14, 1960).

Recent experimental results on nonleptonic hyperon decays are studied on the basis of a doublet approximation for strong and weak interactions, with the implied suggestion that this higher symmetry may be more easily discernible in such reactions in which K particles do not occur explicitly. The doublet approximation is characterized by a doublet spin I which is $\frac{1}{2}$, 1, 0 for baryons, π, K, respectively, and by a K spin. It is not necessary to assume that the strong K interactions are weak compared to the strong π interactions. For the mentioned reactions it is necessary to assume that the strong interactions which do not conserve I play a minor role compared to those which conserve I.

The following refinement of the nonleptonic $\Delta T = 1/2$ rule is proposed. (T = isotopic spin.) The weak nonleptonic interactions consist of two parts $H^{(0)}$, $H^{(1)}$ with $\Delta I = 0$, 1, respectively. In the doublet approximation $H^{(0)}$ and $H^{(1)}$ separately conserve parity in the presence of all strong π and K interactions. $H^{(0)}$ and $H^{(1)}$ together do not conserve parity, however. In addition to $\Delta I = 1$, $H^{(1)}$ should in general satisfy a further constraint, but there are classes of graphs for which $\Delta I = 1$ is sufficient.

Current × current structures for $H^{(0)}$ and $H^{(1)}$ are examined. Results of a foregoing paper can be viewed as a special case of the $\Delta I = 0$, 1 rule. The same is true for results obtained by Feldman, Matthews, and Salam and by Wolfenstein. The considerations of these authors can be extended to wider classes of graphs.

Odd relative helicity and the relation between rates for $\Lambda \to p + \pi^-$, $\Sigma^+ \to p + \pi^0$ are consequences of the $\Delta I = 0$, 1 rule only. So is the prediction that Ξ decay is strongly P-nonconserving.

The parity properties of $H^{(0)}, H^{(1)}$ are sufficient conditions. It is a delicate question whether they are necessary. For a subset of graphs they are not necessary, but this set seems arbitrary. If it is assumed that the parity conditions are necessary, the schizon scheme is ruled out.

It is noted that the nonleptonic weak interactions may be generated by the strong interactions in terms of the following prescription. $H^{(1)}$ is generated by assuming that the π (K) fields have small K (π) components. An $H^{(0)}$ is generated by assuming that the doublets N_1 (N_2) have small N_2 (N_1) components; likewise for N_3 and N_4. This procedure also generates a nonelectromagnetic $\Delta T = 3/2$ interaction. This last coupling is small in the sense that it only contributes to $K_{\pi 2}{}^+$ to the extent that the doublet approximation is not valid.

*Permanent address: Institute for Advanced Study, Princeton, New Jersey.

MANDELSTAM REPRESENTATION WITH ANOMALOUS THRESHOLDS. R. J. Eden, P. V. Landshoff, and J. C. Polkinghorne, Department of Applied Mathematics and Theoretical Physics, University of Cambridge, Cambridge, England,

and J. C. Taylor,* Department of Physics, Imperial College, London, England (Received November 28, 1960).

It is proved that fourth order diagrams provide necessary and sufficient conditions for the Mandelstam representation to be valid for every finite order in perturbation theory.

*Now at the Department of Applied Mathematics and Theoretical Physics, University of Cambridge, Cambridge, England.

EFFECTS OF K-MESON INTERACTIONS ON THE NUCLEON ANOMALOUS MAGNETIC MOMENT.

K. Nishimura, Department of Physics, Rutgers University, New Brunswick, New Jersey (Received November 23, 1960).

A previous calculation of the physical nucleon wave function in static-source pion theory is extended by including the pseudoscalar K-meson interactions, the motivation being that this should increase the scalar part of the nucleon anomalous magnetic moment, thus improving the result of previous calculations. In constructing a trial function for the physical nucleon, the method of moments was used and terms containing up to three mesons were included. Calculation shows that a too strong K-meson coupling is detrimental to the vector part, and that the scalar part can be increased approximately by 10% if the K-meson interaction is made moderately low.

INTERMEDIATE VECTOR BOSON AND RADIATIVE LEPTON DECAY OF THE K MESON.

Akira Kanazawa* and Masao Sugawara, Physics Department, Purdue University, Lafayette, Indiana and Katsumi Tanaka,† Physics Division, Argonne National Laboratory, Argonne, Illinois (Received October 20, 1960).

K-meson decay into electron, neutrino, and photon is analyzed in the lowest order perturbation with respect to weak and electromagnetic interactions, but without making any approximation regarding the strong interaction. The weak interaction is assumed to be transmitted by a single charged intermediate vector meson which interacts with the weak current in the conventional way. It is pointed out here that a certain angular and momentum distribution of decay particles could reveal almost unequivocally whether the intermediate vector meson does exist. It is shown also that other lepton decays of the K meson which include μ mesons and π mesons cannot be used for the same purpose.

*On leave of absence from Physics Department, Hokkaido University, Sapporo, Japan.

†Temporary address for 1960-1961: Istituto di Fisica Teorica dell' Università di Napoli, Mostra dell' Oltremare, Napoli, Italy.

NONLINEAR ELECTRODYNAMICS IN GENERAL RELATIVITY.

Asher Peres, Department of Physics, Israel Institute of Technology, Haifa, Israel (Received November 30, 1960).

General relativistic field equations are derived from a gauge-invariant electromagnetic Lagrangian, which does not involve derivatives of the field, nor any charge density, but otherwise is completely arbitrary. These equations are explicitly solved in the static spherically symmetric case, and it is shown that there are solutions which are everywhere regular and behave, at large distances, like the gravitational and electromagnetic fields of a point charge. Some wave-like solutions are also derived.

INTERNAL SYMMETRIES OF STRONG BARYON-MESON INTERACTIONS.

Yoshio Shimamoto, Brookhaven National Laboratory, Upton, New York (Received November 3, 1960).

A simple model considered previously by Pais in which the Σ and Λ hyperons are regarded as a mass-degenerate supermultiplet in the strong pion interaction is reconsidered. It is shown that recognition of the symmetry exhibited by these hyperons in their pionic coupling leads to certain prescriptions which may be used to break the symmetry via the strong K-meson interactions. The symmetry reduction schemes described make possible the construction of a strong baryon-meson interaction Hamiltonian which requires no more than four coupling constants (rather than the customary eight) and which in no way imposes severe restrictions on the strong interactions. Finally, production and scattering amplitudes based on the 4-symmetry are discussed.